Analysis of Seismic Similarity in Strombolian Eruptions from Mount Erebus, Antarctica

By
David Brent Henderson

Submitted in Partial Fulfillment of
the Requirements for the Degree of
Master of Science in Geophysics (Solid Earth)

New Mexico Institute of Mining and Technology
Department of Earth and Environmental Science
Socorro, New Mexico

January 2007

ABSTRACT

Mount Erebus has long been recognized to produce very similar seismic signatures associated with its Strombolian eruptions. Preliminary research performed on similar seismograms from December 1999 to January 2000 suggested a sudden decorrelation of the coda, accompanied by relative stability in the early seismogram. Using coda wave interferometry, this decorrelation was interpreted as a median change within the volcano. Closer examination of this data in this thesis shows that clipping due to event size variations as well as more subtle features controlled by event size strongly influence such analysis techniques.

Once it became obvious that source effects were very important influences on seismogram similarity, more sophisticated methods were implemented to better understand them. A moving window cross correlation analysis demonstrated more comprehensively that eruption size is a significant factor in seismogram similarity. A surprising discovery to come out of this research was the existence of time bands of strong correlation, probably arising from scatterers within the volcano at some distance (km) from the lava lake, which are even visible in the late coda (30+ s). Invariance is seen in the corresponding correlation lags associated with these scatterers, indicating stability in medium velocity.

Clustering the whole waveform seismograms also showed that size is the primary determiner of seismogram similarity. However, the fact that several clusters can have the same size (and even be active simultaneously) showed that other variable source processes must be involved as well. Videos of eruptions, as well as infrasound data, showed that other possible source process variations that may be important in this context include location of the bubble in the lava lake, lava lake convection phenomena (i.e., the lava lake state during eruption), and the geometry or pressure of the eruptive gas slug. Overall, similarities in how the initial and coda parts of the seismogram cluster also indicate that seismogram variability is due to source processes.

Clustering the infrasound data resulted in completely different clusters then the seismic data. The clusters for the infrasound data were very similar, except for the rate of change of the first motion. This indicates that infrasound clusters are especially sensitive to rupture processes, making them promising for measuring lava lake rupture process.

ACKNOWLEDGMENTS

This research supported by NSF Grants OPP-0116577, OPP-0229305, and OPP-0538414 and by New Mexico Tech Research and Economic Development.

I also wish to thank my fellow students for their help and support on this project, specifically Jana Stankova, Casey Elliott, Hunter Yarbrough, Kyle Jones, and Jonathan MacCarthy.

I would also like to thank my advisor Rick Aster for his input and patience, as well as the rest of my committee for their input (Susan Bilek and Philip Kyle).

TABLE OF CONTENTS

LIST OF TABLES

Page

LIST OF FIGURES

Page

CHAPTER 1

Introduction and Background

Introduction

Mount Erebus is a 3794 m stratovolcano located on Ross Island, Antarctica, that has been essentially continually active since Sir James Ross first observed it in 1841 [*Kyle*, 1994]. The Inner Crater of Mount Erebus contains a persistent, convecting, phonolitic lava lake, which has existed since it was discovered in 1972 [*Giggenbach et al.*, 1973] and probably considerably longer. The lava lake has varied in diameter from ten to sixty meters during that time [*P. Kyle, pers. com.*]. The number and size of Strombolian eruptions from the lava lake has been variable, with no activity during 2003 to unusually strong activity in 1984, during which time the lava lake was briefly buried under the eruptive debris. The end of 2005 and all of 2006 have been marked by a return to strong Strombolian activity (Figure 1.1). The Strombolian eruptions are due to gas slugs forming at an unknown depth below the surface of the lava lake and explosively decompressing when they reach the surface. The gas slugs can have a diameter of up to 10 meters [*Aster et al.*, 2003], with even larger gas slugs occurring since 2005 (possibly filling the whole lake). *Dibble* [1994] first noted that there is a strong seismogram

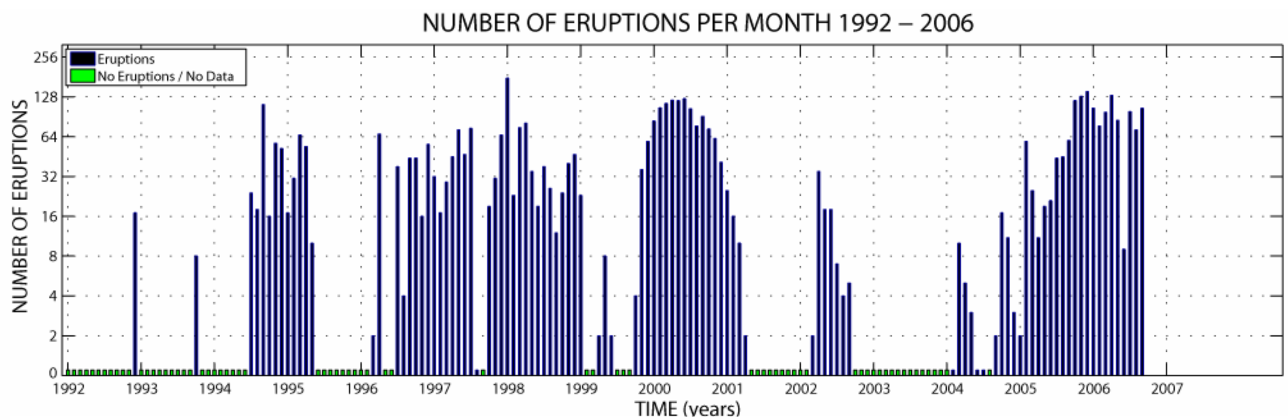

Figure 1.1 - Bar plot of the number of eruptions per month over the last 14 years. The y-axis is plotted on a logarithmic scale, and time in years on the x-axis. Periods of no eruptions or lack of data are shown in green. The prominent gap during 2003 is due to the fact that there were no eruptions during this period. Many earlier gaps are probably due to the loss of instrumentation during the Antarctic winter (*from Jones et al.* [2007] and www.ees.nmt.edu/Geop/Erebus/erebus.html).

similarity between many of the strombolian eruptions due to its self-replicating lava lake eruptive conditions, a key observation that led to the work reported here.

While there is strong seismogram similarity between eruptions, there is also some second order variability. But what does this variability mean, and what can it tell us? Seismogram variability in the coda has been interpreted by *Gret et al.* [2005] to show that the path between the source (Strombolian eruption) and receiver (seismometer) changed. The purpose of this research was to study these results in detail, and expand the study to larger time periods using more comprehensive techniques.

Background

It has been shown that the latter part of a local earthquake seismogram (the coda) consists largely of backscattered waves due to heterogeneities in the crust [*Aki*, 1969; *Aki and Chouet*, 1975]. In other words, waves traveling through a medium are scattered one or more times before arriving at the seismometer. Volcanoes have been shown to be very inhomogeneous, producing especially strong scattering behavior [*Wegler and Luhr*, 2001]. *Aki and Chouet* [1975] noted that seismic waves with frequencies up to 25 Hz are sensitive to the earth's scattering structure. In theory this sensitivity can be used to monitor changes in a medium.

Coda wave interferometry was developed to take advantage of the multiple scattering and sensitivity of coda waves to internal structure. The principle behind coda wave interferometry is that the directly arriving energy is relatively insensitive to small changes in the medium, but that single or (especially) multiply-scattered coda waves may be delicately sensitive to such changes [*Snieder*, 2004]. Possible changes include distributed velocity changes, movement of a scatterer (heterogeneity), changes in the properties of the scatterer, or movement of the source [*Gret et al.*, 2006b; *Snieder*, 2006; *Snieder et al.*, 2002]. If we have a repeating non-destructive source and a permanent receiver, this sensitivity to small changes might thus allow us to use the coda wave as a change detecting ”interferometer”. Conversely, if there is no change between the source and receiver the waveforms will be identical. This technique thus seeks to generally exploit the phase and amplitude information of coda waves to monitor changes in a medium over time [*Snieder*, 2006].

Coda wave interferometry has been successfully tested in the laboratory. For example, the thermal dependence of velocity in granite and aluminum was monitored by using the sensitivity of the coda [*Gret et al.*, 2006b; *Snieder et al.*, 2002]. Using an ultrasonic transducer and receiver, the relative change in velocity was calculated from 20 to 90^{o}C at 5^{o} intervals. The authors found that the directly arriving waves were not significantly affected by small temperature changes, but significant changes were noted in the coda over the same intervals. The velocity was found to vary linearly with temperature, except from 70^{o} to 75^{o} where thermal cracking occurred, causing a rapid velocity decrease. The cracking occurred only on the pristine sample, and afterwards further heating and cooling resulted in a linear velocity change over the entire temperature range [*Gret et al.*, 2006b; *Snieder et al.*, 2002]. Other laboratory tests include the relative velocity changes due to uniaxial stress and due to water saturation in Berea Sandstone [*Gret et al.*, 2006b]. An in situ coda wave interferometry experiment was also carried out at a hard rock mine in Idaho Springs, Idaho. Using a pressure cell installed on a mine column and a hammer as a repeatable source it was possible to measure velocity changes due to pressure changes as small as 8.27 MPa [*Gret et al.*, 2006a].

Velocity changes have been observed in fault zones using coda wave interferometry. *Rubinstein and Beroza* [2004] identified highly similar earthquake doublets and multiplets and used them as a repeating source. The multiplets occurred before, during, and after the M_w 6.9 Loma Prieta earthquake. Using a moving window cross-correlation on the S wave arrival and the S wave coda after the multiplets had been lined up at the P wave arrival, velocity changes were identified. An example of these velocity changes was seen using the moving window correlation after the Loma Prieta earthquake, and were seen as delays in the direct S arrival and S coda. Delays of up to 20 ms were seen in the direct arrival and 50 ms in the S coda. It was concluded that the velocity change was likely due to shallow cracks that formed due to the non-linear ground motion induced by strong motions during the main shock. It was also noted that the magnitude of the velocity change was influenced by the local geology. After the Loma Prieta earthquake, stations located on older (harder) ground produced smaller delays while stations located on newer (softer) ground produced larger. The strength of softer rocks is more easily overcome by strong ground motion, creating larger velocity changes**.** The observed velocity changes recovered over time, probably due to crack healing [*Rubinstein and Beroza*, 2004]. A velocity change was also observed along the Karadera-Düzce Branch of the North Anatolian fault in Turkey after the 1999 M_w 7.1 Düzce main shock. *Peng and Ben-Zion* [2006] noted that the observed velocity change appeared to be due to a very shallow, upper 100 m, heavily damaged surface layer. Once again, non-linear ground motion was implicated. Site effects, consistent with the Loma Prieta finding, were concluded to have influenced the magnitude of the velocity change, and the velocities also recovered over time [*Peng and Ben-Zion*, 2006]. These two observations strengthen the assertion that the coda is affected by geology, crack density, and topography (even relatively subtle topography [*Revenaugh*, 1995]). Conversely, searches for seismic coda variability in quiescent fault regions such as the pre-2004 Parkfield area of the San Andreas Fault [*Antolik et al.*, 1996; *Aster et al.*, 1996] have failed to detect any more gradual changes associated with pre-main shock stress or other changes, although precise repeated vibrator studies have demonstrated coda changes that can be correlated, again, with near-surface variability associate with seasonal precipitation [*Karageorgi et al.*, 1992]

As in all such studies utilizing natural events, the repeatability of the source is key to resolving any clear changes in the propagation medium [*Aster et al.*, 1990; *Aster et al.*, 1996]. For instance, using coda wave interferometry, *Snieder and Vrijlandt* [2005] were able to show that a change in the coda observed for doublets and multiplets along the Hayward Fault was due to changes in source location. They were able to estimate that the source had moved between 63 and 124 meters for the different pairs. These results agreed with results using the double difference source relocation method [*Waldhauser and Ellsworth*, 2000]. Noise was found to be an important factor in calculating the source separation. Noise tended to cause an over estimation of the displacement, and had to be corrected for [*Snieder and Vrijlandt*, 2005]. Thus, coda variations, in differing situations, have been shown to be due to either medium changes or source location changes, a key issue that we will return to later in this thesis.

The heterogeneous structure of volcanoes has been shown to cause strong multiple scattering [*Wegler*, 2003; *Wegler and Luhr*, 2001]. In a seminal study by *Fehler et al.* [1988], an increase in attenuation (changes in the scattering field between the source and receiver, also referred to as Coda Q) was observed at Mount Saint Helens before the September 1981 eruption due to the opening of microcracks. There was a 20-30 percent drop in attenuation after the eruption, which was attributed to the closing of the micro cracks due to the depressurization of the volcano [*Fehler et al.*, 1988]. Before the 1998 eruption of Volcan de Colima in Mexico, an increase in attenuation of 34-38% was observed. This attenuation was also attributed to the opening of microcracks due to over pressurization of the volcano [*Dominguez et al.*, 2003].

Coda wave interferometry can potentially exploit this scattering to examine temporal internal changes at volcanoes worldwide, but again, tradeoffs between medium changes and source location appear to be strong. At Arenal volcano, Costa Rica, *Snieder and Hagerty* [2004] deconvolved infrasonic pulses from the seismic displacement records for different time intervals resulting in a highly repeatable signal. Subsequently using coda wave interferometry (time shifted cross-correlation) it was possible to show that the changes found in the repeatable signal are due to a small-scale source displacement, estimated to be 15 m [*Snieder and Hagerty*, 2004]. Coda wave interferometry was also successfully implemented at Mt. Vesuvius volcano in Italy. Using a moving window cross-correlation on doublets from Mount Vesuvius, *Pandolfi et al.* [2006] reported a velocity change before and after a magnitude 3.6 earthquake. This velocity change was suggested to be due to the over pressurization of the volcano, causing microcracks to open. Coda wave interferometry made it possible to detect both long term and short term velocity changes in the volcano, some of these changes being as small or smaller then 0.4 percent [*Pandolfi et al.*, 2006].

An initial focus of this research is a study in which [*Gret et al.*, 2005] used coda wave interferometry to monitor temporal changes at Mount Erebus. The authors took advantage of the stable lava lake at Mount Erebus, and the repeating, self-reconstructing strombolian eruptive system of the lava lake. In this study of the short period seismograms from strombolian eruptions recorded between the 12th December 1999 and the 25th January 2000, *Gret et al.* [2005] observed a progressive decorrelation of the coda over a short period of time around January 8th (Figure 1.2). The decorrelation was observed by cross correlating the first 7 s of each event with a master event chosen as the earliest eruption. The same was done for the coda of each event, also using a window of approximately 7 s long starting 5 s after the beginning of the seismogram. An example of the sindowes used for correlation can be seen in Figures 1.3 and 1.4. This style of analysis will be referred to as the "Gret style analysis". The decorrelation was attributed to a possible change in the scattering properties of the volcano, leading to this research.

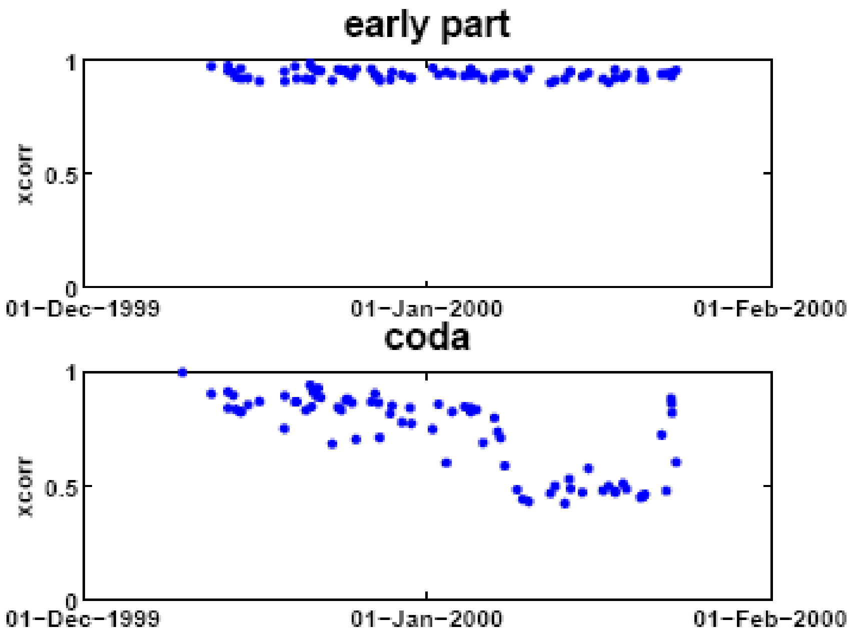

Figure 1.2 – A figure from *Gret et al.* [2005] showing the high correlation of the initial part (top), and the decorrelation of the coda (bottom), around 8 January 2000. These results are from station E1S SP. Note the apparent recovery at the end of the data.

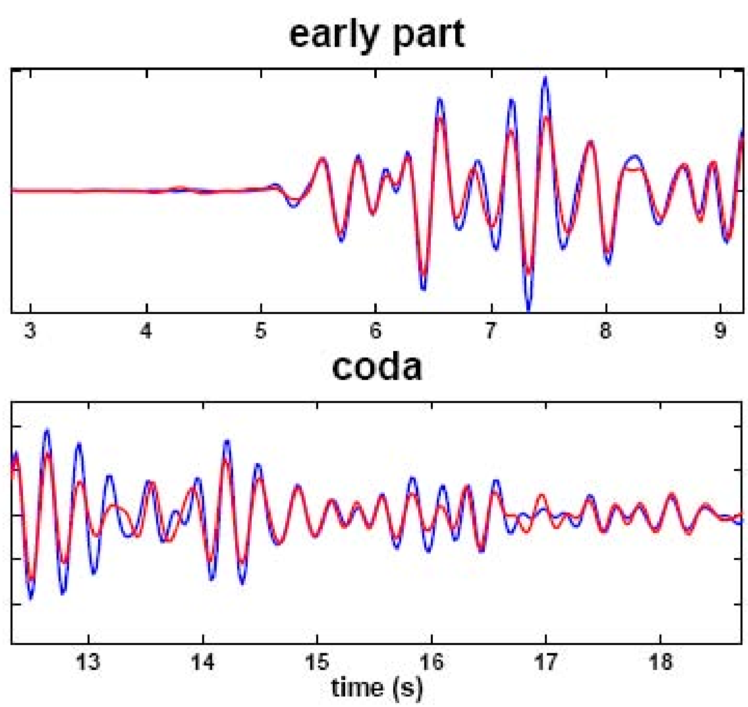

Figure 1.3 – A figure from *Gret et al.* [2005] showing two separate events that are almost identical at station E1S SP. There are only minor differences seen for the early part and the coda.

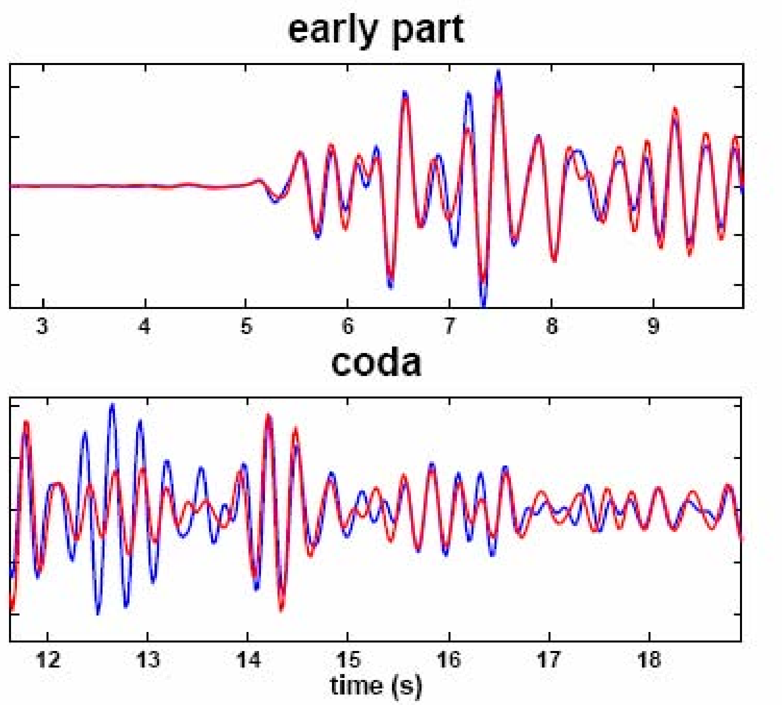

Figure 1.4 – Another figure from *Gret et al.* [2005] showing two events recorded about two weeks apart at E1S SP. The initial parts are once again almost identical. However, this time there are some portions (examples can be seen around 13 and 15 s) of the coda where decorrelation occurs.

CHAPTER 2

Data Used

History of Instrumentation

The first temporary seismometers were deployed on Erebus in 1973, and the first permanent short period digital network was installed during the 1980-81 field season [*Skov*, 1994]. The first generation of Erebus seismometers used were vertical component 1 Hz Mark Products geophones. This network remained unchanged until it was partially removed in January 1987. During this period, the data was radio-telemetered to Scott Base and recorded on an analog magnetic tape recorder. The stations were powered by solar panels and only the seismometer at Scott Base (SBA) was able to collect data year round. During the Antarctic winter all other stations would lose power, although Truncated Cones (CON) and Hooper's Shoulder (HOO) did transmit the entire winter of 1985 due to the addition of large quantities of lead-acid batteries [*Rowe*, 1988].

Mount Erebus Volcano Observatory (MEVO) was created in 1992, providing the means to continuously monitor Mount Erebus and conduct long-term studies. During the 1992-93 field season a new communication system was installed at McMurdo Station. This system allowed the data to be transferred in near real time to the USA. A new, nearly automatic data acquisition and handling system based on PC-hosted IASPEI hardware was also developed at this time, incorporating six permanent Erebus short period stations and a seismometer at McMurdo Station [*Skov*, 1994]. Starting at this time the continuous data was archived at New Mexico Tech. At its peak, the short-period seismic network consisted of nine seismic stations.

The first permanent broadband Erebus seismometer (a 3-component 30-s corner frequency Guralp 40 T) was deployed in January of 2001 at site E1S. Installation of other broadband seismometers occurred during the 2001-2002, 2002-2003, and 2003-2004 field seasons, producing the present six station (E1S, CON, HUT, HOO, RAY, NKB) integrated Surveillance Instrumentation [ISI] network [*Aster et al.*, 2004b]. Each station consists of a 40 T seismometers, GPS receivers, and telemetry hardware. Additional items at various stations include infrasonic microphones, infrared radiometers, tilt meters, gas sensors, weather and instrument monitors, and data acquisition equipment. These instruments were integrated and installed under a Major Research Instrumentation grant from the National Science Foundation (NSF) [*Aster et al.*, 2004b]. In addition to the ISI network, there are also six short period stations (Mark Products L4c) currently [1/07] operating on Mount Erebus (BRD, BOM, SIS, ABB, ICE, and MAC). Infrasound (attached to stations E1S, RAY, and NKB) installed around the crater facilitate the identification of eruptions, and have been especially useful for discriminating between eruptive and non-eruptive events, as well as studying eruptive source processes [*Jones et al.*, 2007]**.** The locations of the current seismometers are shown in Figure 2.1. The seismic data is sampled at forty samples per second, and all information is telemetered via spread spectrum or (in the case of short period stations, FM telemetry) to McMurdo station, where it is assimilated by a Guralp SCREAM and Earthworm data logging system and subsequently transmitted to New Mexico Tech via the Internet. The

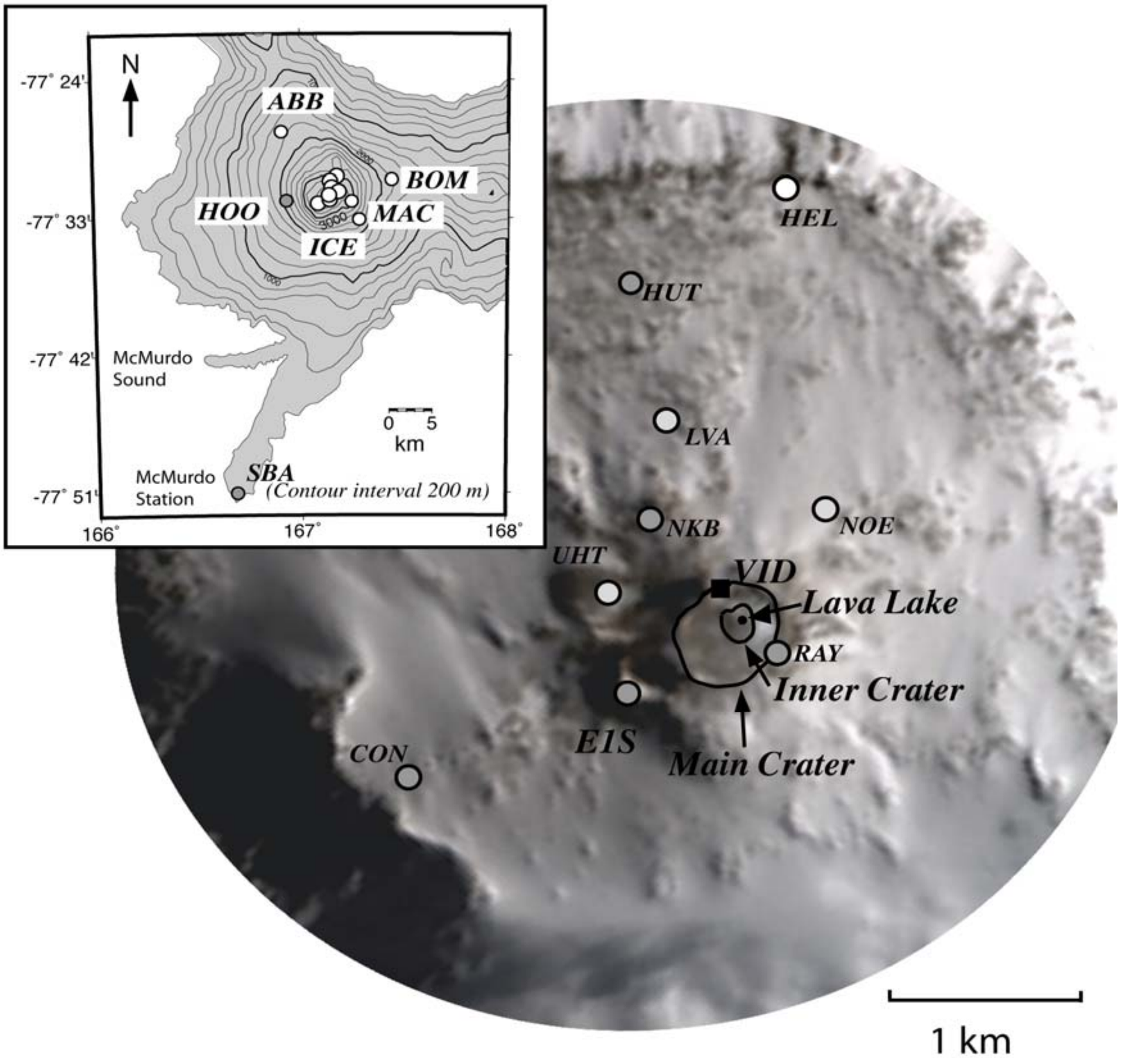

Figure 2.1 – Map of seismometer locations on Mount Erebus. The gray dots are broadband seismometers, the white dots are short period seismometers, and stations UHT, NOE, and LVA were a temporary broadband deployment in Dec 1999-January 2000. SBA, located at Scott Base, is part of the Global Seismic Network (GSN)

broadband stations are powered by solar panels and by wind generators but rarely function all year. This is because of the extreme weather conditions as well as the long dark winters when the sun does not rise. During storms winds can be in excess of 90 knots (more then 104 miles an hour), and temperatures can exceed fifty degrees Celsius below zero. Ice rinds also tend to build up on wind generators, which are used to power the instruments when there is no light. The ice and wind can combine to destroy the wind generators. The equipment is also subjected to extreme cold temperatures during the winter. Station E1S recorded temperatures as low as $-58^{o}C$ during the winter of 2003, and reached $-56^{o}C$ in the winter of 2006, according to ISI telemetry [*P. Kyle, pers. com.*].

Data Format

All lava lake strombolian eruptive events that have been digitally recorded since 1992 were copied from the MEVO archive and put into a data directory for analysis. Each event was stored in a directory that is named by the year-month-day-hour-minute-sec of the approximate eruption time (e.g., 20050206234309). The events were stored as SAC (Seismic Analysis Code) files containing the time series of each station that was functioning at the time of the event. The time series are labeled using the naming convention *station.instrument.ER.sac* (e.g., E1S.BHZ.ER.sac). The left-hand coordinate system components BHZ, BH1, BH2 are standard Federation of Digital Seismographic Network (FDSN) monickers used for the three component broadband stations, with BHZ being the vertical component, and BH1 and BH2 being the horizontal components. At Erebus the BH1 component is deployed radially inward towards the lava lake, and BH2 is tangential to the lava lake. EHZ is the FDSN descriptor used for the short period, single component vertical stations. IS# is used for the infrasonic microphones, where # is the number of the infrasonic microphone, as some stations have had more then one infrasonic microphone.

When talking about the short period data, the stations will be referred to as station name SP (ex E1S SP). The broadband data is referred to as station name BB (ex E1S BB). This is necessary since many short period, temporary deployments, and broadband stations have the same station name. The broadband data from the temporary PASSCAL deployment is differentiated by and E before the station name (ex EE1S BB).

Data used

Various data sets were used in this research. The data sets used consist of the short period data from December 1999 to January 2000, as well data form a temporary PASSCAL deployment during the same period. Broadband data from 2001 until May 2006, containing over 1200 events, was also used in this research. Besides the seismic data, several other datasets were analyzed as well. Data from the infrasound network was examined, as well as digital video that had been recorded between December 2005 and January 2006. All seismic stations and pertinent information [*Ruiz*, 2004]can be found in Table 2.1, and all infrasound detectors and pertinent information can be found in Table 2.2.

Broadband and Short Period Stations			BH* (V = vertical, R=radial, T=tangential): broadband channels EHZ: short period vertical channels			
Station	Channel	Gain ((μm/s)/count)	Azimuth (E of N)	Lat	Long	Elevation (m)
CON	V (BHZ)	8.02E-04		-77.5346432	167.0849	3456
	R (BH1)	7.95E-04	66			
	T (BH2)	7.96E-04	156			
E1S	V (BHZ)	1.09E-03		-77.5304197	167.1397	3712
	R (BH1)	1.10E-03	56			
	T (BH2)	1.10E-03	146			
HOO	V (BHZ)	7.99E-04		-77.5316032	166.9326	2069
	R (BH1)	7.84E-04	85			
	T (BH2)	7.86E-04	175			
LEH	V (BHZ)	7.98E-04		-77.5105992	167.1421	3401
	R (BH1)	7.95E-04	163			
	T (BH2)	8.02E-04	253			
NKB	V (BHZ)	1.10E-03		-77.5219759	167.1475	3627
	R (BH1)	1.10E-03	142			
	T (BH2)	1.10E-03	232			
RAY	V (BHZ)	1.09E-03		-77.528767	167.1706	3769
	R (BH1)	1.10E-03	323			
	T (BH2)	1.10E-03	53			
ABB	EHZ	3.12E-04		-77.4568788	166.9089	1734
BOM	EHZ	1.74E-04		-77.508949	167.4402	1960
BRD	EHZ	6.11E-04		-77.2715	166.7456	1802
CON*	EHZ	1.31E-03		-77.5346432	167.0849	3456
E1S*	EHZ	1.89E-03		-77.5304197	167.1397	3712
HEL	EHZ	6.11E-04		-77.5052519	167.1775	3300
HOO*	EHZ	2.11E-04		-77.5316032	166.9326	2069
MAC	EHZ	7.33E-04		-77.5325291	167.2466	3278
EE1S**	BHZ	1.09E-03		-77.5304197	167.1397	3712

*Replaced by a broadband instrument

**Temporary PASSCAL deployment

Table 2.1 – Seismic stations used in this research (Figure 2.1). Broadband, high dynamic range channels are denoted by BH*, and short period channels vertical channels are denoted by EH*. Latitude, Longitude, elevation, and gain have been included for all stations, and azimuth for the horizontal broadband channels. Gain denotes passband conversion constants from counts to ground velocity.

Station and Channel	Gain ((μPa/s)/count)	Lat (dd)	Long (dd)	Elevation (m)
E1S IS1	4.63E+01	-77.5304548	167.1398375	3712.777
E1S IS2	4.64E+01	-77.53033884	167.1509026	3769.527
E1S IS3	1.74E-04	-77.53045576	167.1398474	3658.712
NKB IS1	4.64E+01	-77.5219889	167.1474033	3627.006
NKB IS2	1.74E-04	-77.52607269	167.1558531	3774.119
RAY IS1	1.74E-04	-77.52855894	167.1708299	3766.506
RAY IS2	1.74E-04	-77.52857064	167.1708488	3765.739

Table 2.2 – List of all infrasound channels along with their locations and gains. Gain denotes passband conversion constants from counts to overpressure.

For the broadband data, only the vertical channel has been used for analysis so far. This is partially because the initial study performed by *Gret et al.* [2005] had been done using short period instruments, which only have a vertical component. Using the vertical component made it easier to compare results. Another reason was that there was a period of time (August – December, 2004) when only the vertical channel for E1S BB was being receive, creating and undesirable data gap. A quick at the horizontal channels did not show anything unexpected, but time constraints prevented further analysis. However, for future research it would be a good idea to include the horizontal stations as well.

Preparing the data for analysis

Broadband seismic data collected in 2002 was sampled at one hundred samples per second. Before these events were added to the archive, they were resampled to forty samples per second using the "resample" command in MATLAB, which performs the necessary filtering and decimation. Appropriate variables in the SAC header were adjusted to the new sampling rate and saved. The resampling was necessary because many of the analysis techniques rely on directly comparing like-sampled time series data.

After the events were added to the archive, they were converted into SAC format and the beginning of each event was picked and saved to the SAC header. The initial picks were not accurate enough for analysis to be performed on the data, so a conjugate gradient least squares (CGLS) algorithm [*Aster et al.*, 2004a] was used to solve for the adjustments needed to better align the events [*Aster and Rowe*, 2000]. In order to prepare the files for the alignment, all of the SAC files were loaded into a uniform length (1600 samples) array within MATLAB. Each seismogram was then detrended and filtered with a 2 pole bandpass filter between 2 and 5 Hz using the "filtfilt" and "butter" commands in MATLAB. Each whole-record seismogram was then cross-correlated with every other event, and the resulting time lags were then put into a system of linear equations. The CGLS algorithm was then applied to solve for the best L-2 norm residual adjustments to the picks [*Rowe et al.*, 2002]. The maximum correlation coefficients were used to weight the system of linear equations used in the CGLS routine in order to try and reduce the effects of outliers (low correlation). An adjusted pick was calculated and saved to the SAC header of each event. The alignment using the original pick can be seen in Figure 2.2a. The improvement of the event alignment using the adjusted pick can be seen in Figure 2.2b. This process worked well for 1-month segments of data. However, adjusting one month segments lined up the events for that month, but subsequent months did not line up with each other. The improvement gained when applying this method to the full broadband dataset was not good enough for my needs.

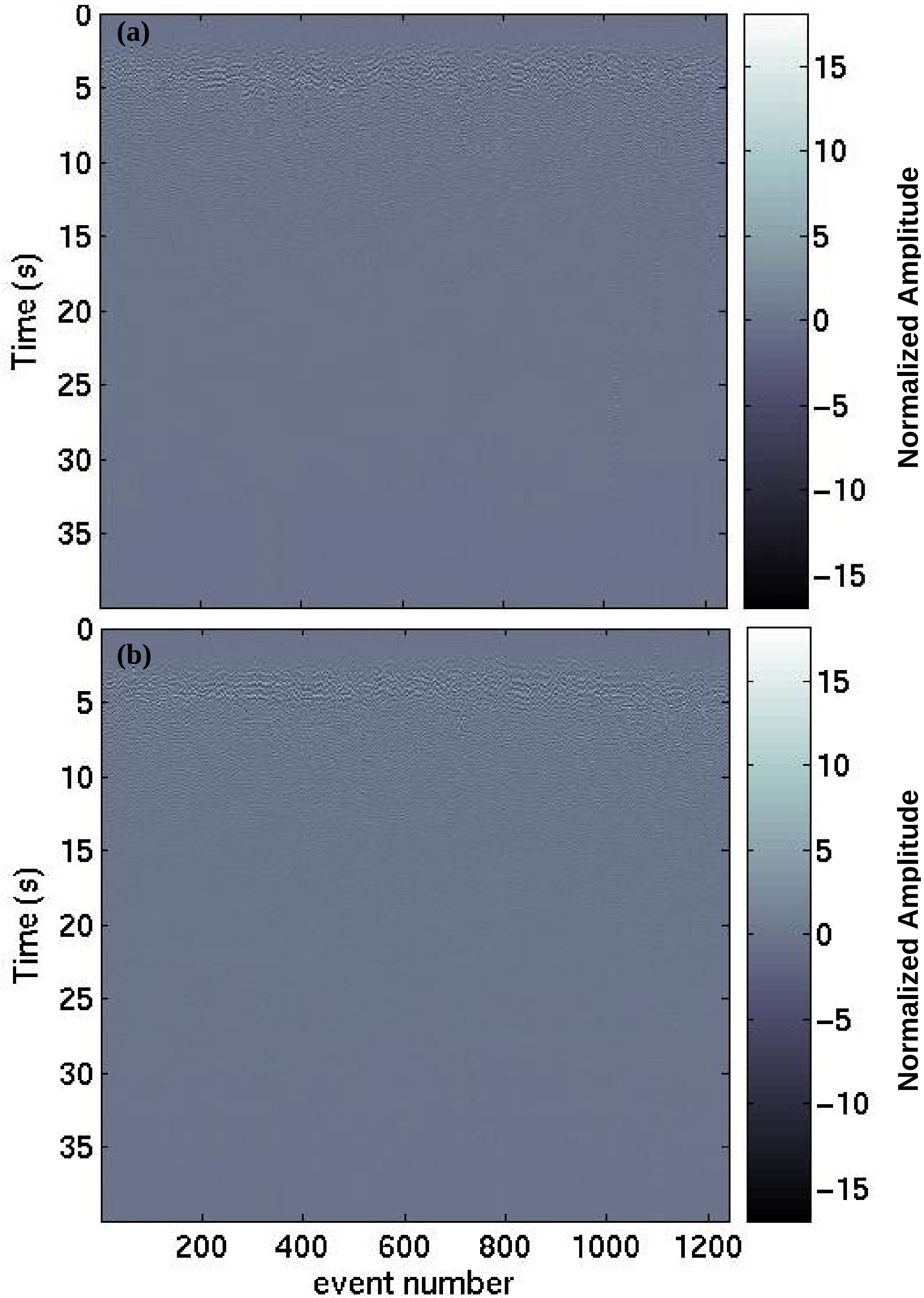

Figure 2.2 – MATLAB *imagesc* plot of all of the Strombolian eruptions, normalized by their RMS value, recorded at E1S BB. (a) All events lined up on the rough pick. As can be seen, the rough alignment is very poor. (b) All events lined on up on their adjusted pick. Although the alignment has improved, there is still enough scatter that when they are stacked together they will have some destructive interference. This alignment is not good enough for analysis that will be performed later. These events have been filtered between 2-5 Hz.

In order to improve the alignment of the events even more, an iterative alignment program was implemented. First, in order to save loading time, a matrix containing all of the desired events was created for each station. This matrix contained vectors of the raw unfiltered data for each seismogram, 1600 samples in length, starting 2 s before the beginning of the event (using the adjusted pick). It was necessary to use the adjusted pick talked about in the previous paragraph because the original event-by-event picks typically were not good enough to seed the alignment process.

Once the data was prepared, it was loaded into the iterative alignment program and filtered for the desired frequency band using a 2-pole Butterworth filter. Each event was then normalized by its RMS value. Once the data was loaded, all of the data was stacked, and each event was cross-correlated with that event stack. The indexes of the events above a specified cross correlation threshold (0.5 was used here) were stored in an array, and these events combined to form the new event stack. This agglomerative process was repeated until the alignments stabilized. Once the process had stabilized, the aligned events were saved along with all of the pertinent variables (maximum size (vertical channel after detrending and filtering), RMS size, index of events used in the final stack, the original data, etc)

The procedure described above produced a remarkable improvement in the alignment of the events (Figure 2.3a) compared to the events lined up on the adjusted pick (Figure 2.2b). An even clearer improvement was seen by plotting only the events used in the final event (cross correlation with the stack of greater than 0.5) stack of the alignment code (Figure 2.3b). I also examined the alignment improvement by looking at

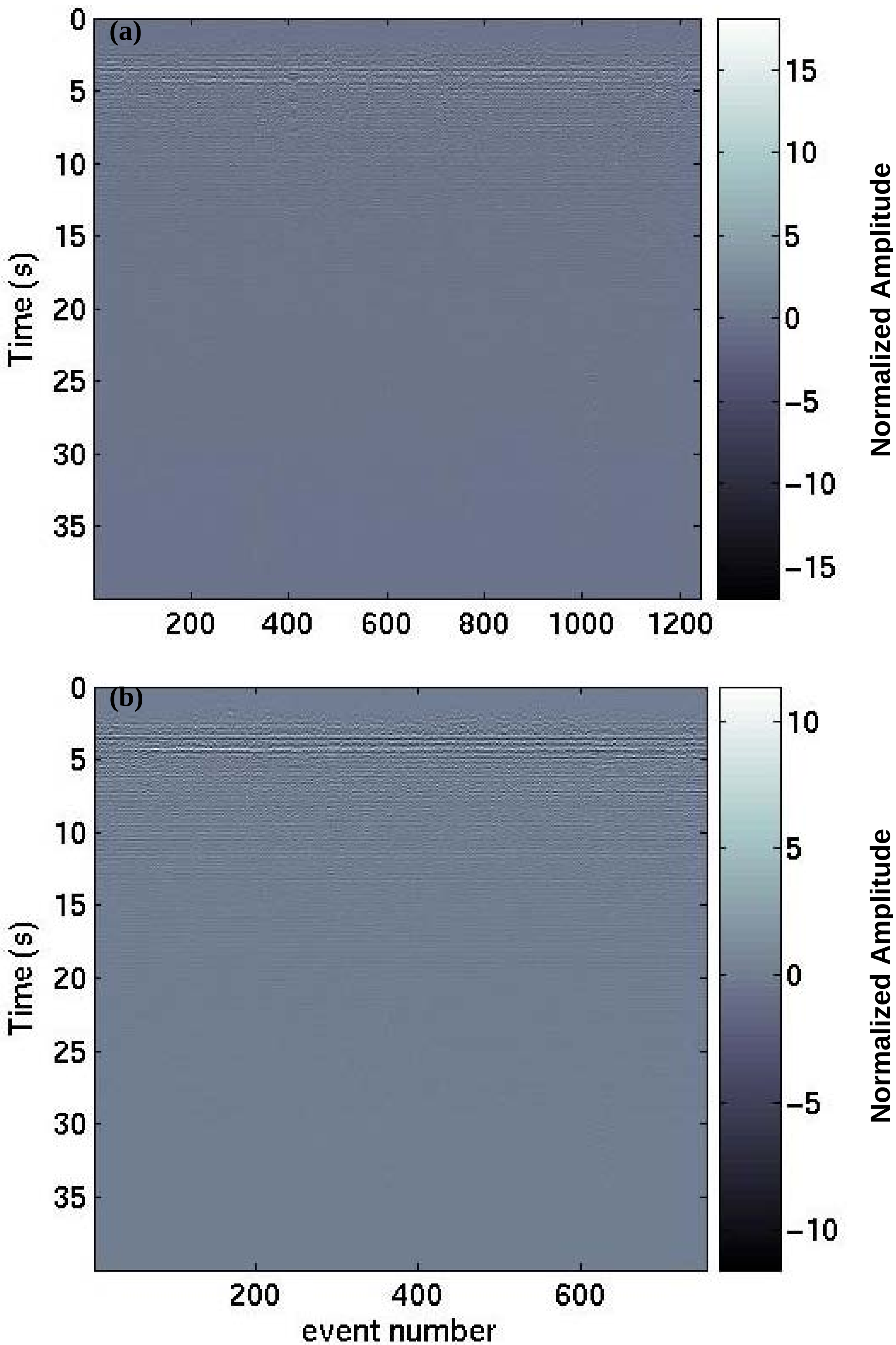

Figure 2.3 – (a) Alignment plot for station E1S BB after implementation of the iterative alignment program. Note the large improvement seen in alignment when compared with Figure 2.1b. (b) Plot of the events with cross correlation coefficients to the stack above 0.5. These are the events that were used for analysis. The improvement in alignment is even more obvious using this subset of events.

a stack of all of the events plotted with one standard deviation, calculated sample-by-sample moving through the seismograms. In Figure 2.4 the pre-alignment stack can be seen. Figure 2.5 shows the incredible improvement gained after running the alignment code. The original event-by-event picks typically were not good enough to seed the alignment process, and intermediate refined picks established using cross correlation were used.

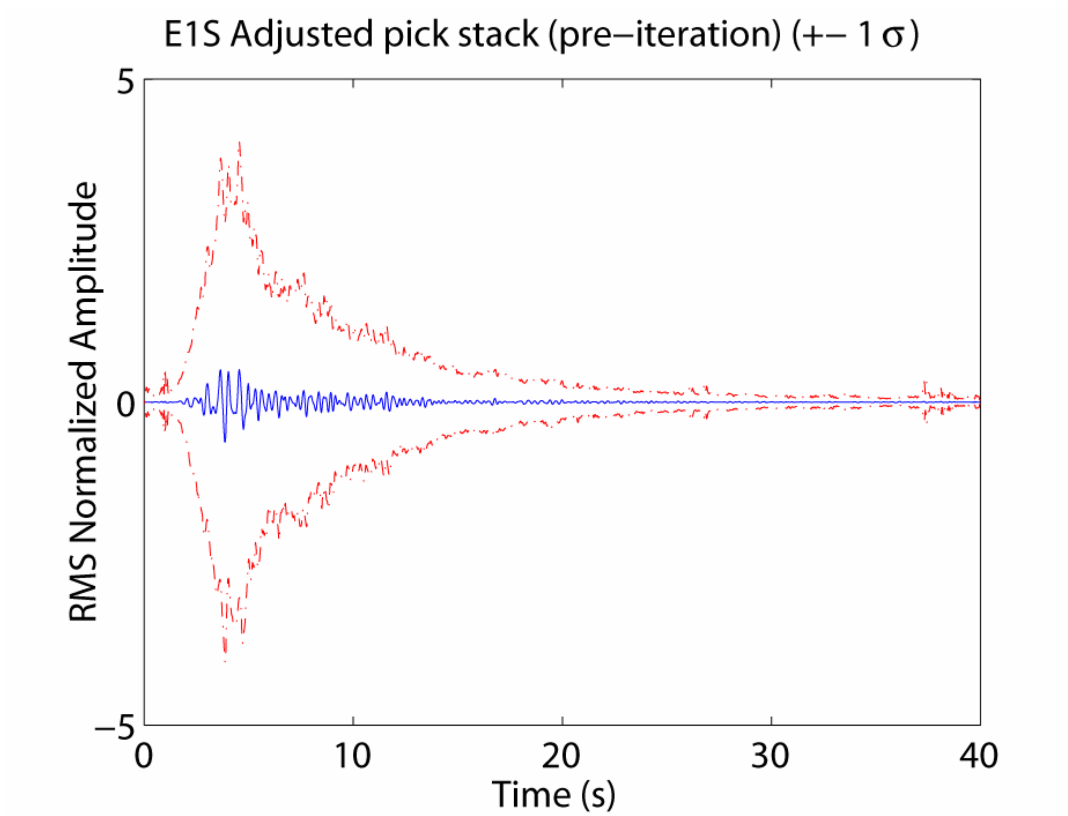

Figure 2.4 – Stack of all of the events aligned on the adjusted pick (Figure 2.2). The red lines are +- one standard deviation. While the adjusted pick is an improvement over the rough pick, it can be seen that the alignment is still not good enough to give us a representative stack.

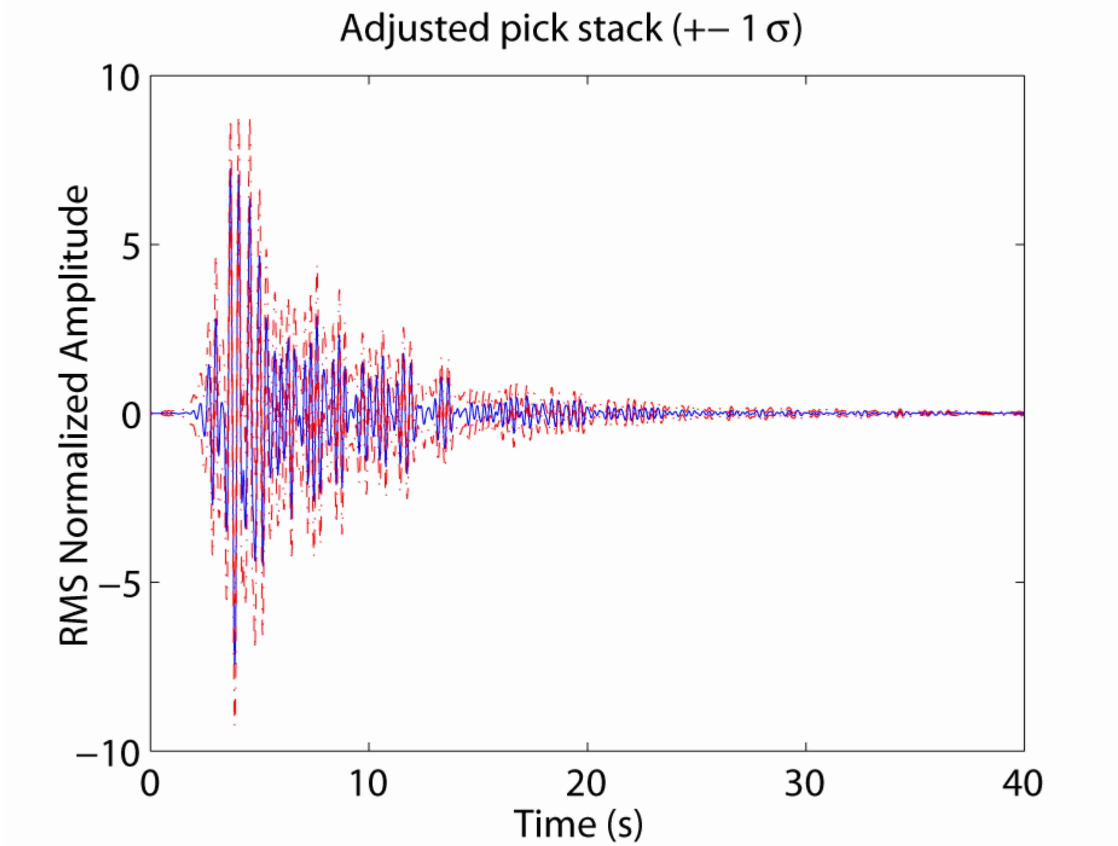

Figure 2.5 – Plot of the final event stack for the events with a correlation coefficient of 0.5 or better (Figure 2.3). The stack now is a reasonably good representation of the repeatable elements of the constituent individual eruptions, as can be seen by the improvement in the standard deviation envelope (red).

CHAPTER 3

Reproducing and Reanalyzing the Results of Gret et al. (2005)

Methods

The first step in analyzing the seismic similarities between Strombolian eruptions was to reproduce the results obtained by *Gret et al.* [2005]. Reproducing those results was not as simple as it first appeared due to the lack of some important information. Unfortunately, I was unable to establish full contact with Gret to get this information (he had moved to Europe and was difficult to correspond productively with). The windows used to correlate the initial parts and the codas were not well specified, nor was the filtering used. However, I was able to estimate these parameters from the figures in the paper where it was clear that the data had been tightly filtered around 4-5 Hz.

In my work, various filtering ranges were examined to see how they affected the correlation of events with each other. This was accomplished by taking a month's worth of eruptions and filtering them over a range of bands and intervals. This was implemented for various months and stations to make sure that there were no significant instrumentation changes over time. First a spectrogram of an event, high-pass filtered at 1 Hz, was created to see where the majority of the energy was in the signal. Because much of the energy was between 2 and 5 Hz (Figure 3.1), though some smaller events seem to have most of their energy between 3 and 6 Hz (Figure 3.2), most of the

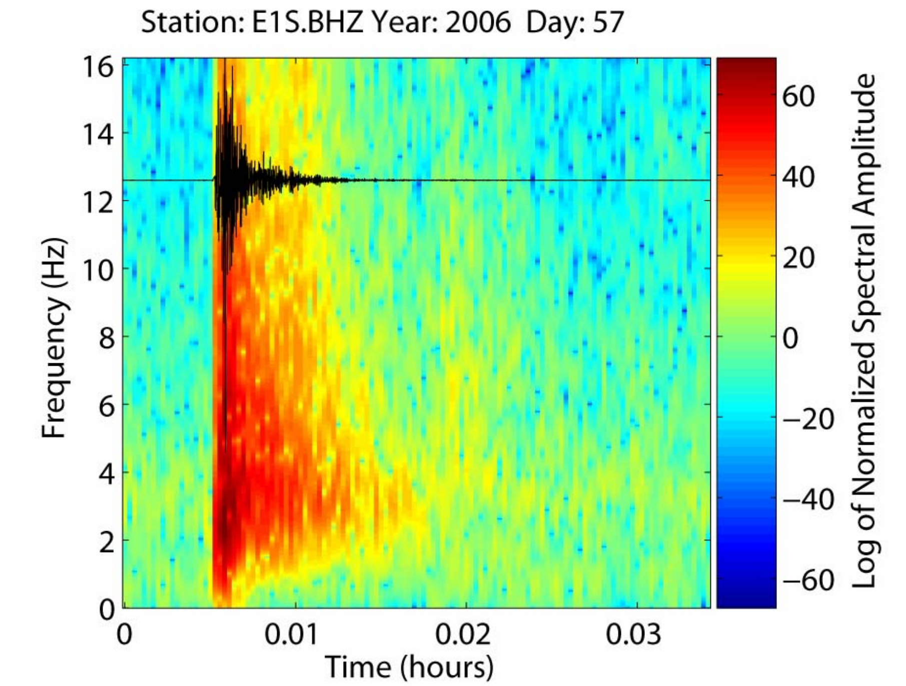

Figure 3.1 – Spectrogram of a typical Strombolian eruption. This eruption was recorded at E1S BB on 26 February 2006, at 01:16 UTC. The majority of the energy for this event is between 2 and 5 Hz. This time series was high-pass filtered at 1 Hz. The overlay is the seismogram of the event, also high pass filtered above 1 Hz.

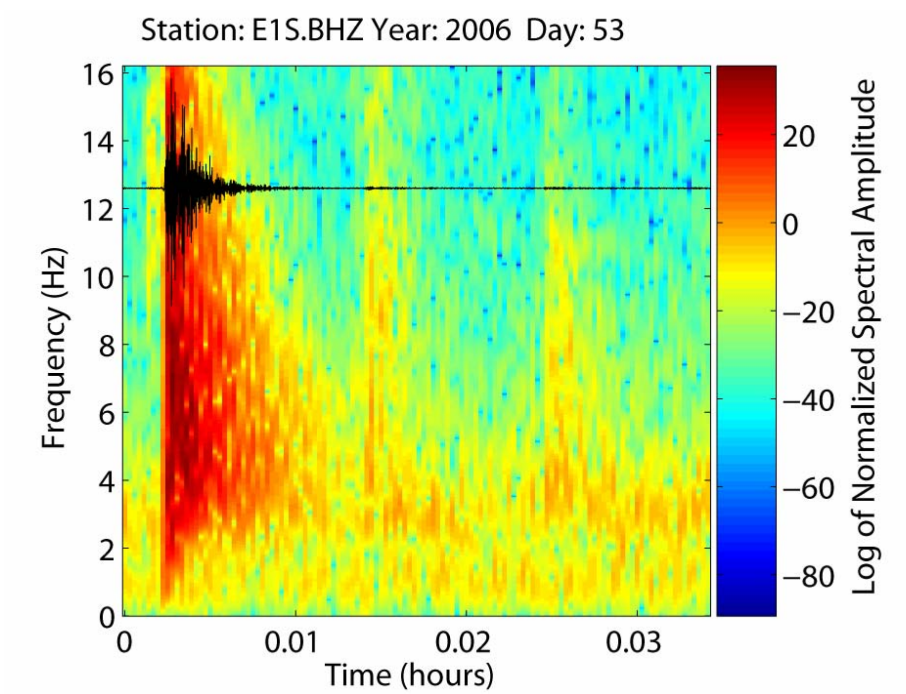

Figure 3.2 – Spectrogram of a small Strombolian eruption on 22 February 2006, at 16:42 UTC, recorded at E1S BB. The majority of the energy in a slightly higher frequency range then the event from Figure 3.1, which was a larger event. The overlay is the seismogram of the event high pass filtered above 1 Hz.

frequency bands and intervals tried were around this range. Figure 3.3 shows the unfiltered broadband seismogram of the same strombolian eruption used in Figure 3.1. Different frequency ranges and bands were observed to see which provided the best correlations (Figures 3.4-6). The frequency band of 2 to 5 Hz was chosen since it encompassed the most energy, and was not so narrow that the filtering produced excessive false similarity due to ringing.

The windows used for the correlation comparison were also estimated from *Gret et al.* [2005]. From Figures 1.3 and 1.4, it appears that a window of approximately 7 s was used, starting at three seconds before the signal onset. For the coda I estimated a 7 s window had been used starting at 12 s (Figure 1.4). Unfortunately there is no guarantee that the windows used in the figures are exactly the same windows used in the actual analysis. The exact dates used in the *Gret et al.* [2005] study are also somewhat uncertain. Most importantly, the event used as a master event to compare with all other eruptions is not specified. Finally there are some discrepancies in the dates specifically mentioned in the paper, and the actual dates of the eruptions and some of the dates mentioned occur on days were there were no eruptions in the archive. This is probably attributable to a misreading of the data file headers by Gret et al.

In investigating the results of *Gret et al.* [2005], I used events that occurred between the 1st of December 1999 and the 31st of January 2000, which is referred to here as the “Gret period”. I also decided on a two-pole bandpass filter between 2 and 5 Hz based on the analysis above. Other frequency bands were tried as well, but a narrower band of filtering did not seem to produce noticeably more illuminating results. For the comparison of the initial part, a window of 7 s duration starting 2 s before the beginning

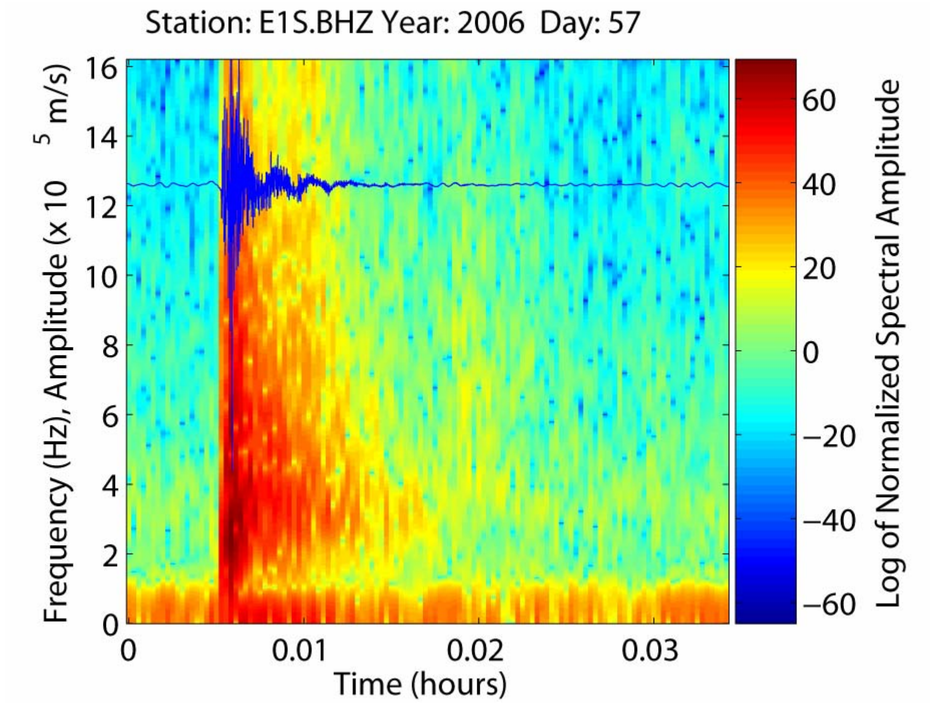

Figure 3.3 – Spectrogram of the same event used in Figure 3.1, except this time unfiltered. The overlay is the seismogram of the unfiltered event.

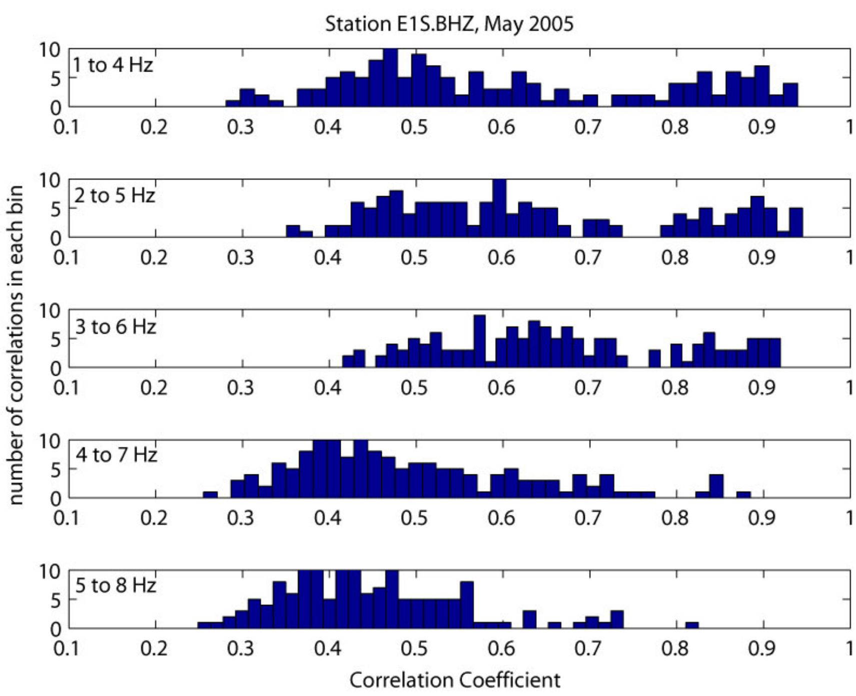

Figure 3.4 – A plot of the maximum correlations for one month of data encompassing a band of 4 Hz for station E1S BB. Each plot band starts one Hz higher then the previous band. The 2 to 5 Hz band has the highest median correlation, however the 3 to 6 band correlates the events with low correlation coefficients better. The analysis for this figure was done for May 2005.

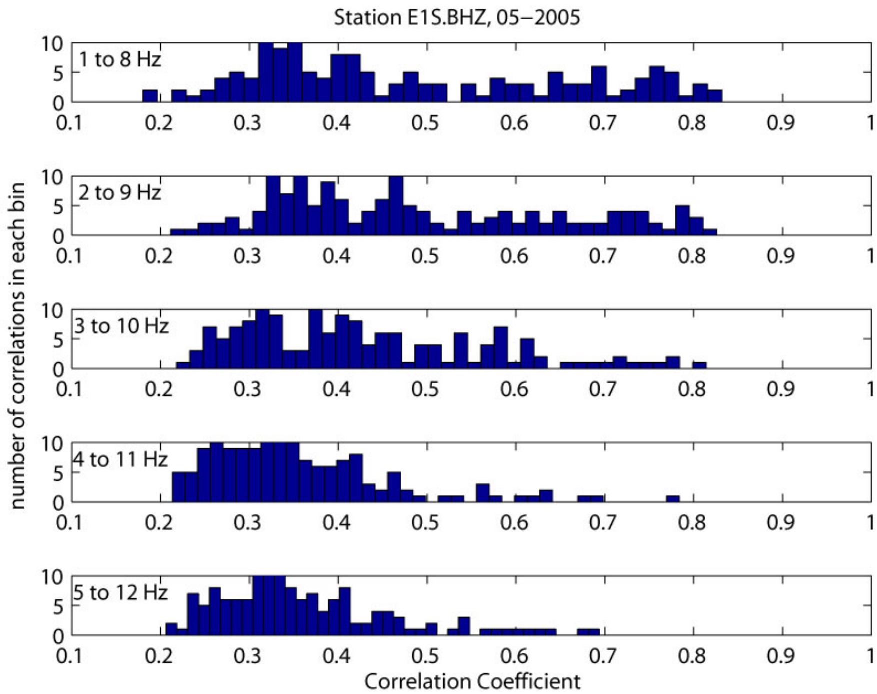

Figure 3.5 – A figure of the 1 to 8 Hz band, incremented by 1 Hz each time, for E1S BB. The 1 to 8 Hz band has the highest median correlation, but once again the next band up (2 to 9 Hz) correlates the outliers slightly better.

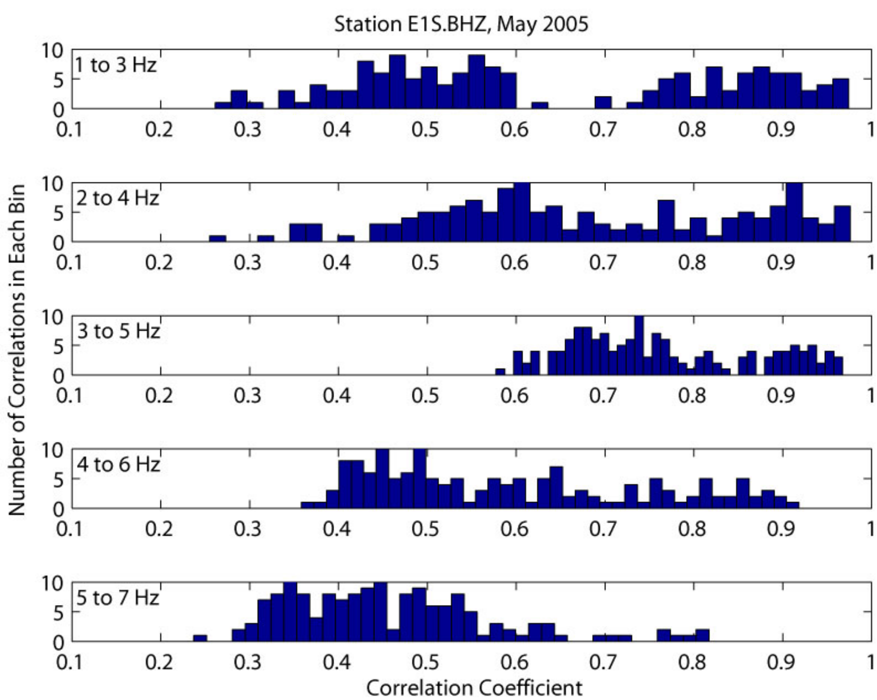

Figure 3.6 – Results from very narrow filtering of E1S BB, between 1-3 Hz. The maximum correlations improve greatly, but filtering the time series with such a narrow band causes the signal to become highly oscillatory, and greatly increases the likelihood of cycle skips.

of the event was used, and a window of 7 s duration starting at 9 s was used for the coda. Different master events were tried to find which one gave a result that most closely mimicked the trend obtained by *Gret et al.* [2005] (Figure 1.2). The strombolian eruption from the 9 December 1999 was the master event used in the final analysis. The data from station E1S SP was analyzed first, and then other short period stations from the Gret period were examined later (ABB, CON, HEL, HOO)

A Gret style analysis was also performed on the full broadband, and high-dynamic range, data set provided by the broadband seismometers install at E1S and other sites starting in 2001. These data do not suffer from any artificial similarity caused by clipping during larger Strombolian eruptions. This analysis was performed between January 2001 and May 10th 2006. During this time there were several periods during which all instruments were down, or there were no identified eruptions (Figure 1.1). The period from September 2002 to December 2004 was one during which no eruptions were identified while the instruments were up [*Jones et al.*, 2007]. Some shorter winter gaps are due to lack of working instruments due to winter power failure. January 2005 marked a return to strong strombolian activity. This was marked by several eruptions every day, as well as the largest eruptions since the 1984 activity (Figure 3.7), with bombs frequently being thrown outside the crater. In fact, on January 1st, 2006 a bomb landed within a meter or two of the digital video cameras on the rim (Figure 3.8). The increase in smaller eruptions in Figure 3.7 may be influenced by the implementation of an automatic triggering system, coupled with the use of infrasonic microphones (K. Jones, pers. com.).

Broadband data from a temporary IRIS PASSCAL deployment was collected in 1999-2000. The PASSCAL instruments were co-located with the stations E1S SP

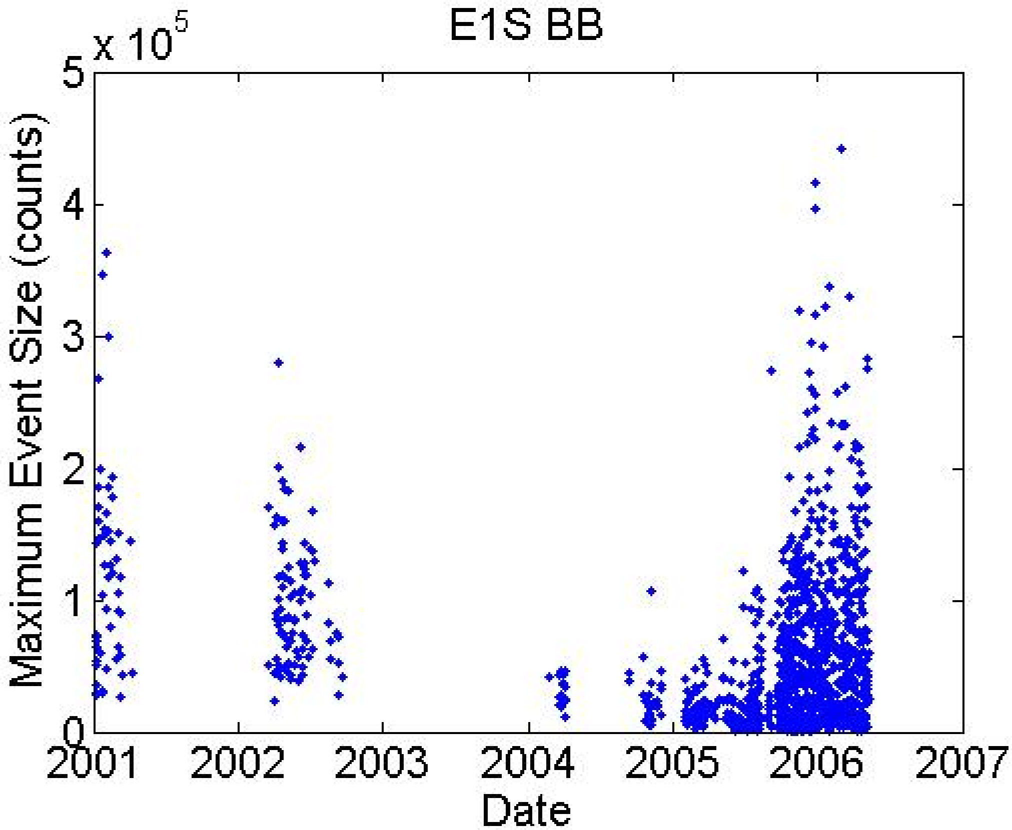

Figure 3.7 – A plot of maximum event size (x-axis) verses time in years (y-axis) for the full broadband data set of station E1S BB. The maximum size is measured from the vertical channel after de-trending and filtering the data. The gaps in data are mostly due to periods of time where the network was down during the Antarctic winter. However, the lack of eruptions during 2003 was due to the fact that no eruptions were identified during this period.

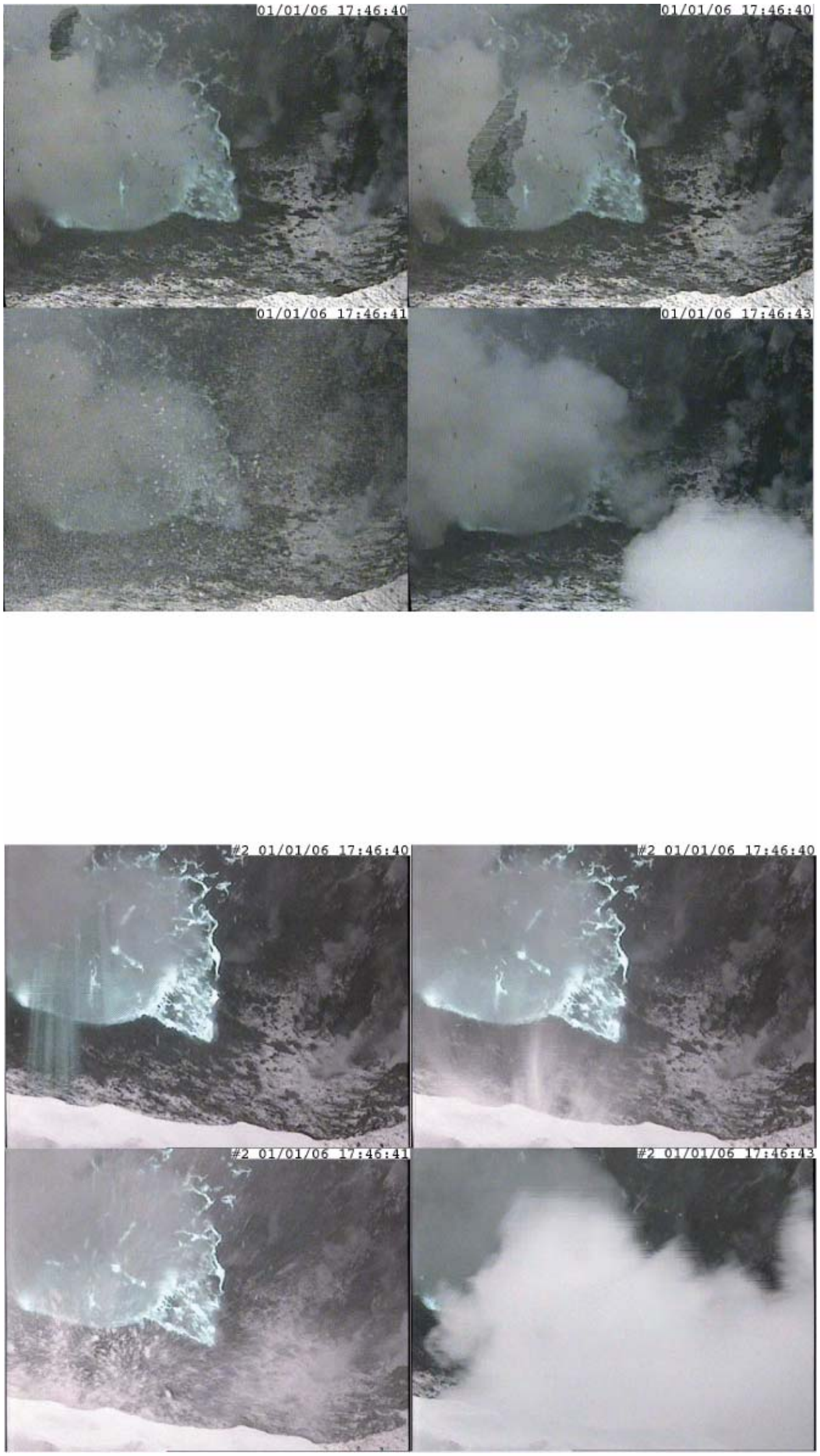

Figure 3.8 – Screenshots of a lava bomb that landed two meters in front of the cameras on the crater rim on January 1, 2006. The top and bottom groups of pictures are from two different cameras that were set up right next to each other.

(referred to here as EE1S), NKB SP, CON SP, as well as at the sites HEL, LVA, HUT, UHT, NOE (Figure 2.1). This dataset contained data collected from 10 December 1999 through 23 January 2000. The same analysis techniques used on the short period data were applied to this data set.

Results

I was never able to produce as clean of results, in the sense of the clear decorrelation trend, as those obtained by *Gret et al.* [2005]. However, I was able to get similar results. For example, using a band of 2 to 5 Hz and a master event from the 10th of December 1999, I was able to get a decorrelation of the coda (Figure 3.9), but it was not as clear as results posted by the authors (Figure 1.2). The initial part correlation was also similar to the authors results, but there is, again, more scatter in my results (Figure 3.10). Using the stack as the master event produced a higher correlation for both the initial part (Figure 3.11) and the coda (Figure 3.12). The higher overall correlation was offset by the fact that the decorrelation of the coda was not as pronounced. The choice of master event generally had a large effect on how the plot of correlations appeared. Also, some choices for the master event produced a decorrelation of the initial part as well (Figure 3.13). Interestingly when I did the same analysis with the 1 to 8 Hz band, the coda results more closely resembled those of the Gret et al. (Figure 3.14), however the overall correlation was lower. Similar decorrelations were seen at the other short period stations as well (Figures 3.15-18).

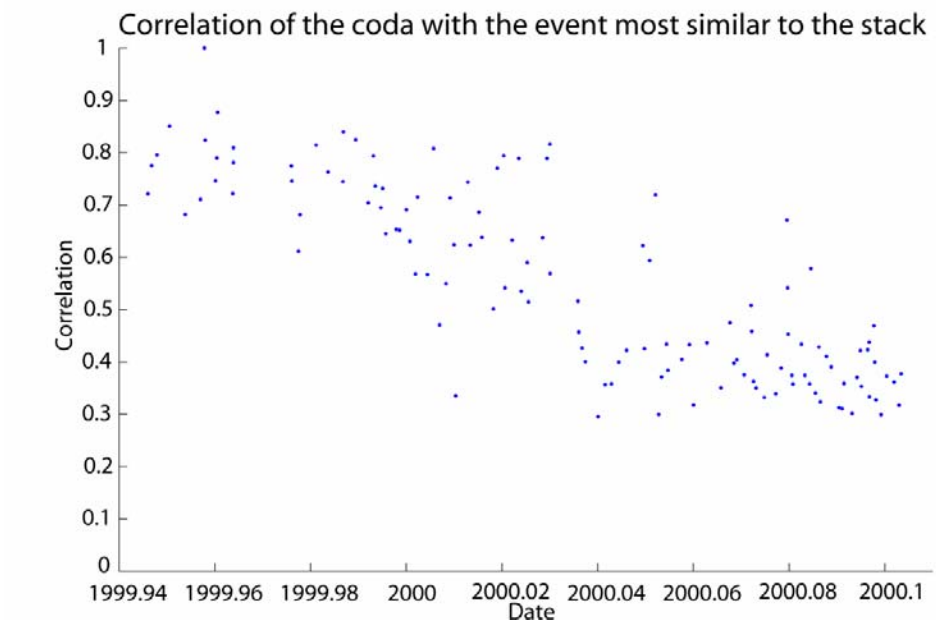

Figure 3.9 – Coda correlations with respect to a master event, for the station E1S SP, during the Gret period. The master (which occurred on December 9, 1999) was chosen because it was the most similar in crosscorrelation to the stack. The data was filtered from 2-5 Hz with a 2-pole Butterworth filter. A fairly abrupt decorrelation of the coda can be seen around 2000.03 (January 8, 2000), which can be compared with the results obtained by *Gret et al*. [2005] (Figure 1.2). Note that unlike the Gret results, there is no apparent recovery.

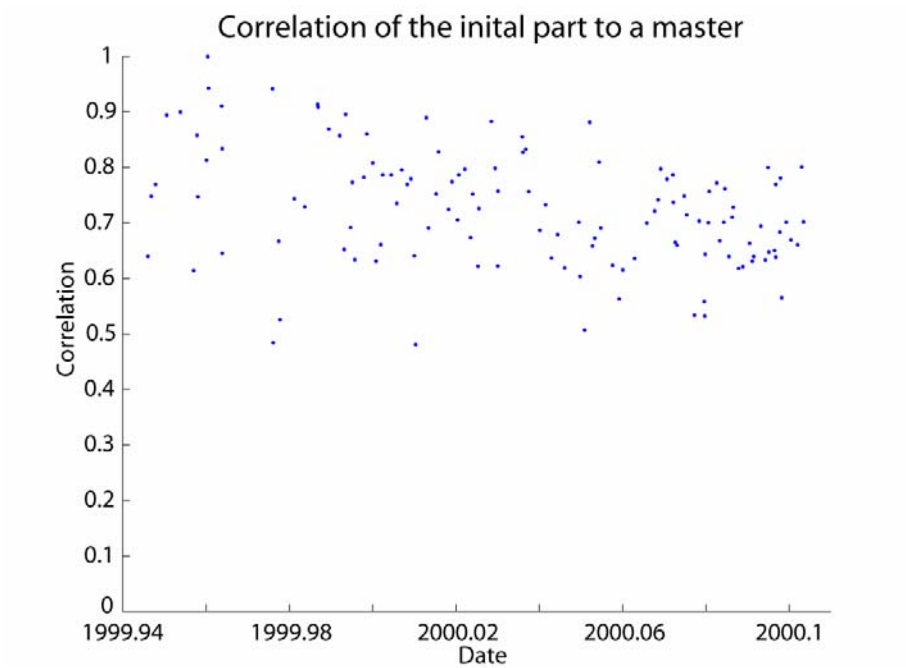

Figure 3.10 – The correlation of the initial part, for station E1S SP, with respect to a master event on December 10, 1999. The data was filtered from 2 - 5 Hz using a 2-pole Butterworth filter. While the correlations are not as high as those obtained by *Gret et al.* [2005] (Figure 1.2), they still show the same lack of an obvious decorrelation.

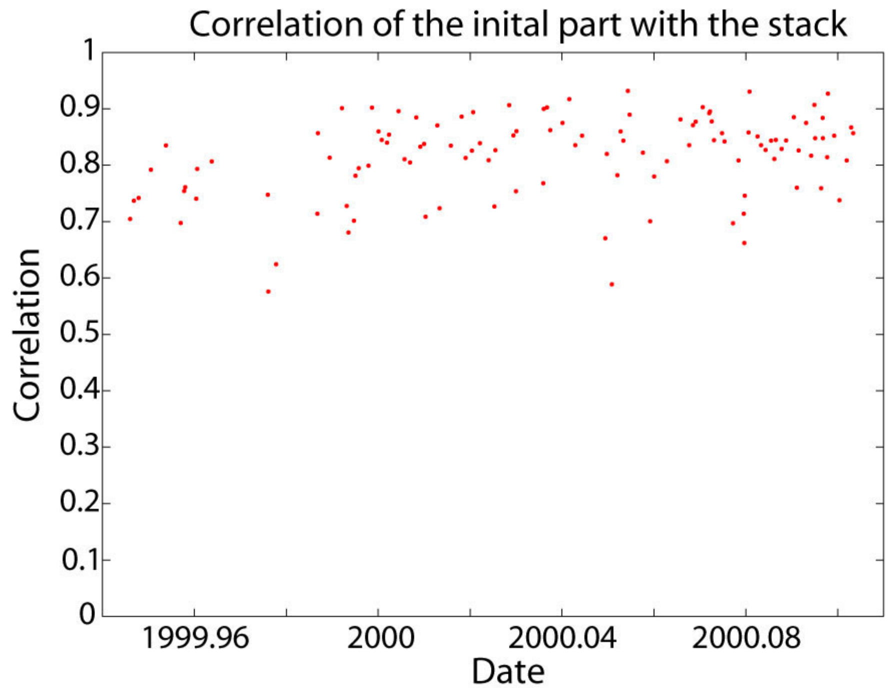

Figure 3.11 – Correlation of the initial part to the stack for station E1S SP. Finding the correlations with respect to the stack produces higher correlations then using a master event, however they are still not as tight as those acquired by *Gret et al.* [2005] (Figure 1.2).

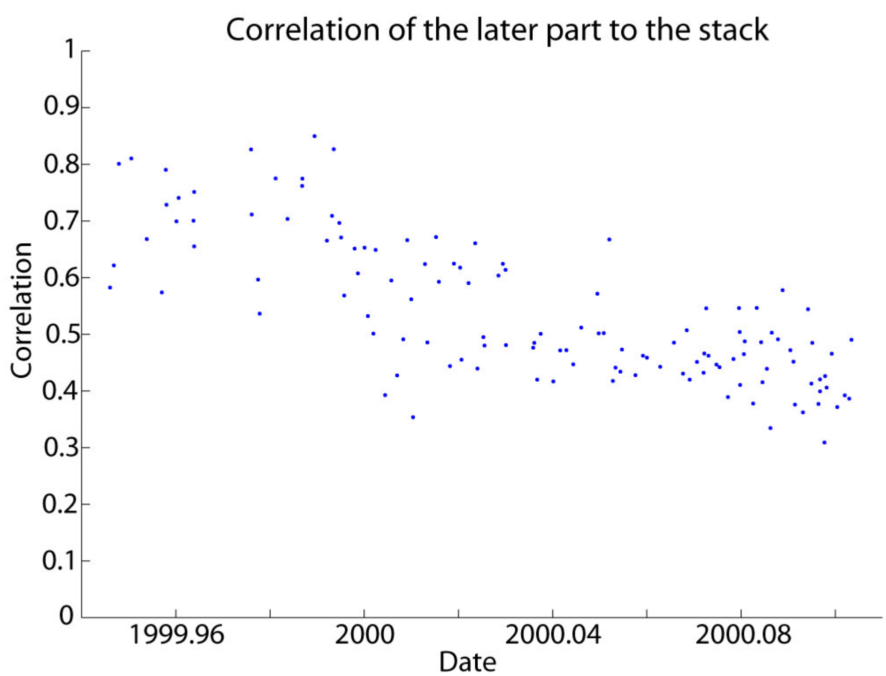

Figure 3.12 – Correlation of the coda to the stack for station E1S SP. The decorrelation around January 8th is still visible, but it is not as extreme compared to using a master event. The correlation of the decorrelated part is also higher then in the Gret results.

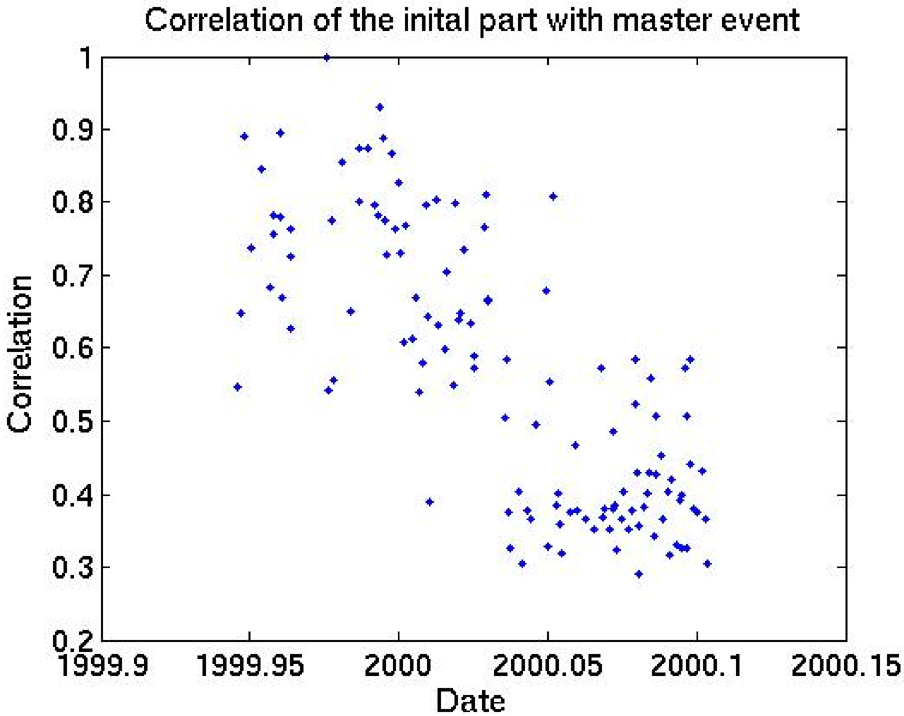

Figure 3.13 – Using an event from 16 December 2000 as a master event produced a large decorrelation for the initial part. While most choices of a master did not show the extreme decorrelations for the initial part as this one did, slight decorrelations of the initial part were not uncommon.

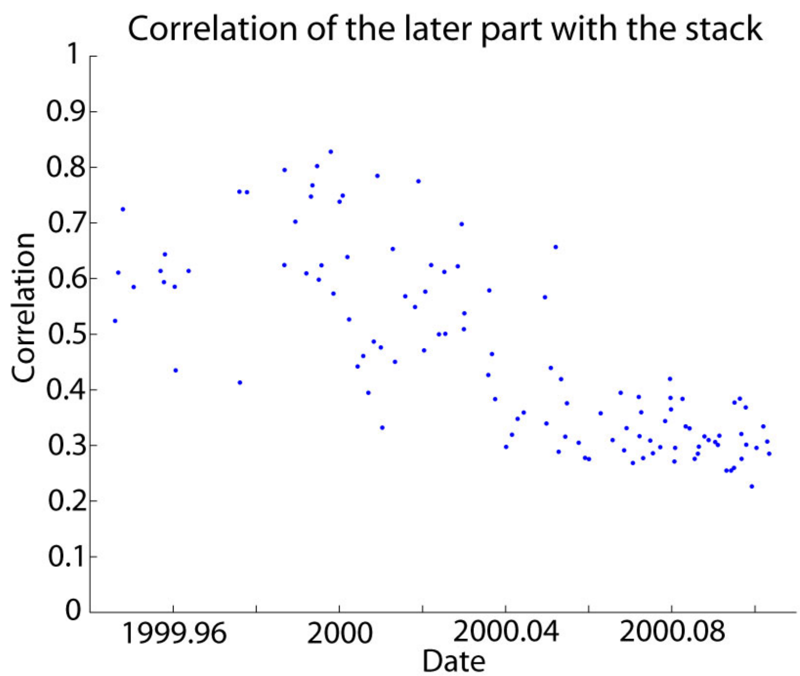

Figure 3.14 – Correlations for the coda filtered from 1 to 8 Hz for station E1S SP, using the stack as a master. While the overall form of the decorrelation in this figure more closely resembles the results in Figure 1.2, the overall correlation is significantly lower.

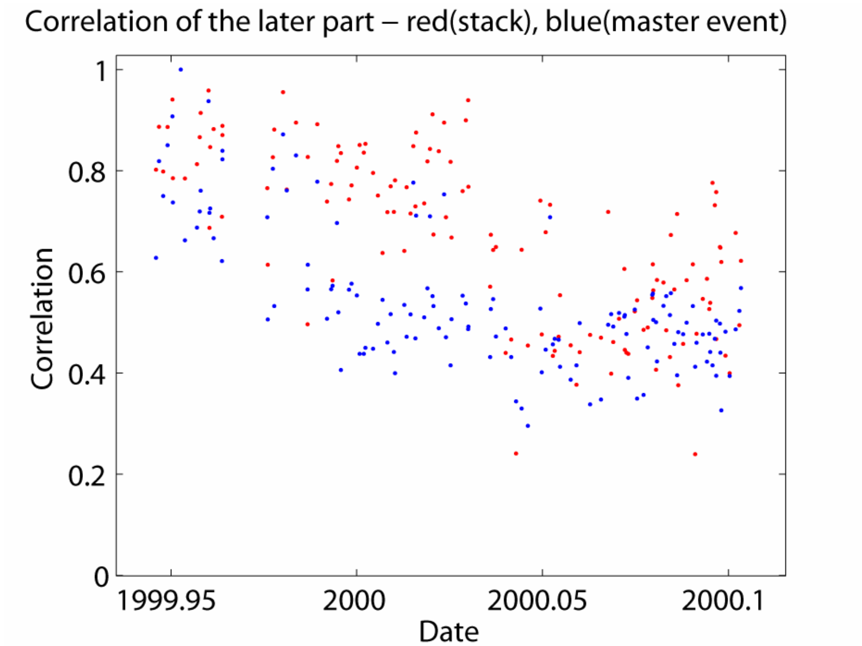

Figure 3.15 – Correlations from the Gret analysis, using the same parameters as before, of the coda for station ABB SP. While the decorrelation of the coda is not as distinct as the one seen at station E1S SP, it is still visible. December 9, 1999 was used as the master event in this case. The red dots indicate correlations with respect to the stack, while the blue dots represent the correlation with respect to the master event.

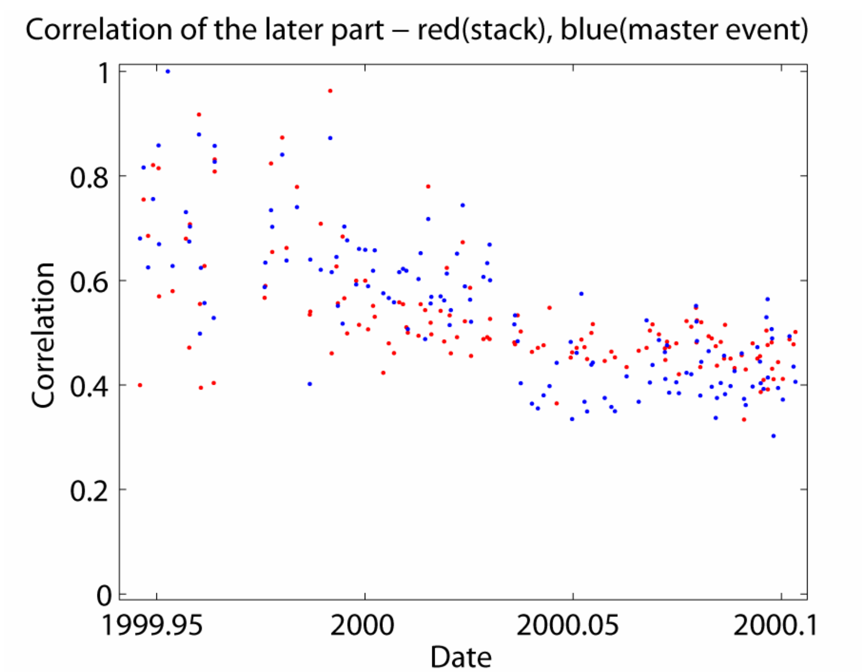

Figure 3.16 – Correlations from the Gret analysis, using the same parameters as before, of the coda for station CON SP. While the decorrelation of the coda is not as distinct as the decorrelation seen at E1S SP, it is still visible. The event of December 9, 1999 was used as the master event. The red dots indicate correlations with respect to the stack, while the blue dots represent the correlation with respect to the master event.

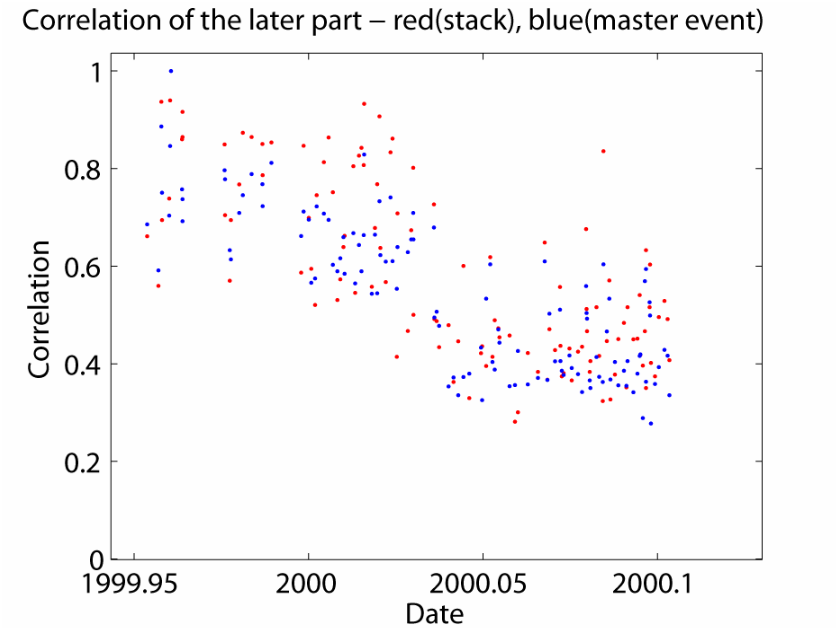

Figure 3.17 – Correlations from the Gret analysis, using the same parameters as before, of the coda for station HEL SP. While the decorrelation of the coda is not as distinct as the decorrelation seen at E1S SP, it is still quite abrupt at this station. The event of December 9, 1999 was used as the master event. The red dots indicate correlations with respect to the stack, while the blue dots represent the correlation with respect to the master event.

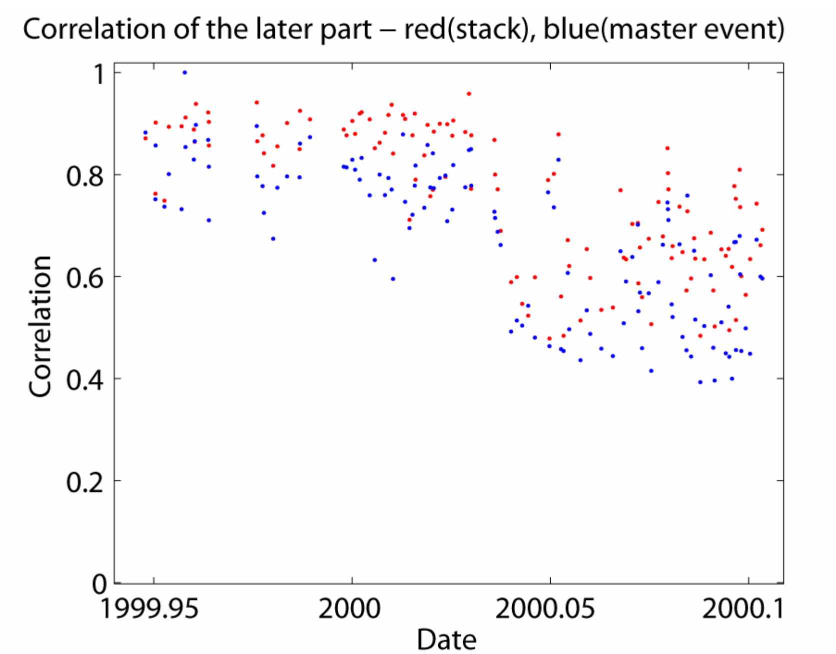

Figure 3.18 – Correlations from the Gret analysis, using the same parameters as before, of the coda for station HOO SP. While the decorrelation of the coda is not as distinct, it is still visible. December 9, 1999 was used as the master event in this case. The red dots indicate correlations with respect to the stack, while the blue dots represent the correlation with respect to the master event.

After trying, with some success, to reproduce the *Gret et al.* [2005] results, there were some indications that changes in the medium may not be the only cause of decorrelation, one clue being the sensitivity of the results on the choice of master event. Some of the other causes looked at were the effects of event size on the correlation (a source effect), as well as the effects of clipping during the Gret period (an instrumental artifact). When I looked at a plot of event size vs. time for the Gret period, there was a plateau where the event sizes no longer increased with time (Figures 3.19 and 3.20). The plots were done with both maximum size or RMS amplitude values versus time. The plateau values begin around January 8th, the same time as the fairly abrupt decorrelation of the coda. Most significantly, when looking at the raw data, before filtering, most of the events are clipped at E1S SP. In fact, only the smallest events are unclipped. Around January 8th, there is a sudden increase in the proportion of the time series that is clipped due to increasing event size (Figures 3.21 and 3.22). It appears that the sudden decorrelation of the coda is thus due to the sudden increase in size of the Strombolian eruptions around January 8th, which results in a sudden change in the waveforms due to the nonlinear effect of clipping. Specifically, the increased clipping appears to extend into the coda, causing an artificial change in the coda. Conversely, the scattering of higher correlations in Figure 3.9 appears to be due to occasional smaller, unclipped, events. Since the clipping is what appears to be causing the decorrelation it is not surprising that the smaller events have a higher correlation since the master event used was also a small event.

As mentioned earlier, the Gret style of analysis was also tried on the complete broadband data set, which has sufficient dynamic range to remain unclipped even for the

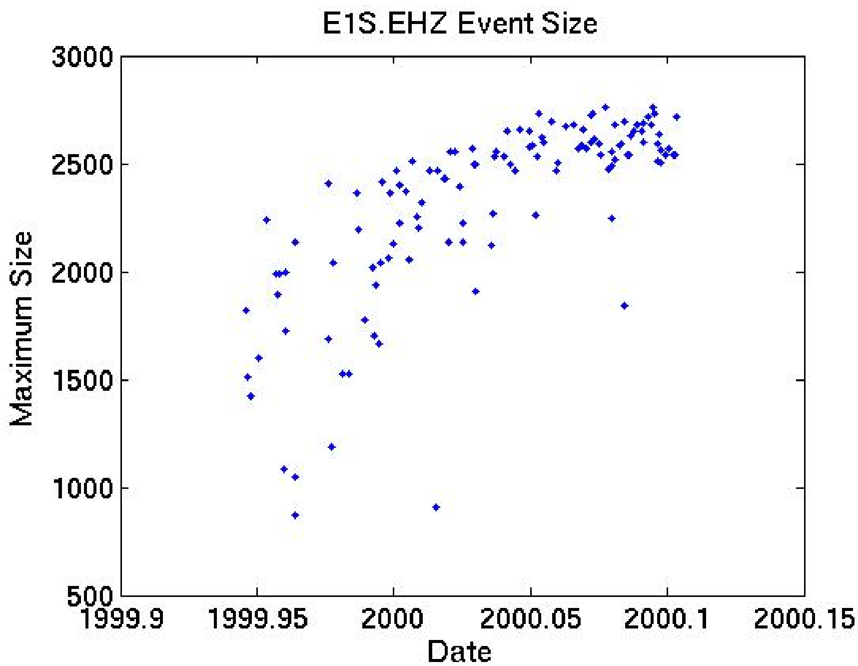

Figure 3.19 – A plot of maximum event size (RMS counts) versus time for E1S SP during the Gret period. Note how the size increases until around January 8th, then plateaus. This is due to the clipping of the data creating an artificial maximum eruption size.

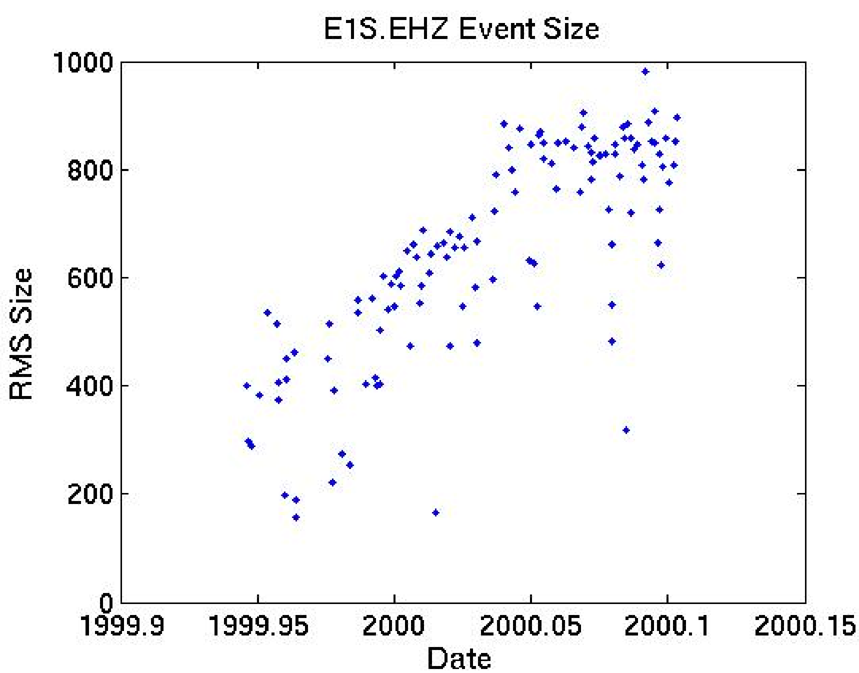

Figure 3.20– A plot of the RMS event size plotted against time for station E1S SP. Once again the size increases until around January 8th, then caps out like in the plot of maximum size (Figure 3.19). Once again clipping is creating a false maximum size.

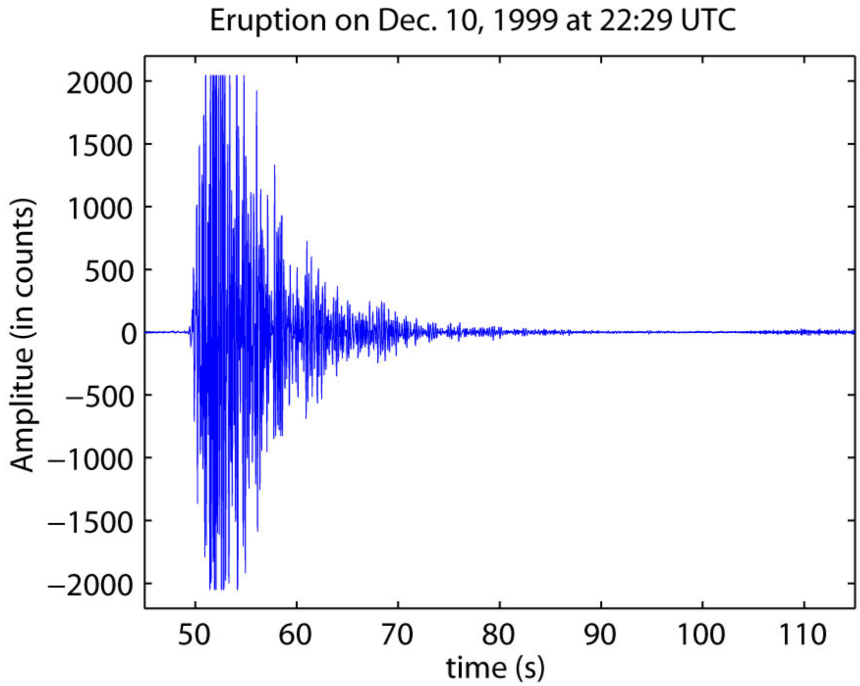

Figure 3.21 – The unfiltered seismogram from a Strombolian eruption recorded at E1S SP, that occurred on 10 December 1999. Note how the initial part is clipped, creating an artificial similarity for the initial part that is then filtered to look like a normal waveform. This is a representative example of how all but the smallest eruptions look unfiltered.

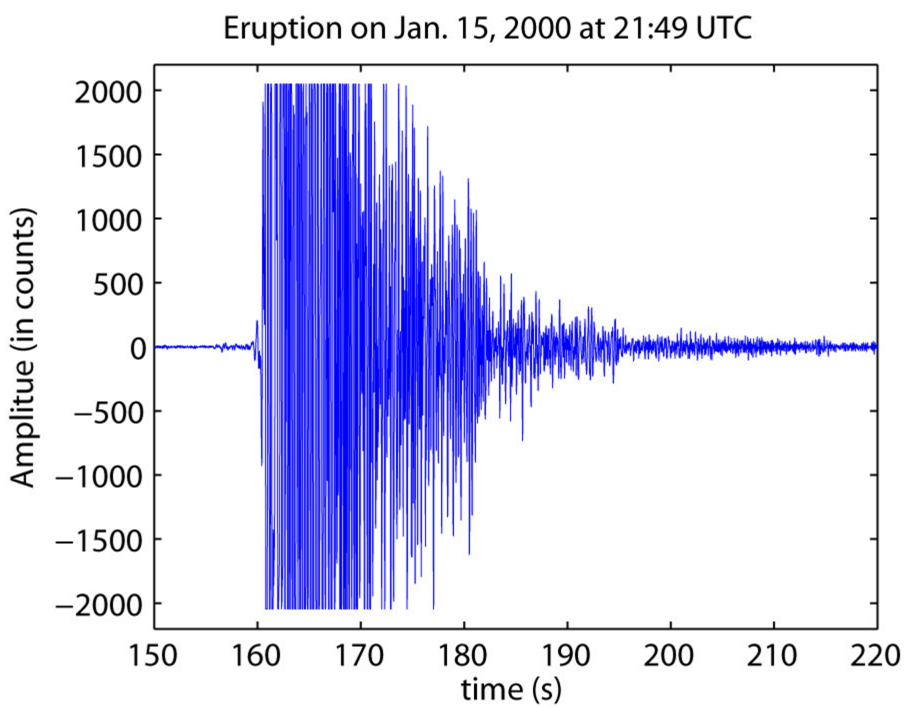

Figure 3.22 – An unfiltered seismogram from a Strombolian eruption recorded at E1S SP, that occurred at on 15 January 2000. This is a representative example of typical January Strombolian eruption. Note how much more of the seismogram is now clipped compared to figure 3.21.

largest events. The correlations to a master and the stack where plotted for the initial and coda parts of the signal. As can be seen from Figures 3.23 and 3.24 there are no discernable trends over time, and the plots of maximum correlation just looks like random scatter. Even when you zoom into the plot for a period with prolific eruptions, there are still no discernable trends (Figure 3.25)

When the broadband data for station EE1S from the temporary deployment was analyzed, it showed a similar decorrelation of the coda (Figure 3.26) as the short period data. However, the initial part of the signal also showed a large decorrelation at the same time (Figure 3.27), and thus the key differential correlation effect reported by *Gret et al.* [2005] was not observed. This decorrelation of the initial part of the seismogram, irrespective of time into the seismogram, strongly suggests that the events are what is changing, rather than the medium. This argues for a change of source characteristics, and indicates that, for these purposes, the eruptive signals are not identical. Plotting the maximum amplitude vs. time for this data set shows that the trend of increasing size continues throughout January (Figure 3.28), further demonstrating that the plateau in Figures 3.19 -3.20 was due to clipping. It is also interesting to note that the return to smaller eruptions around October 22 –23 corresponds to a return to higher correlations in the coda and initial parts. This suggests that the smaller events more nearly resemble true Green’s functions that are representative of the transfer function of the medium

In order to better understand how the broadband data related to the short period data, two events were plotted on top of each other in the form of Figures (1.3 –1.4). This was so it would be possible to see that without the clipping, the initial parts were not that similar. The first two events from 13 of December and 14 of December were plotted on

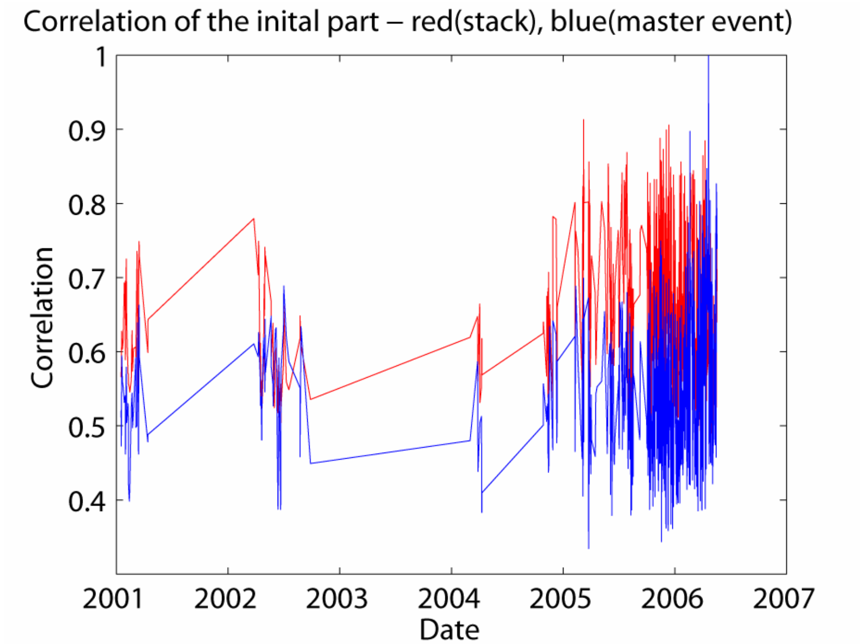

Figure 3.23 – Gret-style analysis for the initial part of the seismogram, for E1S broadband dataset. Once again the data has been filtered from 2-5 Hz using a 2 pole bandpass filter. The correlations are very chaotic, with no obvious trends. Unlike the data from the Gret period the maximum correlations are highly variable. The points were plotted with a line through them to help facilitate the identification of trends.

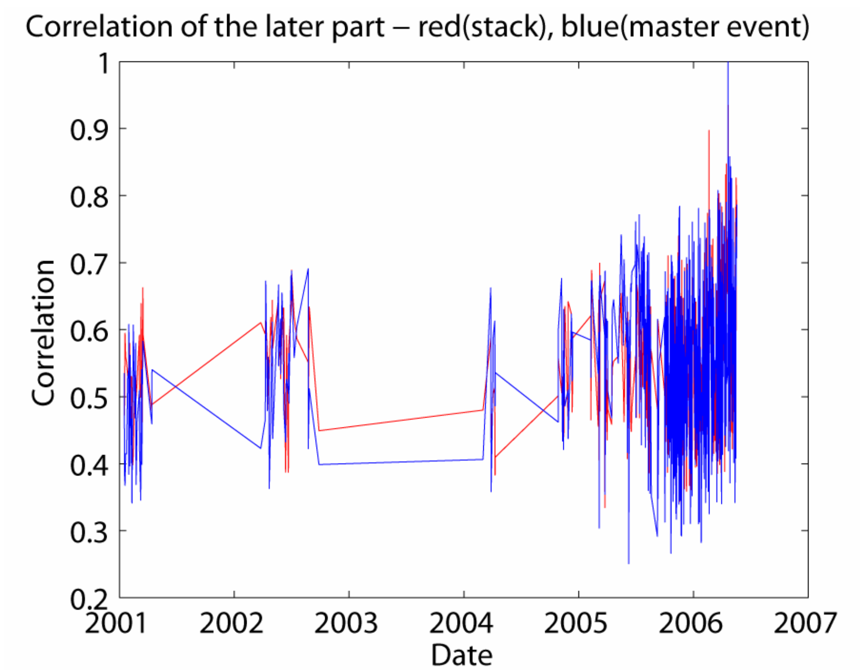

Figure 3.24 – Gret-style correlations for the coda part of the seismogram, for E1S broadband dataset. Once again the data has been filtered from 2-5 Hz using a 2 pole bandpass filter. The correlations are very chaotic, with no obvious trends. Unlike the data from the Gret period the maximum correlations are highly variable, with no distinct periods of decorrelation.

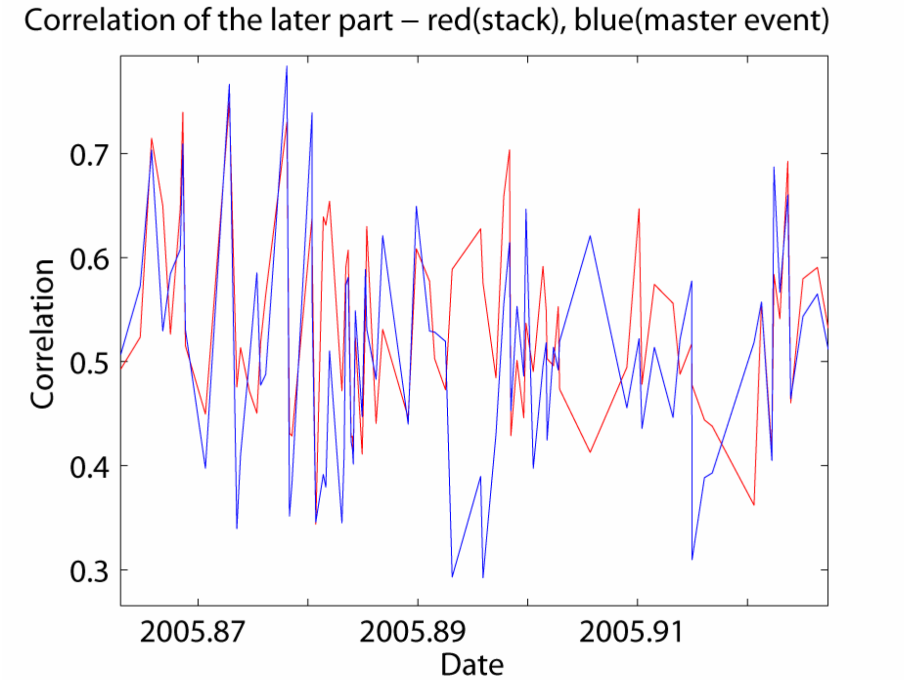

Figure 3.25 – A zoomed in plot of Figure 3.24 showing the coda correlations for E1S BB during an especially active period. Even zoomed in there are no apparent trends, with the correlations jumping all over the place seemingly at random.

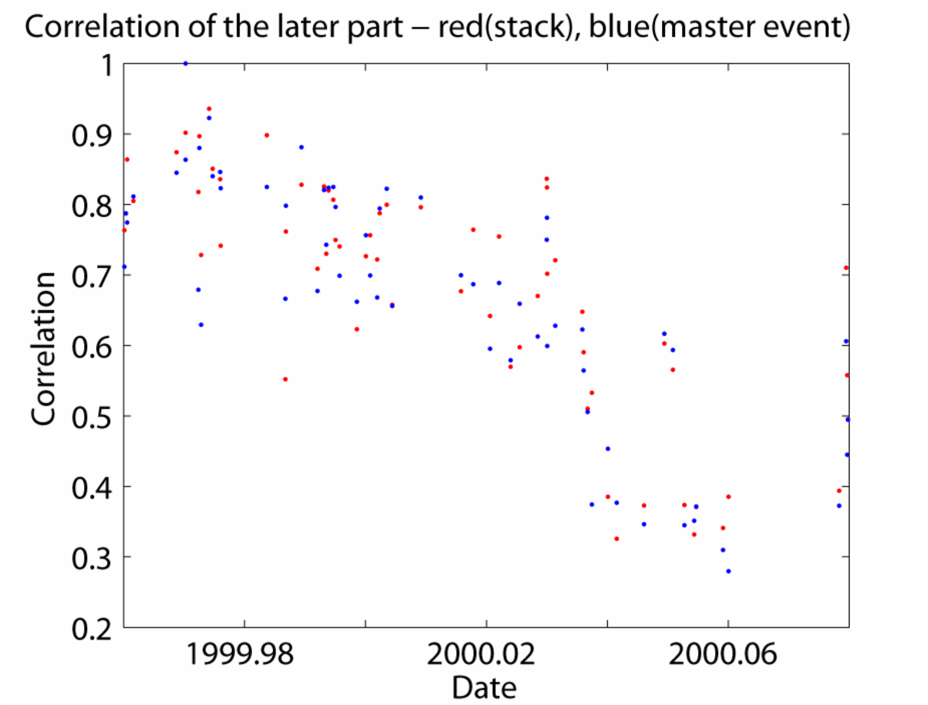

Figure 3.26 – Decorrelation of the coda with respect to the stack (red) and a master event (blue) at EE1S during the Gret period. The apparent recovery around 2000.08 and the period of higher correlating events around 2000.05 correspond to small events with sizes similar to the early December events (figure 3.28)

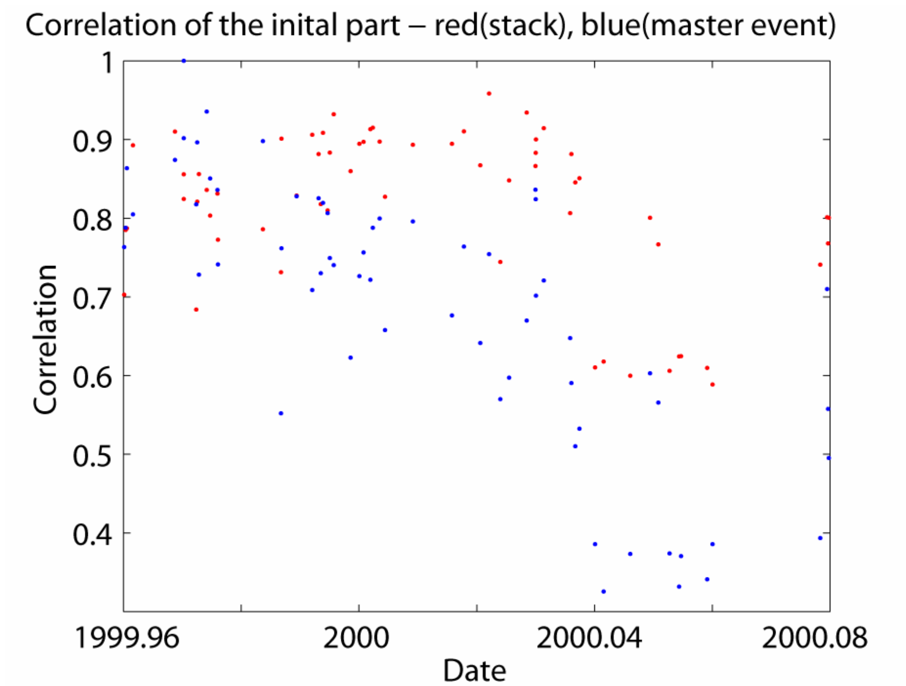

Figure 3.27 – A figure of the correlations of the initial part with respect to the stack (red) and a master event (blue) for the broadband data from the Gret period. Note the decorrelation of the initial part at the same time as the decorrelation of the coda in figure 3.26, which is masked by the clipping of short period stations.

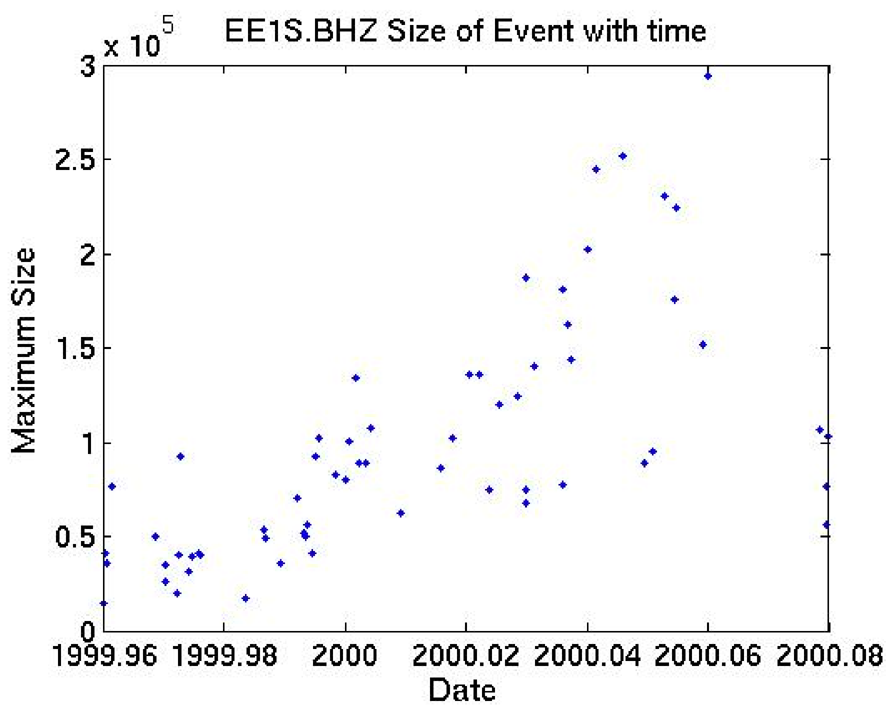

Figure 3.28 – Plot of maximum event size vs. time for the broadband data from EE1S during the Gret period. Note the return to smaller eruptions around 2000.08, and how it corresponds to a return to high correlation for the coda and initial parts in figures 3.26 and 3.27. Also notice there is no longer a size plateau.

top of each other and windowed like Figure 1.3. Similar to the results from the Gret et al. 2005 paper, the initial parts (Figure 3.29) and the coda (Figure 3.30) were almost identical. However, when I plotted an event from the 13 of January 2000 over the 13 of December event both the initial (Figure 3.31) and coda parts (Figure 3.32) were significantly different. This differs from the Gret results (Figure 1.4) where clipping has not been taken into consideration.

After performing the analysis on the Gret period and the broadband data sets, it must be concluded that the *Gret et al.* [2005] results were premature. It also appears the data was tightly filtered, which can cause higher similarity, and can mask the obvious time-domain effects of clipping visible in a broadband signal. It is also clear that the effects of clipping on the correlation were not considered. In fact, clipping occurred at all of the short period stations after January 8th, 2000. In addition it is clear that the clipping is causing artificial similarity by effectively creating a square wave (subsequently filtered) over the clipped region. Some coda pairs with higher correlations occurred in the zone of decorrelation (Figure 3.9). When examined, these events were found to be small eruptions that had very little clipping like the December eruptions (Figure 3.21). These observations are confirmed by the analysis done on the EE1S unclipped broadband data set from the same period. It also suggests that the seismic signals from the eruptions are not as self-similar through time as initially suspected. Plotting a broadband event from the period of decorrelation over a broadband event from early December supports this contention by noting that with clipping removed, the early part of the seismogram is no longer as highly similar.

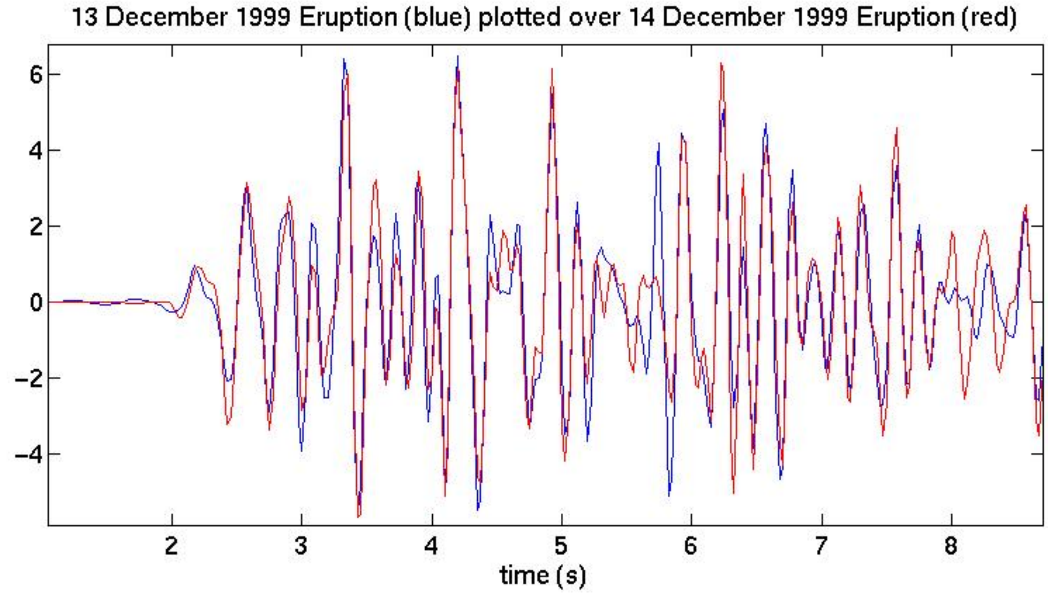

Figure 3.29– Plot of the initial parts of a broadband eruption from the 13 of December and one from the 14 of December, recorded at E1S BB. These events are very similar, as was shown by Gret et al., 2005 (Figure 1.3). These events were filtered from 2-5 Hz using a 2-pole Butterworth filter.

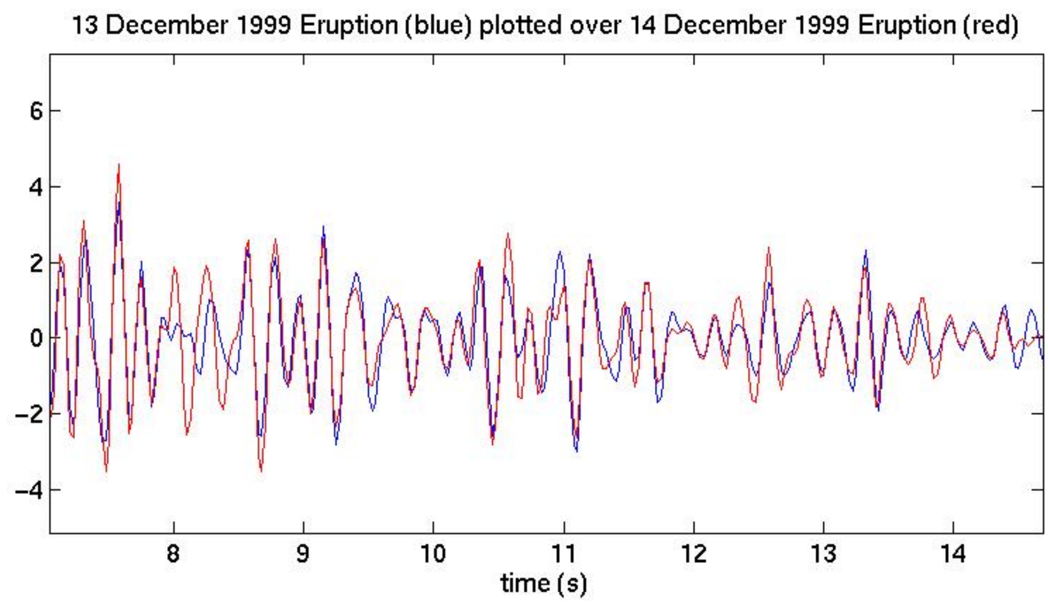

Figure 3.30 – Plot of the coda of a broadband eruption recorded at station EE1S on 13 of December and one from the 14 of December. These codas for these events are very similar, as was shown by Gret et al., 2005 (Figure 1.3). These events were filtered from 2-5 Hz using a 2-pole Butterworth filter.

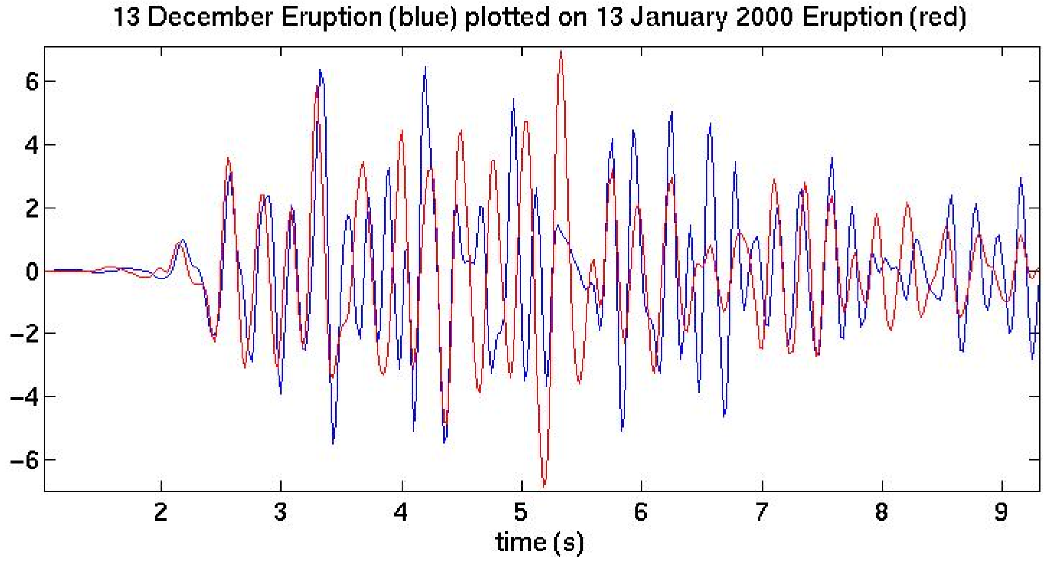

Figure 3.31 - Plot of the initial part of a broadband eruption recorded at station EE1S on the 13 of December 1999 and one from the 13 of January 2000. Except for first 1.5 seconds of the initial part, these waveforms are not highly similar like the short period records of the same period show. This is different then what was seen in the Gret et al, 2005 paper. (Figure 1.4) These events were filtered from 2-5 Hz using a 2-pole Butterworth filter.

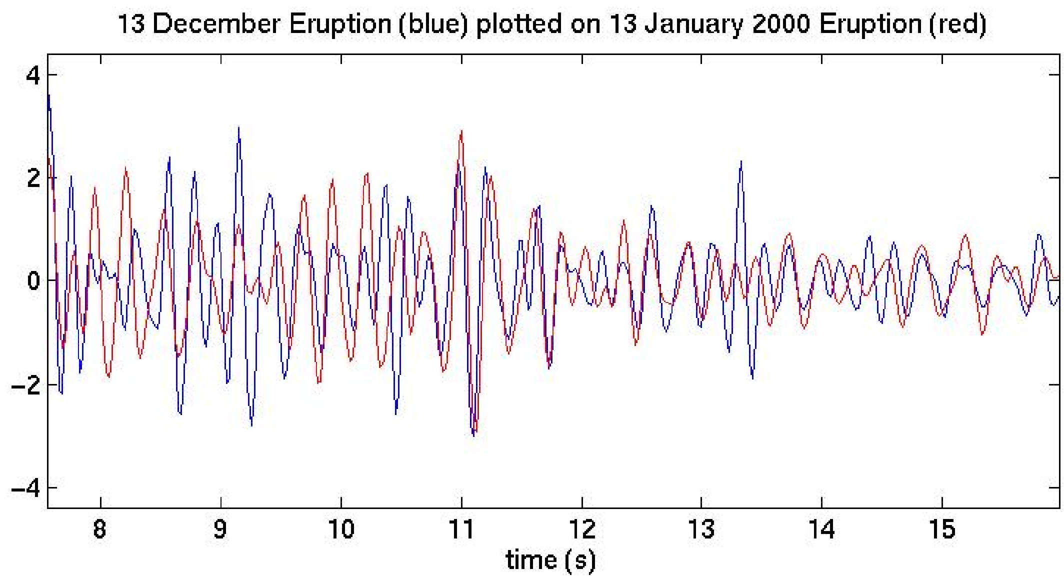

Figure 3.32 - Plot of the coda of a broadband eruption recorded at EE1S for the 13 of December 1999 and one from the 13 of January 2000. Except of a few periods of correlation (11s 12.5 s, etc), most of the signal does not correlate very well. This agrees with the findings of Gret et al., 2005 (Figure 1.4). These events were filtered from 2-5 Hz using a 2-pole Butterworth filter.

CHAPTER 4

Moving Window Analysis

While looking at the data from the Gret period, I noticed that there were small intervals throughout the coda (with durations of around 1 s) where the signals would decorrelate. However, at seemingly irregular intervals there were also places (durations of about 0.5 s) in the coda that would correlate (Figure 4.1). Another example of this time-varying correlation of the signal can be seen in Figure 3.37 at 11 s, 12.5 s and 14 s. These areas of correlation were observed as late as 40 s into the coda.

Methods

In order to examine the behavior of these features a moving window correlation was implemented. This method is similar to the technique used by *Rubistien and Beroza* [2004]. Moving window cross correlations are implemented in many of the papers where coda wave interferometry is used [*Pandolfi et al.*, 2006; *Peng and Ben-Zion*, 2006; *Rubinstein and Beroza*, 2004; *Snieder and Vrijlandt*, 2005]. This method provides a more general way of looking at the similarity between seismograms.

The moving window correlation uses a pre-defined window that steps through the time series. This method takes the data in the window and compares it to a correlation-aligned master event (which may be a stack) for the same period in the seismogram. The maximum correlation coefficients and corresponding lags are calculated for the window and saved. For this project, 50% overlapping windows were used. Window lengths were varied between 0.5 and 2 s. For a comparison to a tectonic environment, this analysis was also carried out on a series of highly similar events from a local swarm in the Socorro area. The swarm started on October 30, 2005, and lasted about a month [*Stankova et al.*, 2006].

Results

The moving window analysis was first implemented on the Gret period short period data set described in Chapter 3. The initial part of the seismogram correlated relatively well for these short windows, which is not surprising since this is dominated by the direct arriving wave (and clipping induced similarity), and should be relatively insensitive to small changes in the source or medium [*Snieder*, 2006]. As can be seen in Figures 4.2 and 4.3, the directly arriving part (up to around 3 s) at E1S SP has relatively stable correlations when correlated with a master event or stack. This analysis technique is essentially a shorter time window version of the analysis from Chapter 3. However, an intriguing phenomenon was observed starting with the early coda and extending for 40 s or more. We observe time bands of highly correlated signal intermingled with bands of decorrelated signal (Figures 4.2, 4.3). These bands are not limited to just the Gret period. When the same analysis was done for E1S BB similar band could also be seen (Figure 4.4). These correlation/decorrelation bands are clearly somewhat stable throughout time. Using a master event brings out the bands a little more by reducing the correlation of the

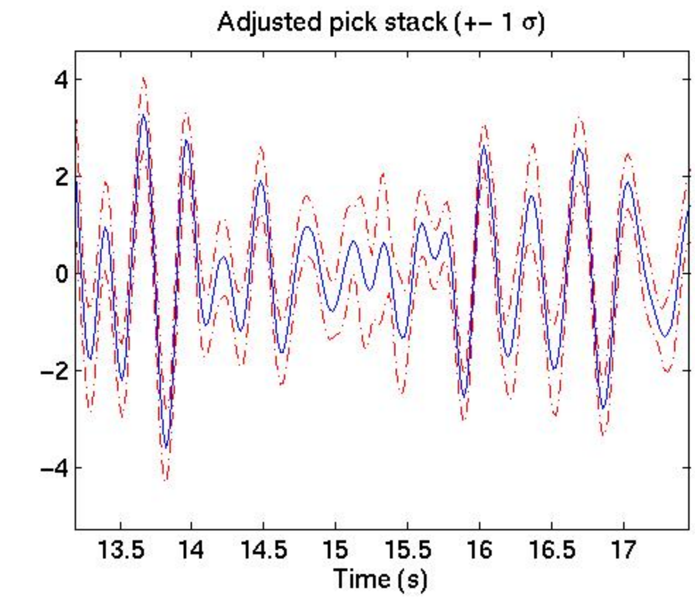

Figure 4.1 – Example of periods of correlation and decorrelation in the coda. This data comes from the stack of station CON SP between 13 and 17.5 seconds. The data has been plotted with lines of 1 standard deviation. Periods of high correlation, lasting approximately 0.5 s can be seen at approximately 13.5 s, 14.5s, 16 s, and 16.7 s. A period of strong decorrelation can be seen around 15 seconds. These periods of strong correlation occur through at least 40 s.

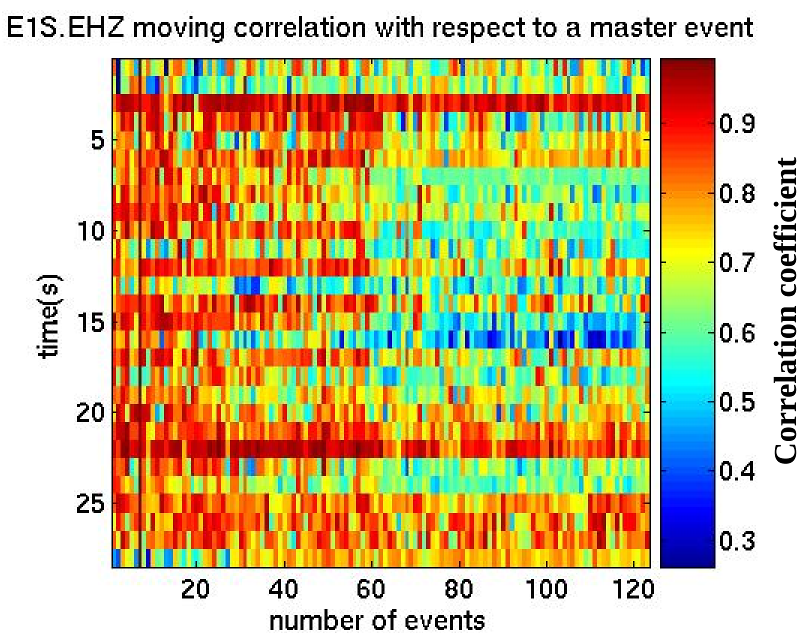

Figure 4.2 – Plot of the moving window correlation for E1S SP during the Gret period, using an event on Dec 9, 1999 as the master and a window of two seconds. Note the high bands of correlation, even late in the coda. Also notice how some of the bands seem to come and go. The band around 3 seconds is the direct arrival, and the area of decorrelation from 9 –7 s is due to the increase in clipping during that period. For this analysis the data has been bandpass filtered between 2 & 5 Hz.

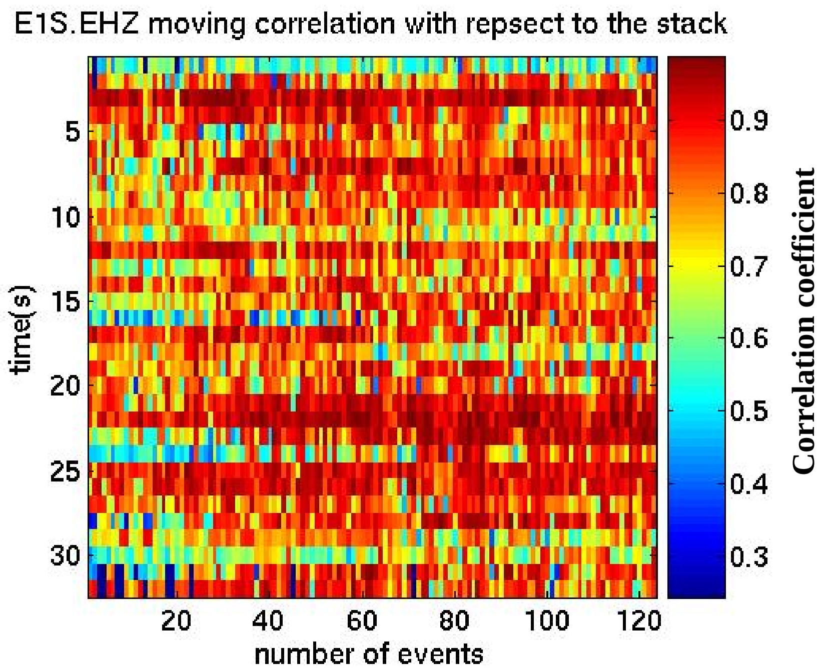

Figure 4.3 – Same analysis as figure 4.2, except the stack is used as the master event. There are still some bands that come and go, but overall the correlation is higher and a little more stable due to the stack being an average of all events. The largest events influence the stack the most resulting in the higher overall correlations of the latter events.

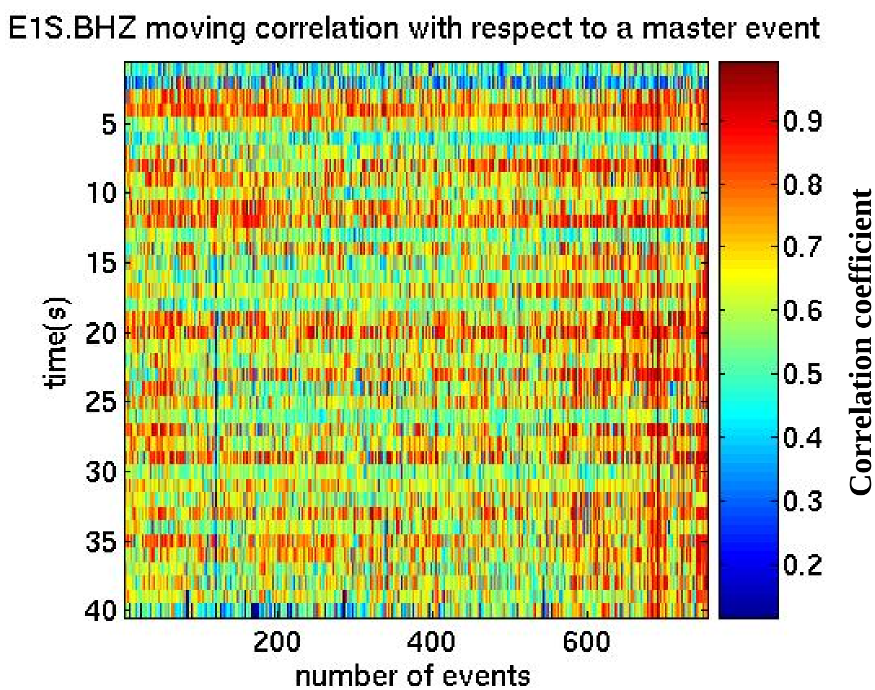

Figure 4.4 – Correlations for the moving window analysis performed on E1S BB. The filtering and windows used for the Gret period were applied here as well. Note how once again some bands of correlation are stable while others seem to come and go.

decorrelated bands and makes them more obvious. However, performing the moving window analysis using the stack as the master produces better overall correlation (as one would expect, because the stack is simply the mean).

To see if this is a phenomenon unique to Mount Erebus (or volcanic environment), or if a similar analysis done for a tectonic environment would show the same time bands of correlation, a moving window analysis was done on a dataset of multiplets from a small earthquake sequence starting around October 30, 2005 [*Stankova et al.*, 2006]. These earthquakes occurred in the Socorro, New Mexico area, and were recorded on the local short period network. After filtering the earthquakes with the same filtering range used for the Erebus events, and running them through the preparation programs, the moving window correlation was performed. Station WTX showed a band of correlation for the initial P and S waves, but nowhere else, though there was a possible hint of a band around 8 seconds (Figure 4.5). Station LEM was the same as WTX, except at this station reflections of the Socorro magma body are common. With a 2 s time window, and the events lined up with the initial P wave, there was a band of correlation corresponding to the magma body reflection at eight (SzP) and ten (SzS) seconds (Figure 4.6). The stack for LEM shows the magma body reflections clearly (Figure 4.7)[*Balch*, 1997; *Hartse*, 1991; *Stankova et al.*, 2006].

The moving window analysis was also performed on the full broadband data set as well the Gret period broadband dataset. In both cases it was noted that there were time bands of high correlation that were relatively stable, and others that seemed to vary with time (Figures 4.2 and 4.4). This was especially noticeable during the Gret period of prolific activity (Figure 4.2). When the maximum correlation of a band was plotted

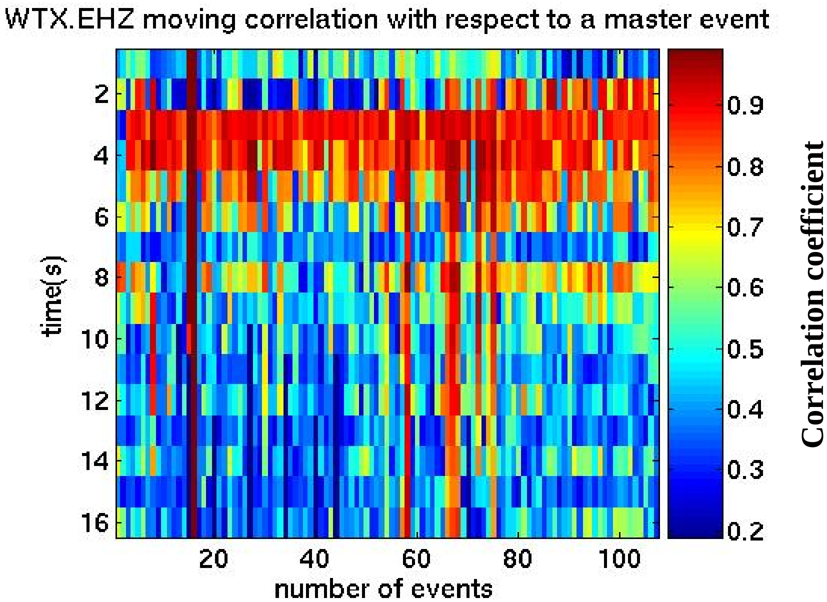

Figure 4.5 – Moving window analysis done on the local short period station WTX. Notice how the directly arriving energy is highly correlated, but there is an absence of bands of high correlation in the coda. There does appear to be a hint of a band around 8 seconds though. The filtering and windows used for the Gret period were applied here as well.

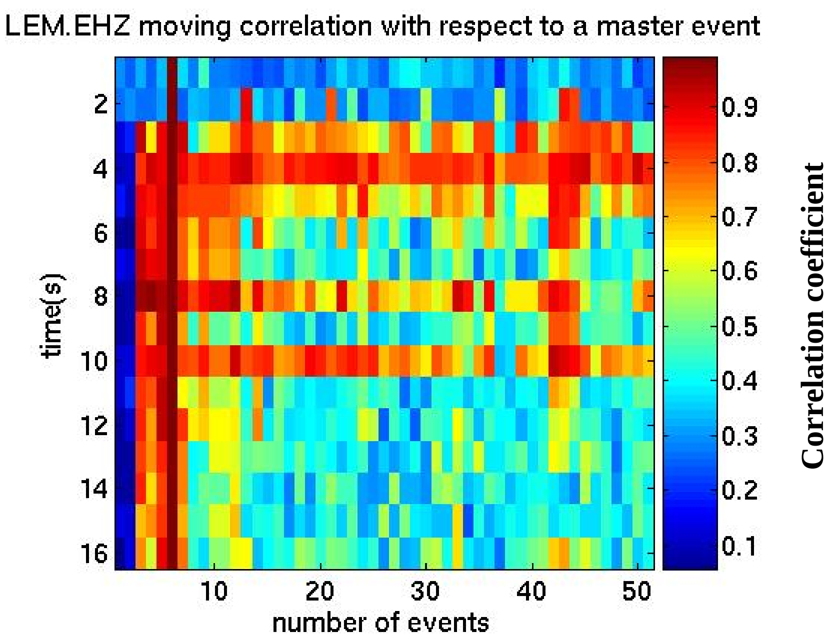

Figure 4.6 – Moving window analysis done for the local short period station LEM, using the event most similar to the stack as the master event. Once again the initial arrivals result in a band of high correlation. It is interesting to note that LEM has two bands of high correlation in the coda at eight and 10 seconds. These bands are due to the magma body reflections, called SzP and SzS, that are seen at this station. The filtering and windows used for the Gret period were applied here as well.

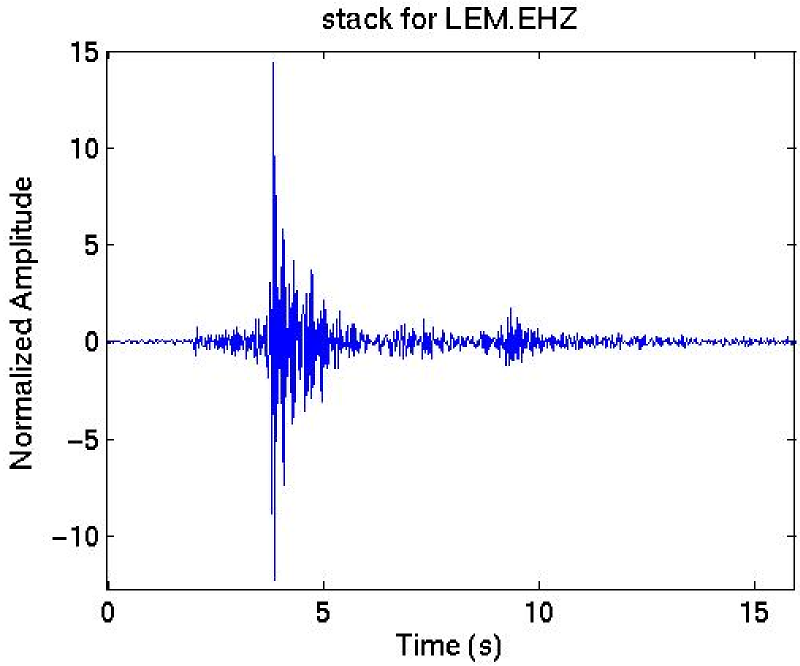

Figure 4.7 - Plot of the stack for local station LEM. Note how the SzP (7-8s) and SzS (9-10s) magma body reflections occur at the same time as the high bands of correlation in figure 4.6.

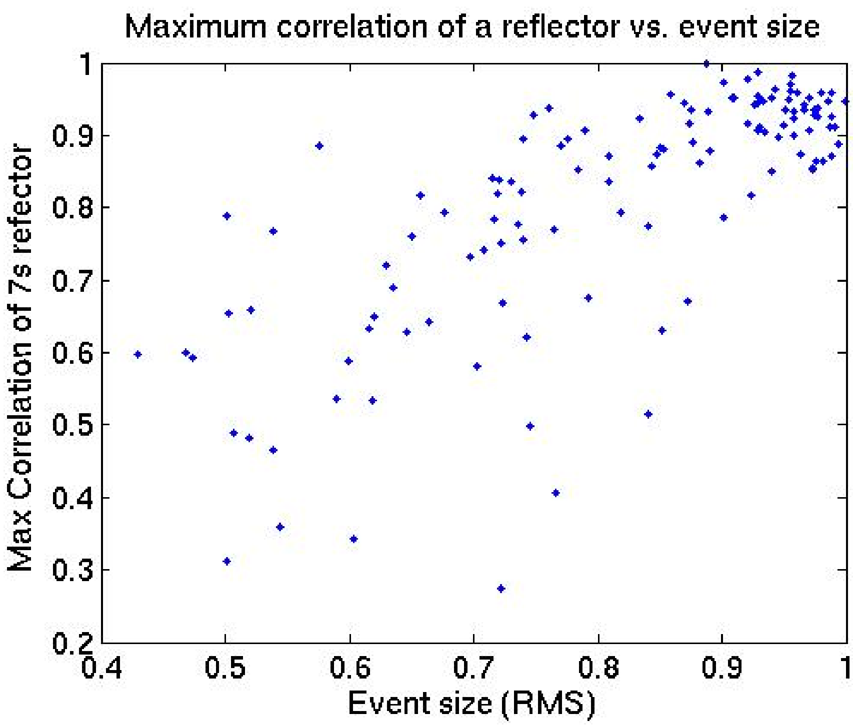

Figure 4.8 – Plot of the strong 7 s band of correlation from Figure 4.3. The maximum correlation of the reflection has been plotted against the maximum event size. Notice how the correlation increases with increasing size.

versus RMS size (Figure 4.8), as well as maximum correlation versus time over-plotted with maximum size (Figure 4.9), there was a noticeable correlation between size and maximum correlation. It is interesting to note that while in many cases the maximum correlation increased with maximum size, the correlation of some bands decrease as the eruptions get larger (Figures 4.10 and 4.11). The correlations of the initial seismogram do not show any comparable trends when plotted against maximum event size (Figures 4.12 and 4.13).

I also looked at the lags produced by the moving window correlations to see if there was any change through time. In Figure 4.13 the lags for the E1S BB data set are plotted using a color scale. As can be seen from Figure 4.13, the lags are surprisingly stable through time, even 30 s into the coda. It is also interesting to see that the bands of strong correlation (Figure 4.3) have resulting bands of stable lags, usually around zero, whereas the bands of decorrelation tended to have resulting lags. It is interesting to see that the lags for these bands of decorrelation seem to alternating between positive and negative, as you get later in the coda (Figures 4.14). This may be due to the overlapping window picking up the bands of high correlation. In contrast, the first 2 - 3 s of Figure 4.14 are more chaotic and contain both positive and negative lags. A figure of the lags for the Gret period, using EE1S BB, was also created (Figure 4.15), and showed the same results.

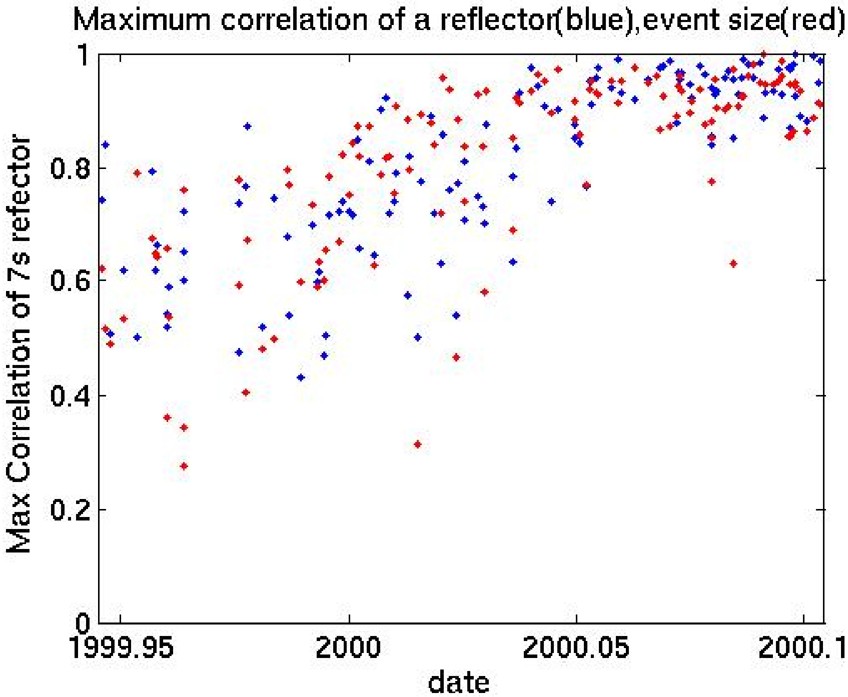

Figure 4.9 – Plot of maximum correlation for the 7 s band of correlation plotted against time (blue). The RMS event size with respect to time has been over (red). Notice how the maximum correlation of this band increase with increasing size, until it plateaus along with event size.

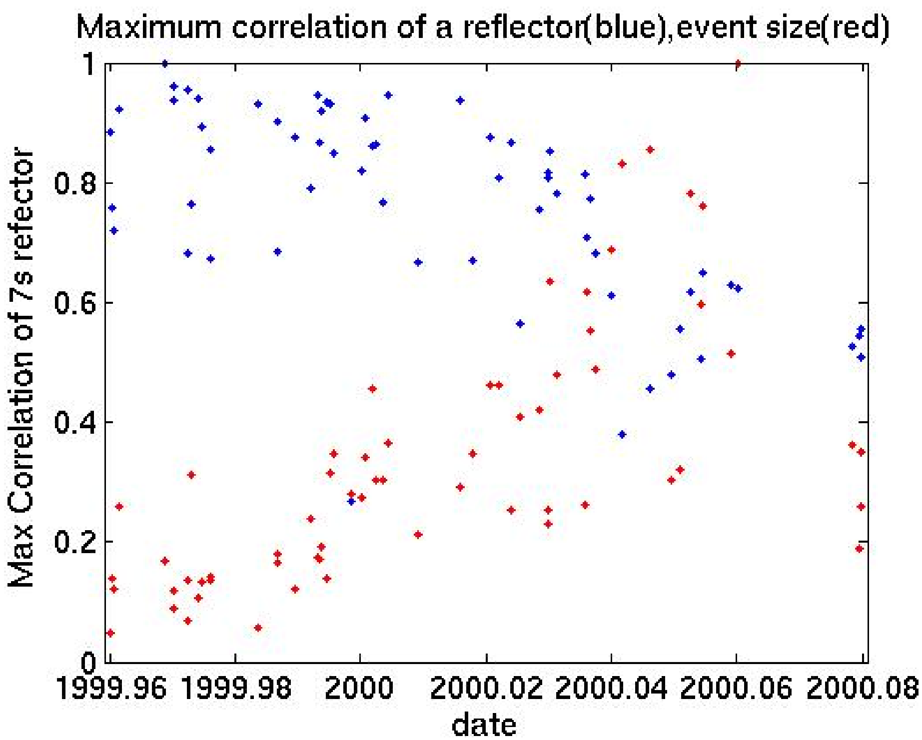

Figure 4.10 – Example of a band of high correlation from EE1S. Notice how the correlations decrease with increasing size.

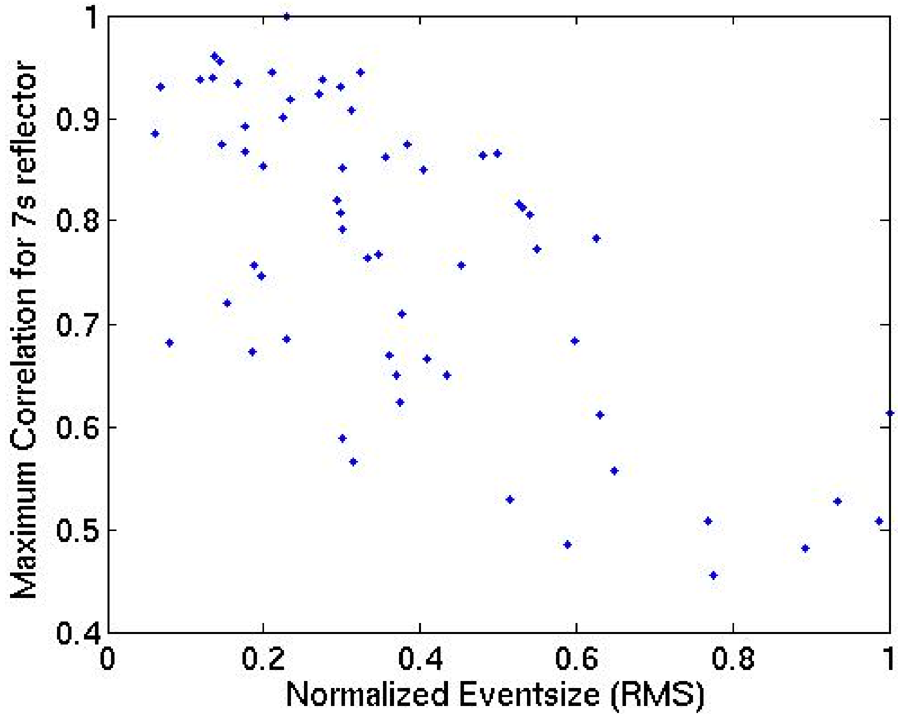

Figure 4.11 – Plot of the Correlation of the 7 s reflector versus maximum size for EE1S showing reversed correlation.

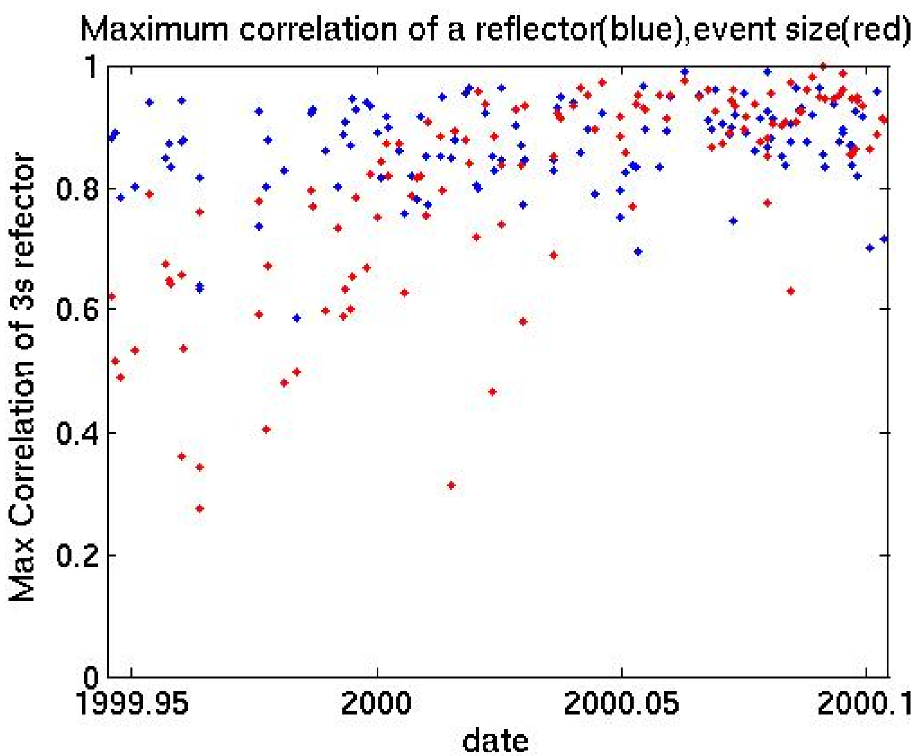

Figure 4.12 – Plot of the directly arriving wave from E1S SP (Figure 4.3) plotted against RMS size. Notice how size does not affect the directly arriving waves.

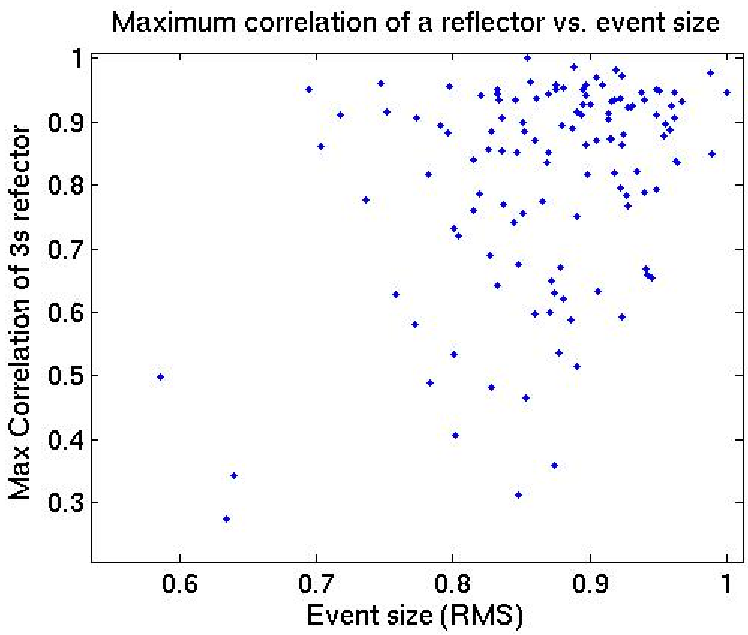

Figure 4.13 – Plot of maximum correlation versus event size for E1S SP. Once again there is no obvious trend for the directly arriving part. There is some scatter with the smaller events, but that is probably due to the fact that most of the signal is unclipped.

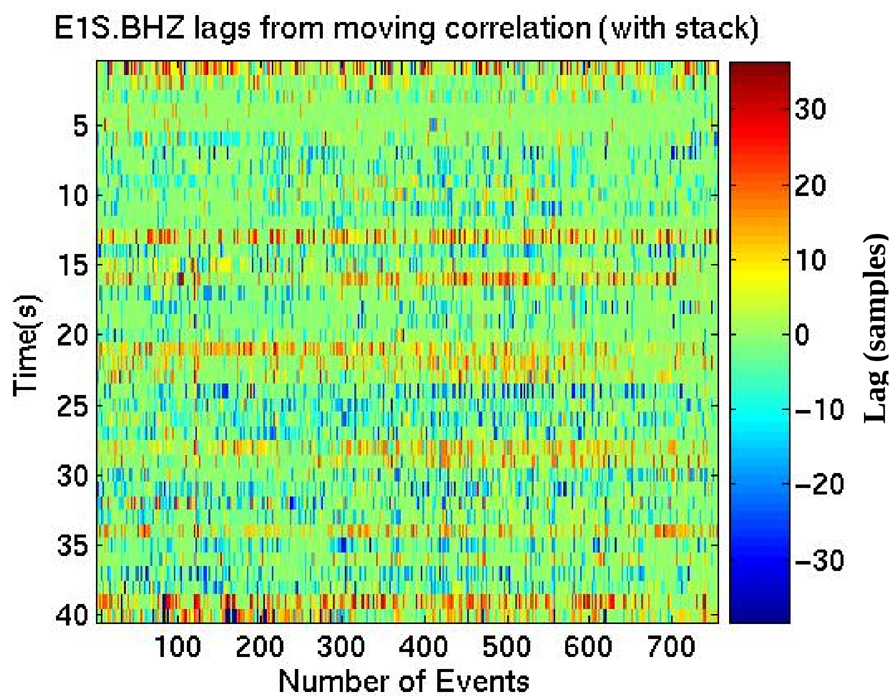

Figure 4.14 – Lags to be best correlation for the moving window analysis. These are the lags for E1S BB. Note that there are strong bands of higher lag, and that many of these bands correspond to bands of decorrelation in the moving window analysis (Figure 4.4). It should also be noted that there are no systematic changes in the lags over time. In fact, event the areas of decoration are surprisingly similar.

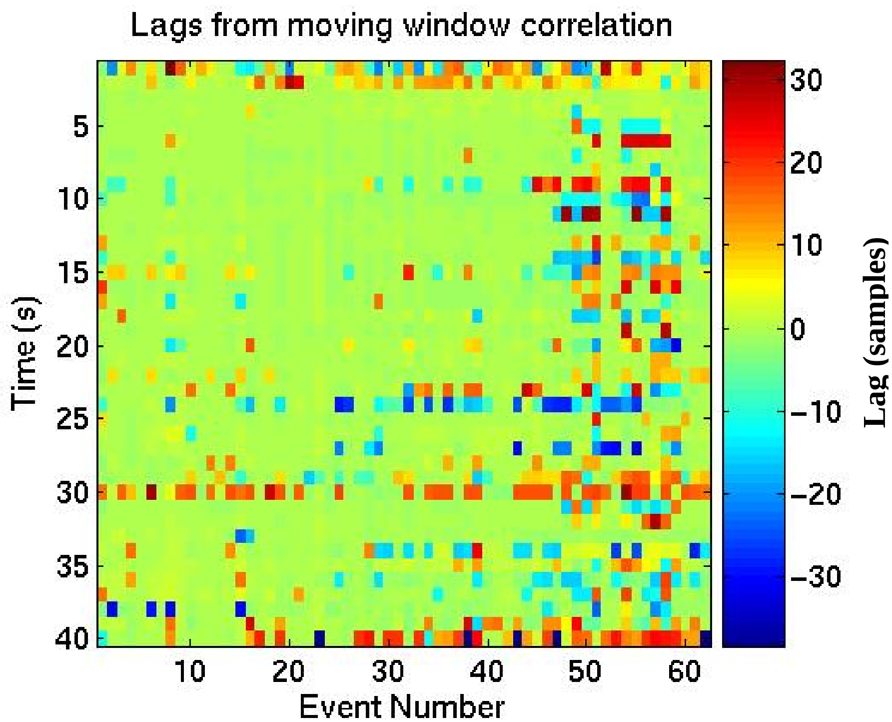

Figure 4.15 – Lags for EE1S BB during the Gret period. Once again the bands of high correlation have little or no lag, even 30 seconds into the coda. As before, the bands of lags correspond to bands of low correlation.

Scatterer analysis

The nature of the high correlation bands is not known, but they are clearly scatterers of some sort residing within the volcano. It is not known at this point whether these features are due to energy trapped within the Mount Erebus magma column (where [*Dibble*, 1994] suggested there should be extensive trapped energy due to strong impedance contrasts and a strong velocity gradient), or scatterers elsewhere (e.g., within or at the edges of an underlying magma chamber or features elsewhere in the Erebus edifice). A scatterer analysis of the waveforms at different stations was carried out to try and understand the cause of these periods of correlation. First, three high signal-to-noise small events that were almost identical and occurred within hours of each other

(20051028212958, 20051028231935, 20051029010934) were filtered between 2 and 5 Hz, and stacked to modestly improve the signal to noise ratio (Figure 4.16). This analysis was implemented for the stations E1S BB, CON BB, and LEH BB (Figure 1). These stations were first crosscorrelated with E1S BB and then lined up at the best correlation. Each station was then plotted over the top of E1S BB, and inspected to see how the strong the reflections lined up. Reflection spacing was examined by normalizing the events by maximum amplitude, then plotting the correlation-aligned seismograms on top of each other. In order to make it easier to see what was happening the absolute value of the time series was taken for each station and plotted on top of E1S BB at the appropriate time lag.

It has been hypothesized that the similarity of the events and the dominant features of the early coda are due to magma column resonances in the immediate vicinity of the lava lake, such as the near-surface conduit system (e.g., *Dibble* [1994]). If trapped energy within the near-lava-lake magma column is the source of the coda scattering features observed here, the scatters are in the near-source regime, and thus should appear at similar times in records from relatively distant stations. This is not, however, what is seen when the events are lined up at the highest correlation (Figure 4.17 and 18). Instead we note that initial (direct arriving) part matches quite well, but few if any of the other prominent reflections line up after that at different stations. While it does not rule out vibration of the conduit as a source of some coda features, it does show that much of the repeatable energy (strong reflections) is arising from subsurface scatters that are of significant distance from the source region (the lava lake) relative to the (several km) station spacing of E1S, CON, and LEH.

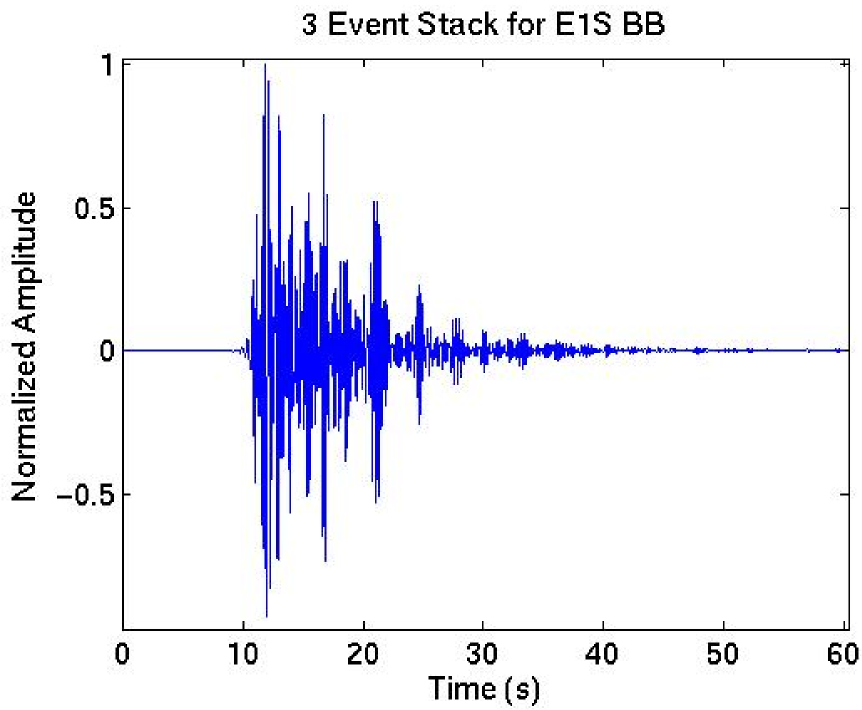

Figure 4.16 – Stack of three highly similar events recorded at E1S BB on October 28-29, 2005. Note the reflection coming in about every 5 seconds starting at about 20 seconds. Those reflections correspond to the bands of high correlation seen in figure 4.4.

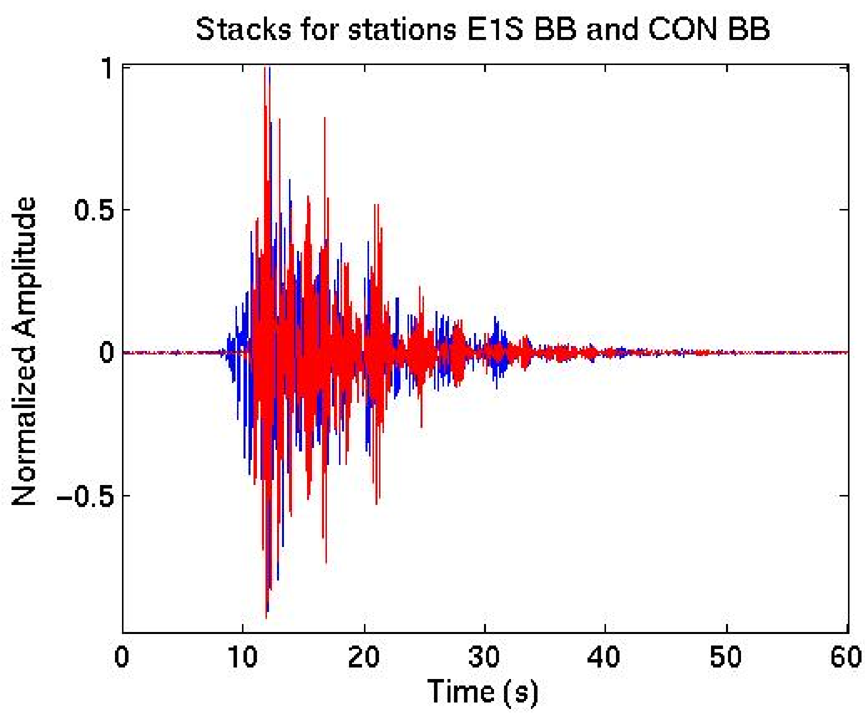

Figure 4.17 – Example of the scatterer analysis performed on the broadband network. There seem to be a few similarities, but overall there is no correlation between strong reflections/refractors at these stations (E1S BB and CON BB).

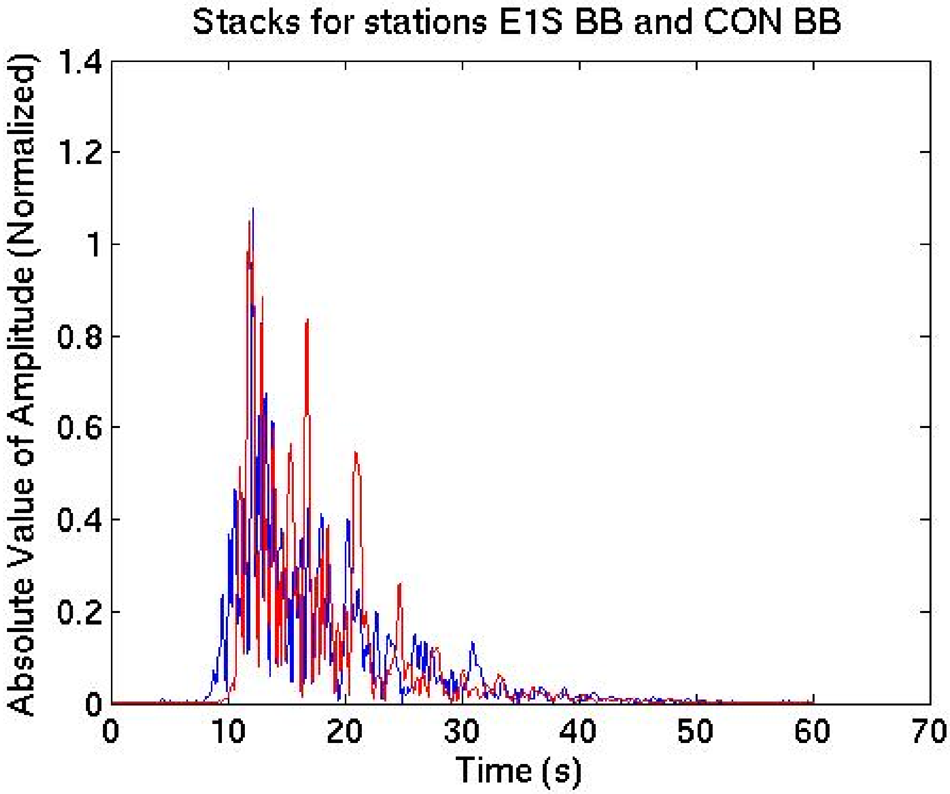

Figure 4.18 – Same analysis and stations as Figure 4.17, except that they have been plotted by the absolute value of their amplitude to make it easier to see similarities.

CHAPTER 5

Cluster Analysis

Methods

Examining the moving window cross correlation analysis it became obvious that there were significant differences between events. There were also periods where there seemed to be clusters of events with higher than normal similarity. An example of a period of higher then normal similarity is the events used for the scatterer analysis (Figure 4.16). Even with the noise in the data it is difficult to tell visually they are different events. The data set was broken into clusters defined by crosscorrelation coefficients to allow us to look at individual groups of highly similar events. This also allows us to see if these highly similar groups are clustered in time, or show other temporal trends that hinge on the key question of whether coda variability is primarily source or medium related.

The clustering analysis was accomplished by using the linkage and cluster programs in the MATLAB 7.0 Statistics Toolbox. Linkage creates a hierarchical tree of clusters by a method supplied by the user [*Aster and Rowe,* 2000; *Rowe et al.,* 2002]. The methods examined for this analysis are single (nearest distance), complete (furthest distance), weighted (weighted average distance), and average (average distance) [*Rowe et* *al.*, 2002]. The average method was chosen for the analysis because it provided the largest clusters and had similar or better median correlations when compared to the other methods. The correlations were done with a 40 s time series starting 2 s before the eruption signal onset. The linkage program works by taking a dissimilarity matrix, finding the closest neighbors, and linking them together. The dissimilarity matrix used was created using the maximum correlation coefficients for each event pair, and subtracting the correlations from 1. For this analysis a minimum correlation coefficient of 0.6 was used to perform the clustering. A correlation coefficient of 0.6 was chosen because it provided the largest cluster size while keeping a reasonable correlation between events in the clusters. A minimum cluster size of 8 events was used when examining resulting groups (clusters smaller than this were considered too small to provide useful comparisons). As always occurs with such methods, higher minimum correlation coefficients resulted in fewer and smaller clusters, though when put into the alignment program some clusters were produced that had very high correlation coefficients (above 0.9). For the clustering analysis a Butterworth 2-pole band pass filter between 1 and 8 Hz was applied prior to crosscorrelation to preserve more of the signal structure than some of the earlier filters (e.g., Chapter 3).

Once the broadband database had been broken down into clusters, each cluster was saved as a separate file and put in a directory with the files from the other clusters. The original data and corresponding cluster information was also saved to the same directory, because with over one thousand events it takes hours for the clustering program to run. This also facilitated direct comparisons of cluster characteristics. E1S BB was the first station to be analyzed. Then once the best parameters had been determined, the rest of the broadband stations (RAY, CON, NKB and HOO) were analyzed, and compared to E1S BB. The clustering analysis was also done specifically for the broadband data from the Gret period, (December 1999-January 2000; see Chapter 3) using the same parameters as the full broadband data set.

Once the data had been broken into clusters of highly similar events, characteristic aspects of the clusters were examined. The first aspect analyzed was the distribution of the clusters through time. This was done to see if the clusters changed gradually through time, if they were randomly distributed, or if they showed other characteristic trends. If the clusters changed gradually, this might be an indication that the scattering characteristics of the volcano were also gradually changing over time. Conversely, tight temporal clustering of similar events might suggest a strong source influence on the seismograms. As can be seen in Figure 5.1, the clusters do not change gradually. In fact, multiple clusters can occur simultaneously and can some clusters also span the whole data set (note that the cluster number is just an arbitrary index to distinguish the clusters from each other). The first line of data on Figure 5.1 shows periods of time where data exists. This analysis was also done for the Gret period broadband data from EE1S (Figure 5.2). It is interesting to see that there are only two clusters for this data, and that they are two discreet clusters in time.

Once it was realized that the cluster were not gradually changing through time due to changes in the medium, other causes of dissimilarity were examined. First, I examined how maximum event size affected the clusters since earlier investigation had shown that it had an influence on similarity (Chapter 3). To see the relation of event size to cluster index the average cluster size was calculated and plotted with error bars of one

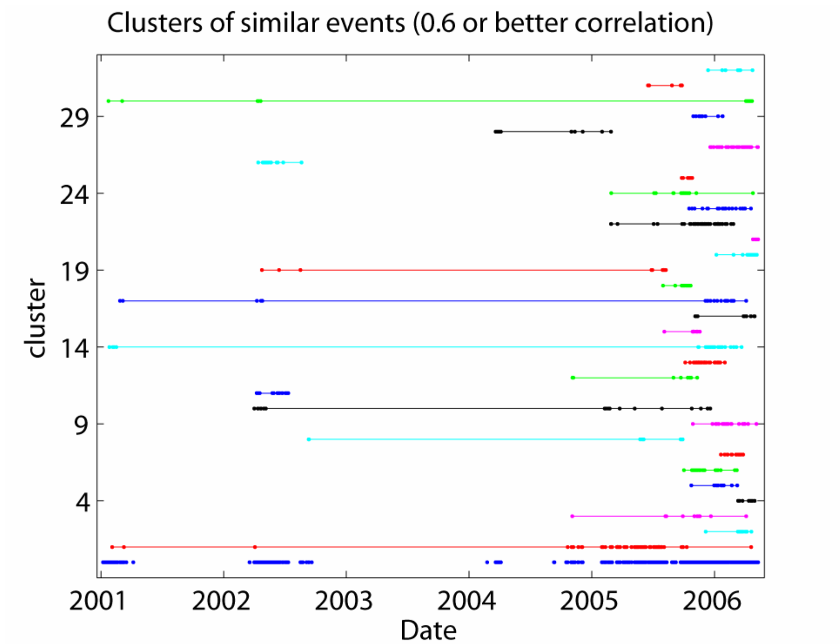

Figure 5.1 – Temporal distribution of the clusters for the entire E1S BB dataset. Some clusters are quite long lived, and can even span essentially the entire dataset. It is also common for more then one cluster to be active at any given time. The blue dots at the very bottom show the cluster of all events, which illustrates the time periods where there are lava lake eruptions. The cluster number is an arbitrary index. The increase in clusters beginning in 2005 corresponds to the increase in eruptive activity, as well as the improved ability to detecting small eruptions.

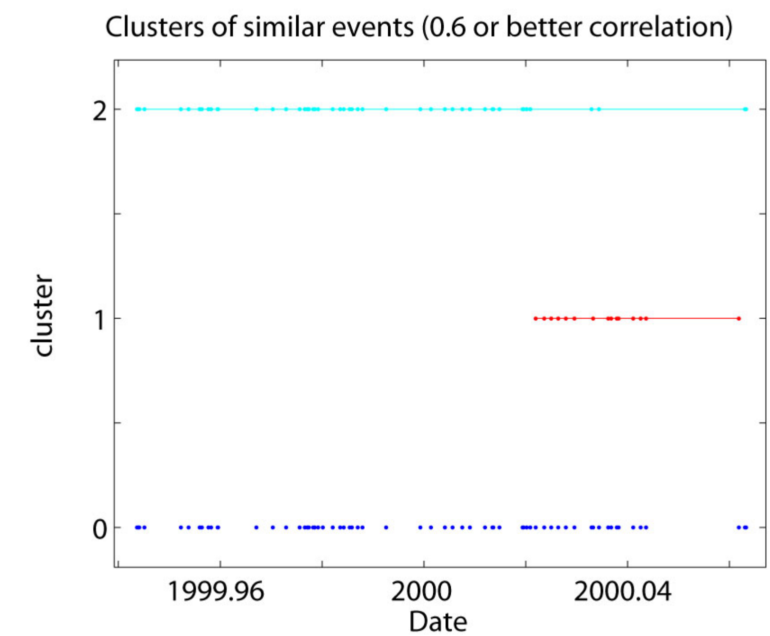

Figure 5.2 – Temporal distribution of clusters for broadband station EE1S for the Gret period. Notice that there are two main clusters with very little overlap. The events that do overlap correspond to the events of higher correlation (around 2000.03) in Figure 3.30. Once again cluster 0 is the cluster of all events.

standard deviation (Figure 5.3). From Figure 5.3 it can be seen that size indeed has an effect on cluster assignment (and thus on seismogram similarity). Clusters with the smallest events also have the smallest error bars, indicating that some aspects of similarity can be linked with small size. What is surprising is that there are so many separate clusters with similar size ranges containing the smallest events, considering the smallest events should theoretically be the most similar since they are the most impulsive. It is also surprising how many of the largest events cluster together. It had been thought that they were the most likely to be dissimilar due to the extended length of the eruption, and theoretically more complicated source processes (non impulsive). The same analysis was performed on the EE1S data from the Gret period, and it is reassuring to see that the average size of the clusters and error bars does not overlap for the two clusters (Figure 5.4), lending credence to the suspicion that the Gret period was one of unusual source stability.

In order to better understand the clusters, especially ones with similar size ranges, the effects of event size were examined. First the average maximum cluster sizes were plotted with time (Figure 5.5). As can be seen in Figure 5.5, clusters with almost identical average sizes are active concurrently. It is also common for the clusters with different averages sizes to be active at the same time. The increase in the number of active clusters seen in Figure 5.1 coincides with the increase of eruptive activity (Figure 1.1). Another method used to understand the effect of size on clusters was to plot the average cluster size verses the number of events within the cluster (Figure 5.6). If one simply equates source size with greater complexity, as occurs with earthquake sources, one would expect the largest clusters were expected to contain the smallest sized events,

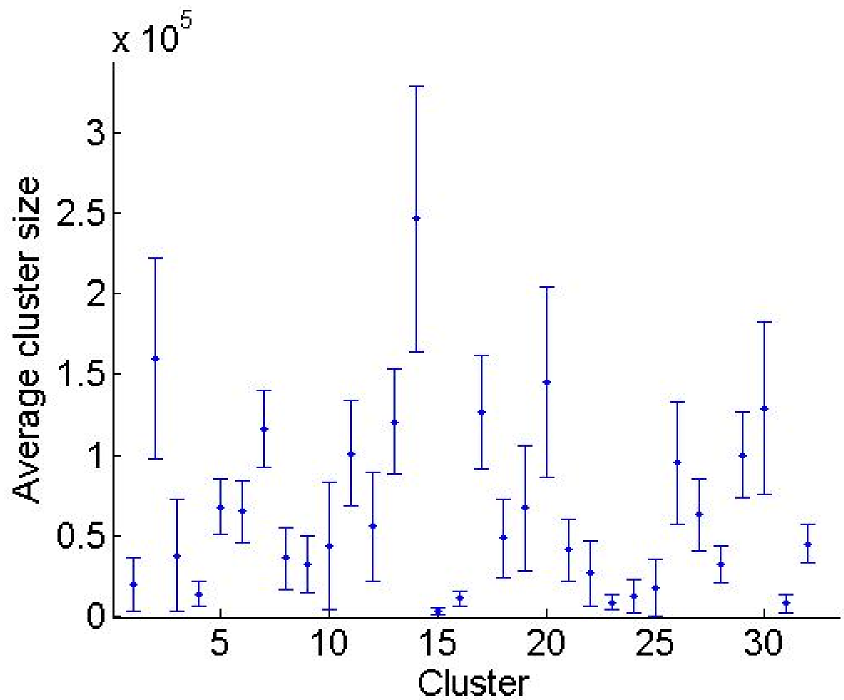

Figure 5.3 – Average cluster size (with one standard deviation error bars) for E1S BB. Notice how there are several clusters containing the smallest events with similar size ranges. Also notice how many of the largest events have clustered together in a single cluster

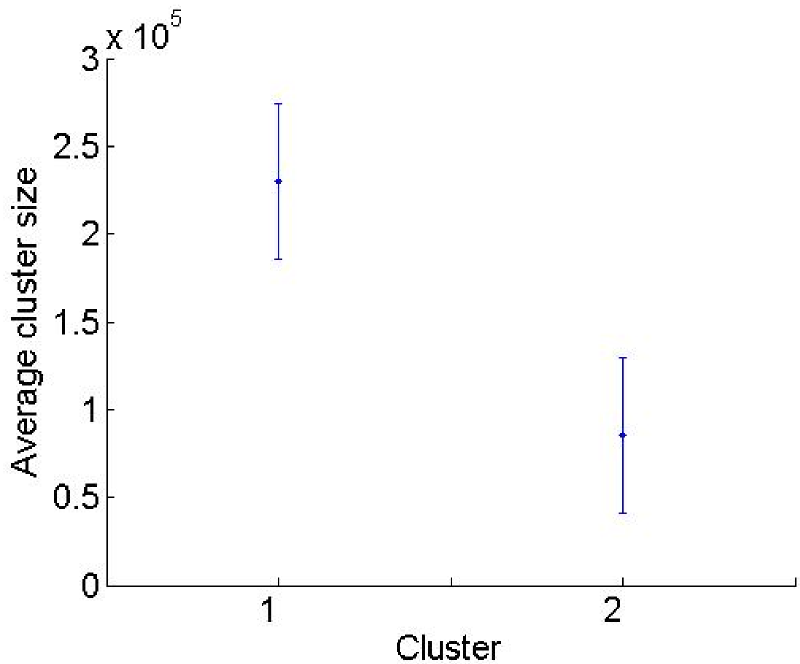

Figure 5.4 – Average cluster sizes for broadband station EE1S recorded during the Gret period. Notice how the size ranges for the two clusters (Figure 5.2) do not overlap. This supports the observation that size is an important aspect of clustering, once again showing that source processes are affecting similarity.

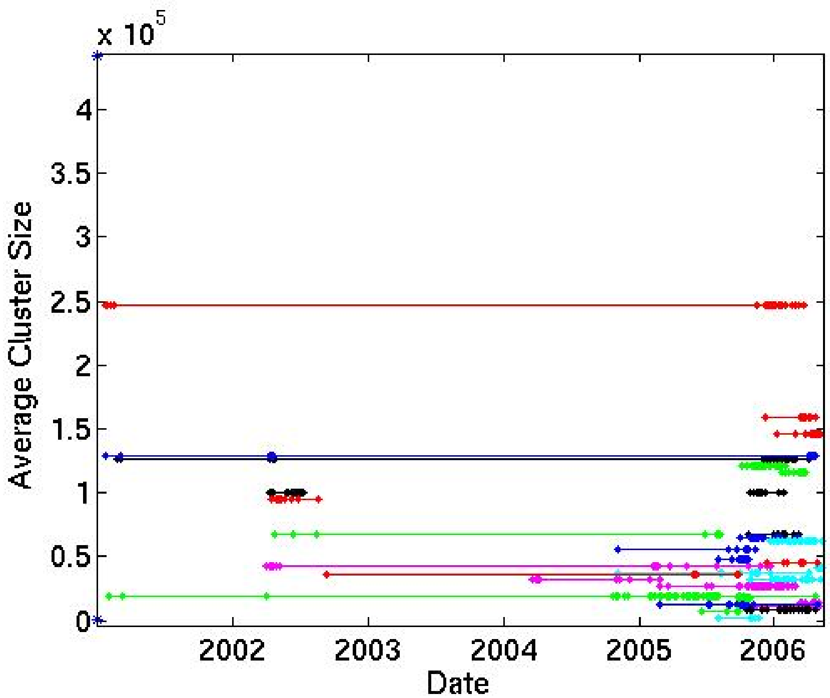

Figure 5.5 – E1S BB clusters plotted by the average size of the events (RMS amplitude in counts) within them. It is interesting that clusters of almost identical average size are active concurrently, indicating that more than pure event size influences waveform similarity. An example can be seen around 2002.5 for the red and black clusters near event size range 10^5.

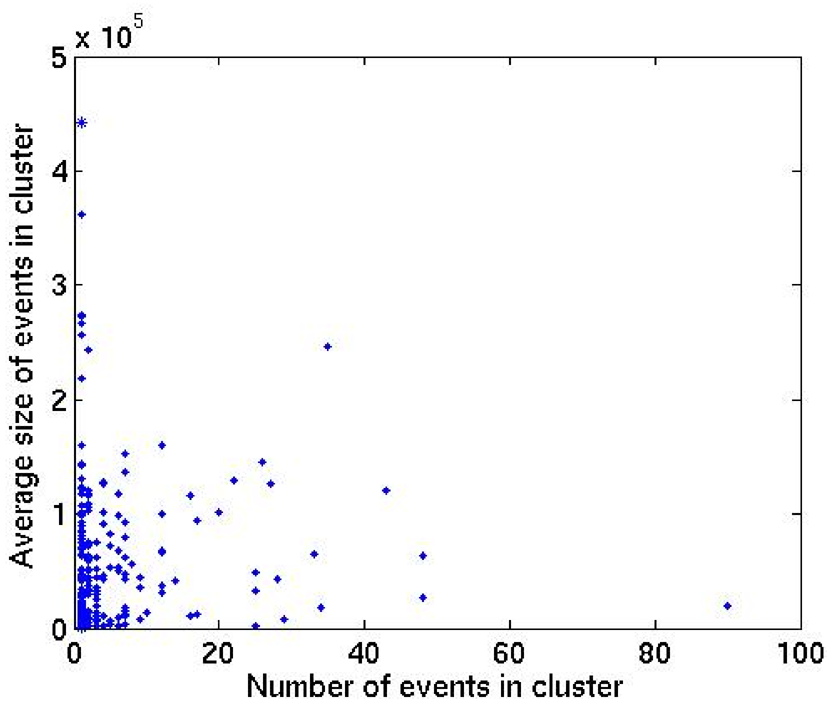

Figure 5.6 – Number of events in the E1S BB clusters verses the average size (RMS amplitude in counts) of constituent events.

and the smaller clusters to contain the largest size events. However, this was not the case. In fact one of the larger clusters contained many of the largest eruptions. It was also surprising how many of the smallest events did not cluster, or only clustered with one or two other events.

Even though the clusters were overlapping in time, and, in a few cases temporally extensive (Figure 5.1), I wanted to examine further to what extent single clusters were active at any give time. To study what particular clusters where active during discrete time periods, groups of 50 events were plotted using a bar plot (Figure 5.7 and 5.8) with the number of events from each cluster, during that period, plotted on the Y-axis. More often then not there was one cluster that was more active than the others for any particular group of events, but it was also not unusual for more than one cluster to be active during a given group (Figure 5.8). Interpreting this type of plot, it must be emphasized that the code takes a fixed 50 events every time, but does not take into account gaps in the data. It is not possible to see if the events in the active cluster are occurring all at once or distributed throughout the group of events**.** If the active cluster occurs for a unique period (without dissimilar events mixed in) it may indicate that while the source processes are variable, they may also be mutually exclusive, resulting in only one type of event occurring at a time.

Since there were several cases where clusters with similar size ranges were active at the same time (Figure 5.5) the characteristics of the individual clusters were further examined. First each event in the cluster was lined up using the iterative alignment program described in Chapter 3. Once the events in the cluster were lined up, the events were stacked to get a representative seismogram for the cluster. An aligned cluster and

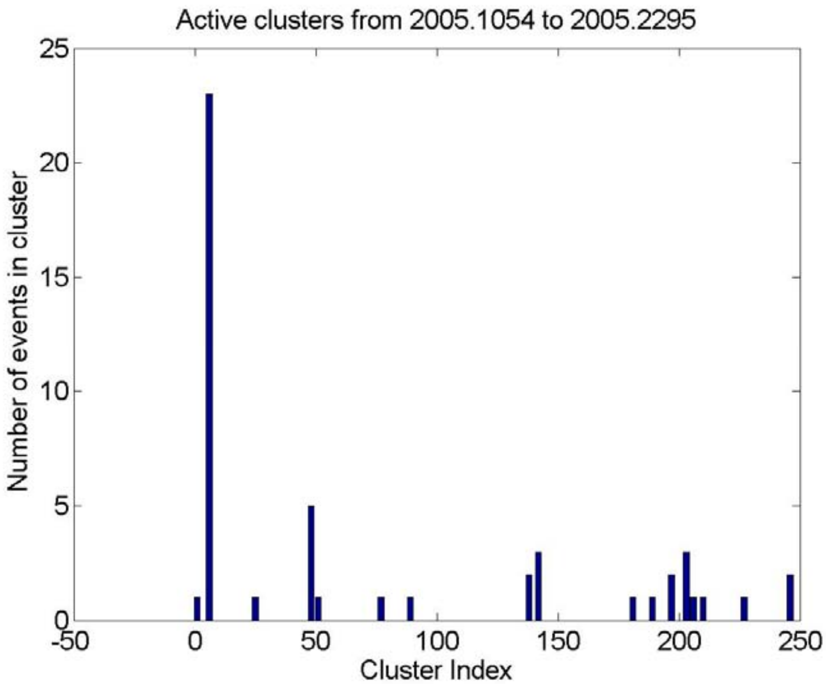

Figure 5.7 – Histogram of the most active clusters for a representative group of 50 events for station E1S BB that occurred during the indicated time periods. In this case Cluster 2 is by far the most active cluster. Once again the cluster index is arbitrary.

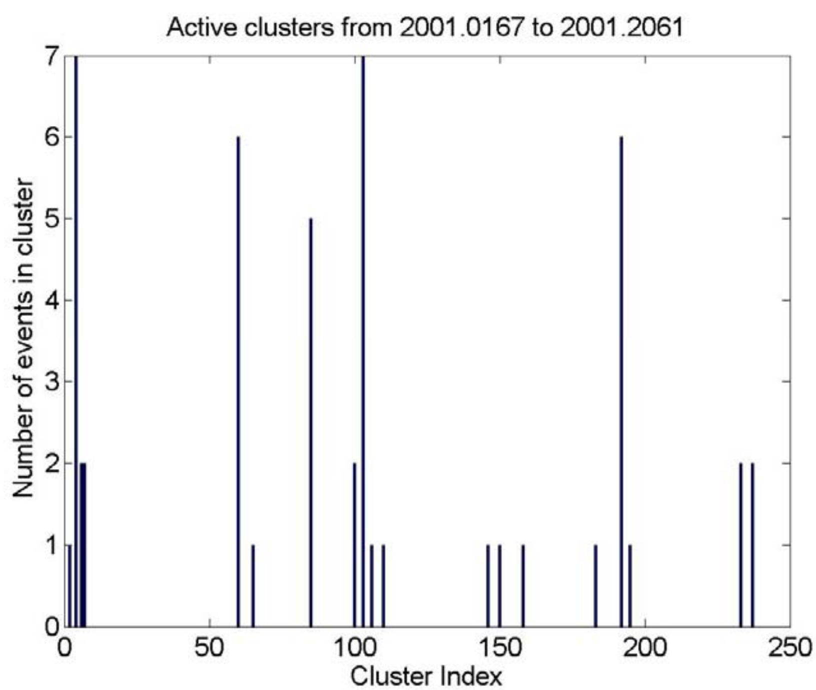

Figure 5.8 – Histogram of the most active clusters for a representative group of 50 events for station E1S BB during the indicated time period. Notice how, unlike Figure 5.7, this group of 50 events contains several active clusters, not just one dominant cluster.

representative stack can be seen in Figure 5.9. This plot allows for the examination of event variability within the clusters. The events were also plotted in time to examine the temporal distribution of the cluster (Figure 5.10). Once all of the stacks for the clusters had been created, the stacks were lined up and plotted (Figure 5.11) to see how they compared to each other.

To see if the coda clustered the same as the initial part of the seismogram, the time series for each event was broken into an initial part (600 samples; 15 s) and a coda (next 600 samples). The initial and coda sections of the time series were then clustered to assess differences between them, since the initial clustering analysis had been done using the whole seismogram. When this analysis was done for E1S BB, the initial window and coda window formed similar clusters. However when the same analysis was done for the station HOO, the initial part (first 600 samples) formed a large main cluster with only a few smaller clusters. On the other hand the coda part (second 600 samples) formed more, but small clusters. This is not entirely surprising since it had been observed that HOO appears to have some strong local site effects.

Videos of eruptions were examined to investigate what source differences might be causing the observed seismogram differences between clusters. During December 2005 a digital camera was installed at NKB, unfortunately it went down in mid-February 2006 during a strong storm and never came back up until servicing in Dec. 2006. However, it was possible to use the video collected during the active time period of December and January 2005 - 2006 to look for visual similarity within clusters. Cloudy days, steam within the crater, or ice on the camera also limited how many eruptions were

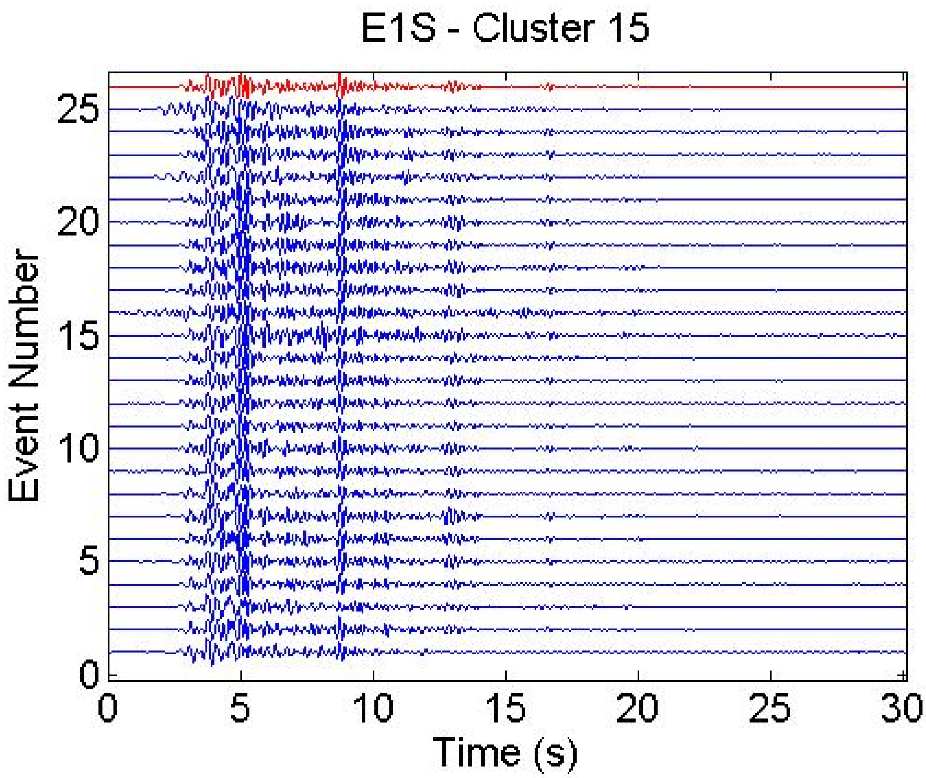

Figure 5.9 – A plot of one of the clusters from E1S BB. The red event at the top is the stack of all preceding events. The earliest events are on the bottom, and they get progressively younger towards the top. Notice the stability throughout the duration of the cluster.

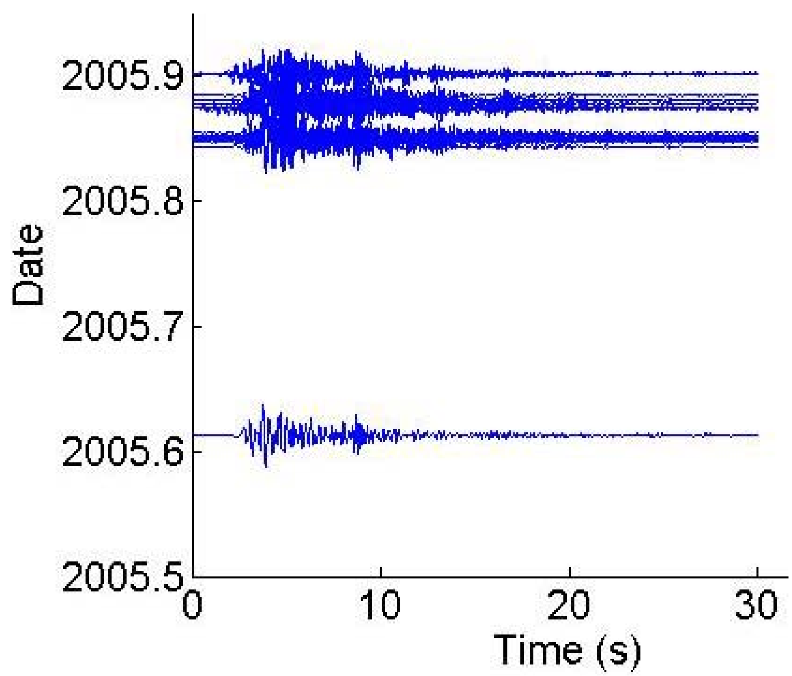

Figure 5.10 – The cluster of Figure 5.9 plotted with respect to time on the y-axis. This cluster comprises many of the smallest events in the catalogue (Figure 5.3 cluster 15).

well captured on video. However, there were enough good videos from the larger clusters to provide a sample of eruption characteristics for some of the clusters

Infrasound was another method used to try and understand source effects that might be correlated with seismic differences between events. The infrasound signal should be an accurate indication of the source of the eruptions since it only passes through the atmosphere before being recorded, whereas seismic signals are propagating through the highly heterogeneous interior of the volcano. Theoretically any differences seen in the infrasound would be essentially due to source processes only. Because of this, the infrasound was clustered to see if the infrasound clusters could be correlated with the seismic clusters from E1S BB. This would demonstrate that the cause of the variability was due to inconsistency of the source rather then changes within the volcano.

During the 2005/2006 field season, a new high dynamic range infrasound microphone was installed at the station RAY on Mount Erebus. Data from this microphone was recorded from the beginning of January through April 13, when RAY went down for the winter. The data from the other microphones around Mount Erebus was not usable for clustering because the dynamic range of those instruments was not high enough, resulting in clipping during many of the larger eruptions. For this reason clusters could only be created for the beginning of 2006. A correlation threshold of over 0.9 (0.97 being used in the end) had to be used in order to get the infrasound data to break into clusters. Creating clusters with the same filtering range as the broadband seismic data was also tried. An example of an infrasound cluster and its stack can be seen in Figure 5.12.

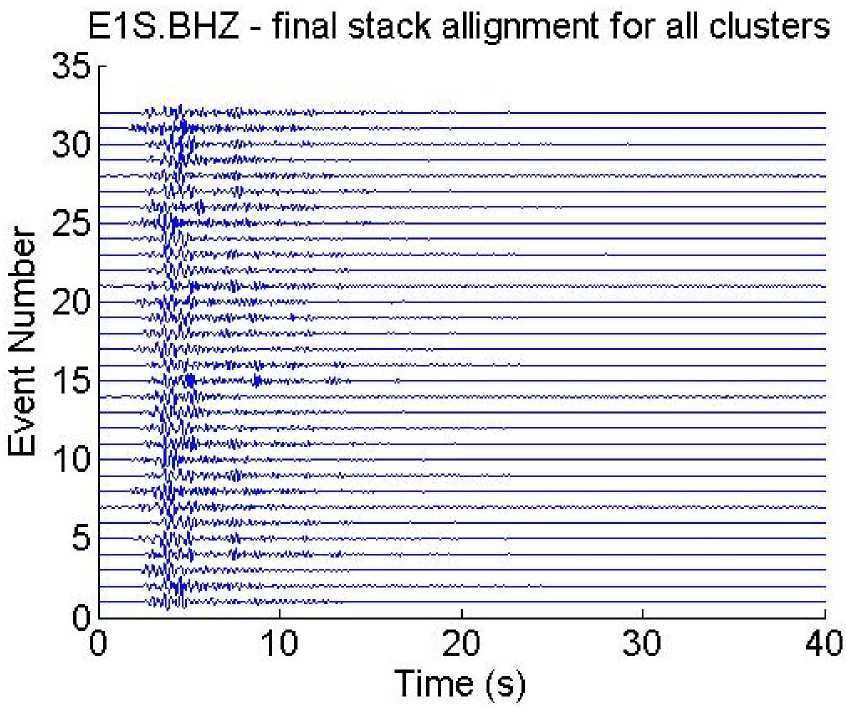

Figure 5.11 – All the stacks created from the E1S BB clusters and plotted to better see the degree of variability between clusters.

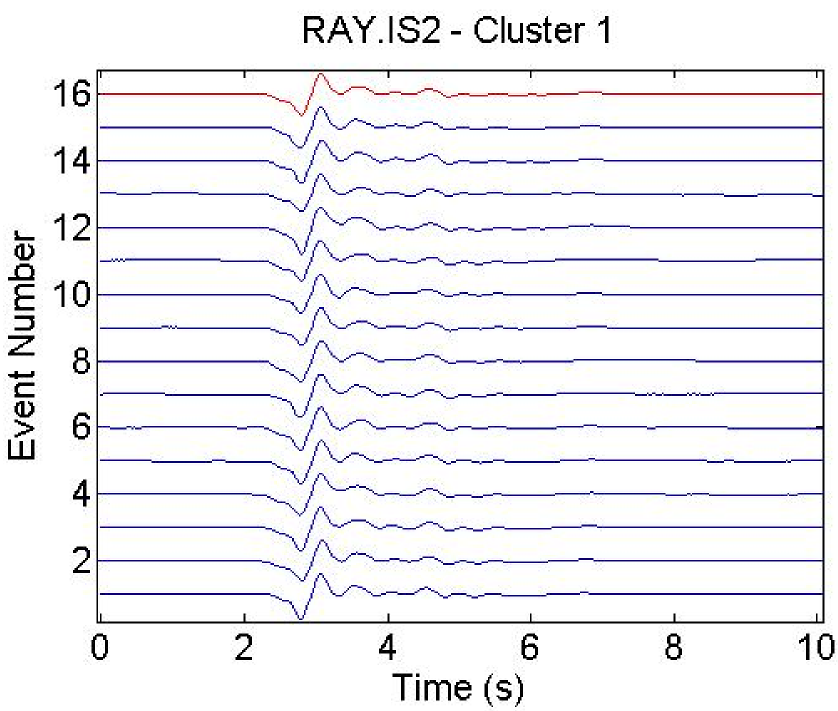

Figure 5.12 – A cluster of the infrasound data from RAY.IS2. The events in this cluster are extremely similar, with correlation coefficients above 0.97.

The array of infrasound detectors around the crater of Mount Erebus has been used to automatically locate the location of the eruption. This is done using a gridsearch program written by Jeff Johnson [*Jones et al.*, 2007]. The program uses infrasound detectors at RAY, E1S, and NKB to calculate the source location of the eruption. The program has the ability to show variability of eruption locations around the lava lake.

To see if the seismic clusters were originating from the same part of the lava lake, the location program was used for the seismic clusters. This was done by taking the clusters during the period the infrasound network was running, getting the corresponding infrasound data from that period, and finding the infrasound locations for those clusters. An example of the locations of one of the clusters can be seen in Figure 5.13.

Results

The clustering clearly shows that clusters are not mutually exclusive, but can be active simultaneously. Some clusters are also active over the entire span of the broadband network (Figure 5.1). This largely punctuated behavior suggests that the variability of the clusters is due to variations of the source because it is inconsistent with gradual changes in the volcano. The average size of the clusters and their error bars show that the clusters also contain discreet size ranges, and thus have some correlation with source size, the easiest measure of source heterogeneity (Figure 5.3). Clusters made up of smaller events have a tighter size range, while the bigger events have a larger size range. It was actually surprising how many of the largest events clustered together, including the largest eruption in the dataset (Figure 5.14). This suggests that some of the larger events also have common source components, such as characteristic changes in

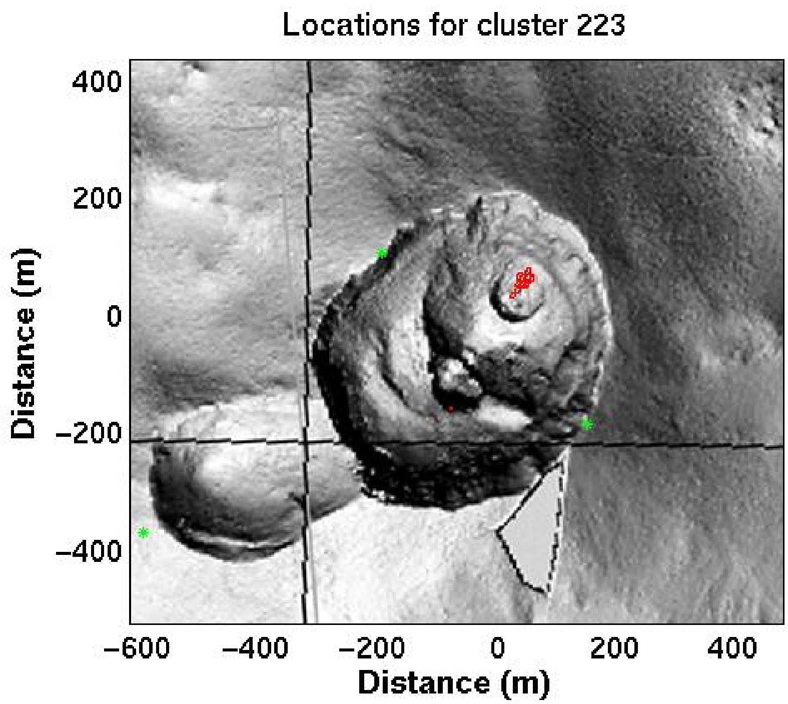

Figure 5.13 – Infrasonic locations for a cluster of strombolian events (red circles) determined by and *Jones et al.* [2007]. The green asterisks are the three stations used for obtaining the locations (lower left corner: E1S; at top: NKB, at right: RAY). Unfortunately the grid search is limited where it can plot the locations some many events are plotted on top of each other.

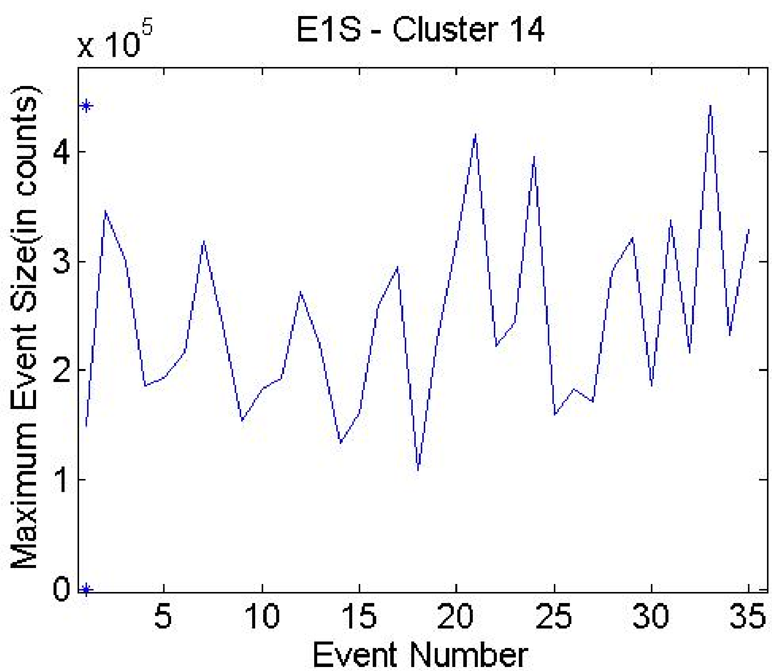

Figure 5.14 – Maximum event sizes for cluster 14. The asterisks on the top left and bottom left are the size of the largest and smallest eruptions recorded at E1S BB. This cluster contains the largest eruption recorded since the broadband network was installed.

frequency content, that lead to continued clustering at large event sizes, as opposed to larger events becoming more and more “orphans” that do not resemble any other events. The cluster of Figure 5.15 has one of the lowest average correlations, but it contains 35 ofthe largest events recorded since the broadband network was installed. The stack for this cluster (Figure 5.15) produces one of the least detailed codas of all of the stacks (Figure 5.11; stack 14). Apparently, many of the later reflections do not line up as well as they do for the smaller events, causing destructive interference and smoothing the stack.

There are some issues involved with clustering that make it difficult to establish the significance of the clustering results between stations and parts. The removal of a single event and can change the structure of event associations and thus affect how the clusters form. This is not entirely unexpected, but it does mean that to compare clusters, say at different stations, it is necessary to make sure to use the same events for each station. With stations going down at different times during the winter, that can be especially difficult to ensure. The decrease in the signal to noise ratio at stations further away from the lava lake also causes changes in correlations that result in difficulties for comparing clusters between stations.

Size is an obvious source of dissimilarity in this data set, as has also been shown in Chapters 3 and 4. However, figures 5.2 and 5.4 showed that there are a surprising number of clusters with very similar average sizes, especially when looking at the smaller events. This indicates that, while the size of the eruption is an important factor influencing how the events cluster, other source effects are apparently also responsible for some of the differences.

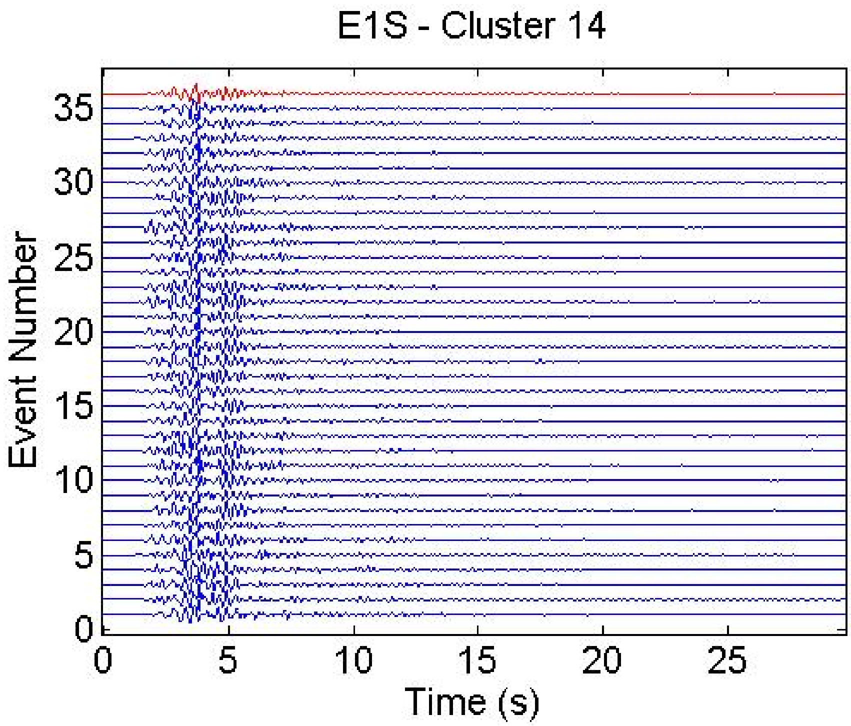

Figure 5.15 – Plot of cluster 14, which contains some of the largest (including the largest) events recorded at E1S BB since the broadband network was installed (stack shown in red). The y-axis shows the constituent event number.

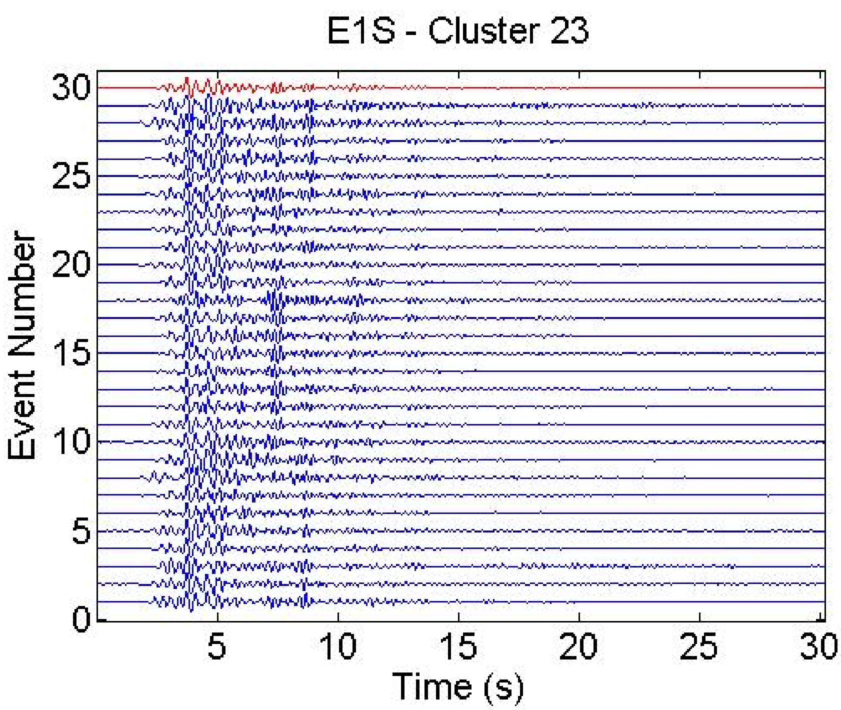

Figure 5.16 – Example E1S BB cluster number 23 (stack at top, in red) and its constituent subgroups. These subgroups are also shown with respect to their temporal spacing in Figure 5.17.

Looking at individual clusters I found that some groups were exceptionally similar throughout time (Figure 5.9), even when the cluster spanned the whole dataset (Figure 5.10). However, other clusters have what appear to be sub-groups within the cluster that change with time (Figure 5.16). The changes usually, but not always, occur between gaps in the data (Figure 5.17). The top subgroup in Figure 5.16 does not appear to coincide with a time gap. A higher correlation threshold would probably cause the subgroups in Figure 5.16 to break apart. Conversely, if the threshold were lowered some of the groups forming the similar stacks in Figure 5.11 would combine. Figure 5.11 also shows there are clusters that are significantly different from each other (ex. - stack 22 and 23). This is especially noticeable with the clusters containing the smallest events.

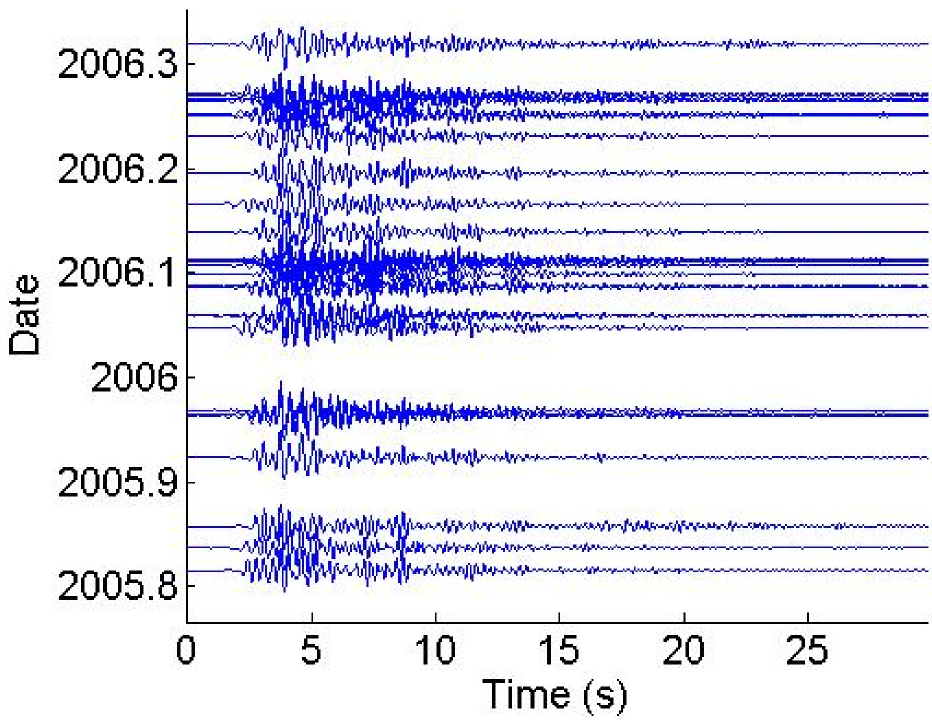

Figure 5.17 – The same cluster stack traces as Figure 5.16, but plotted as a function of time on the y-axis. Some of the changes visible on the previous figure appear to correspond to the events that occur in late 2005. However, the most recent period, 2006.05 – 2006.28, is particularly well sampled in time.

Intriguingly, the strong reflections/reflectors within individual clusters seem to change strength over time. An example of this is seen in Figure 5.16, where the amplitude of some scatterers is variable between subgroups. For further work, I recommend that analysis focus on these unusually similar groups that show this scatterer behavior.

When the videos for individual seismic clusters were examined, it was immediately noticeable that many clusters had similar size ranges. This was especially obvious for the clusters containing the smallest eruptions, which visually looked almost identical. There is some indication that clusters usually, but not always, had similar rupture characteristics and possibly similar bubble size, but more complete and exhaustive video data is necessary to investigate this adequately. There were some events that seemed like outliers, and these are probably events that barely cluster. There were some obvious differences between clusters as well. Some eruptions would cause a bulge in the lave lake that would then rupture, other times there would be little (rise of the overall level of the lava lake) or no warning and the rupture would burst through the surface of the lava lake. Examples of some different rupture characteristics can be seen in Figure 5.18. For the smaller eruptions, the location where the bubble rose to the surface was variable, but with the largest eruptions the bubble is so large that there is little variability. The eruptions seem to occur mainly in the lower 2/3 of the lava lake (with respect to the camera). The video of one of the outliers "orphans" from the clustering was examined (it didn't link with any other events (correlation of 0.1 or less)). This event turned out to be an ash eruption from a subsidiary vent (Figure 5.18).

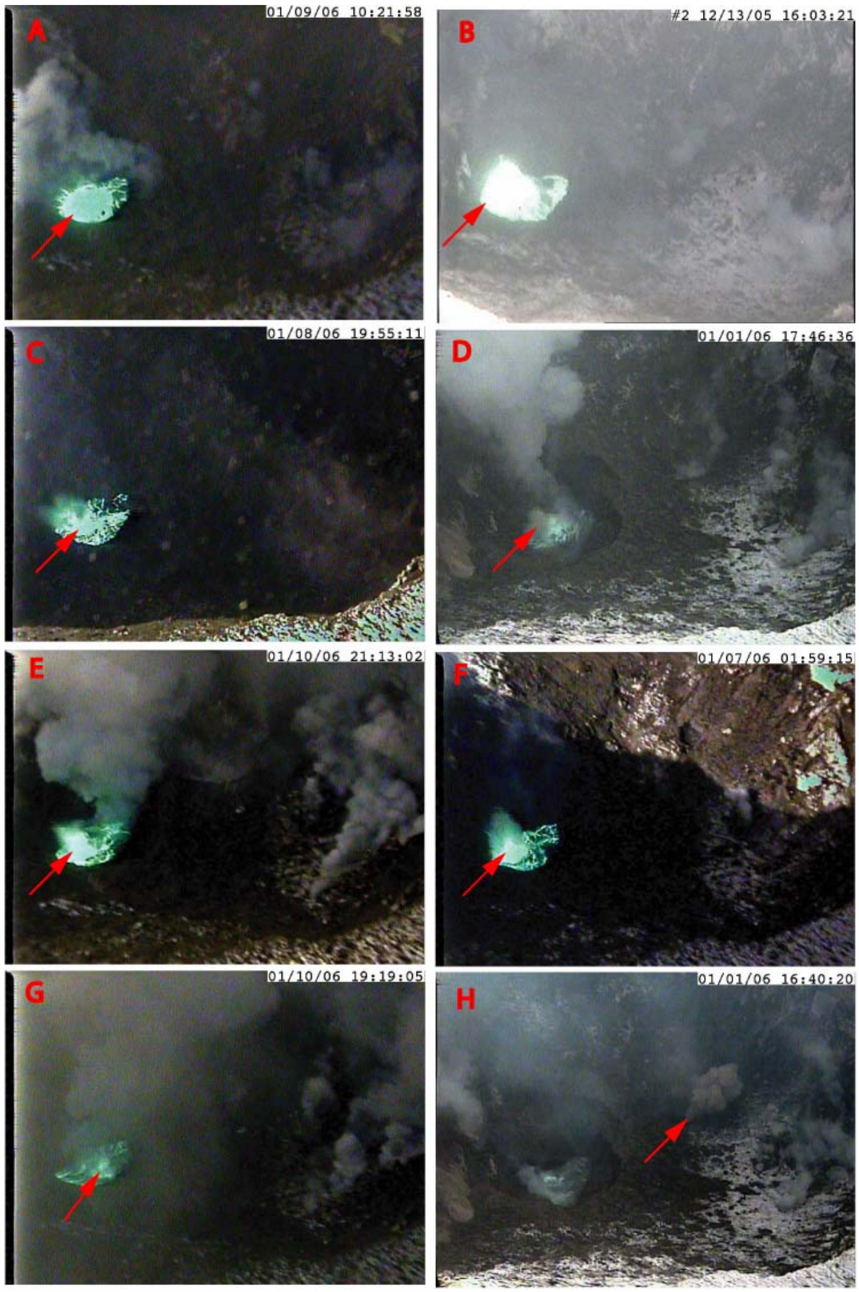

Figure 5.18 – Both A and B are from cluster of small events (cluster 15, 17 events), which bulge before bursting. A emerged from the bottom center of the lake, and B emerged from the bottom left corner. All events in this cluster looked very similar. C is a large event blowing out near the lower left side of the crater wall. There was no bulge before the eruption, and this event did not cluster with any other event. D is a typical large eruption. There was no bulge or warning before the eruption (except a slight rise in the level of the lava lake). E and F are two medium sized eruptions, with E bursting on the left side of the lava lake and F bursting in the center. Neither event produced a bulge before rupture. H is an ash eruption from a subsidiary vent. This event was orphaned (correlation coefficient < 0.1) during clustering.

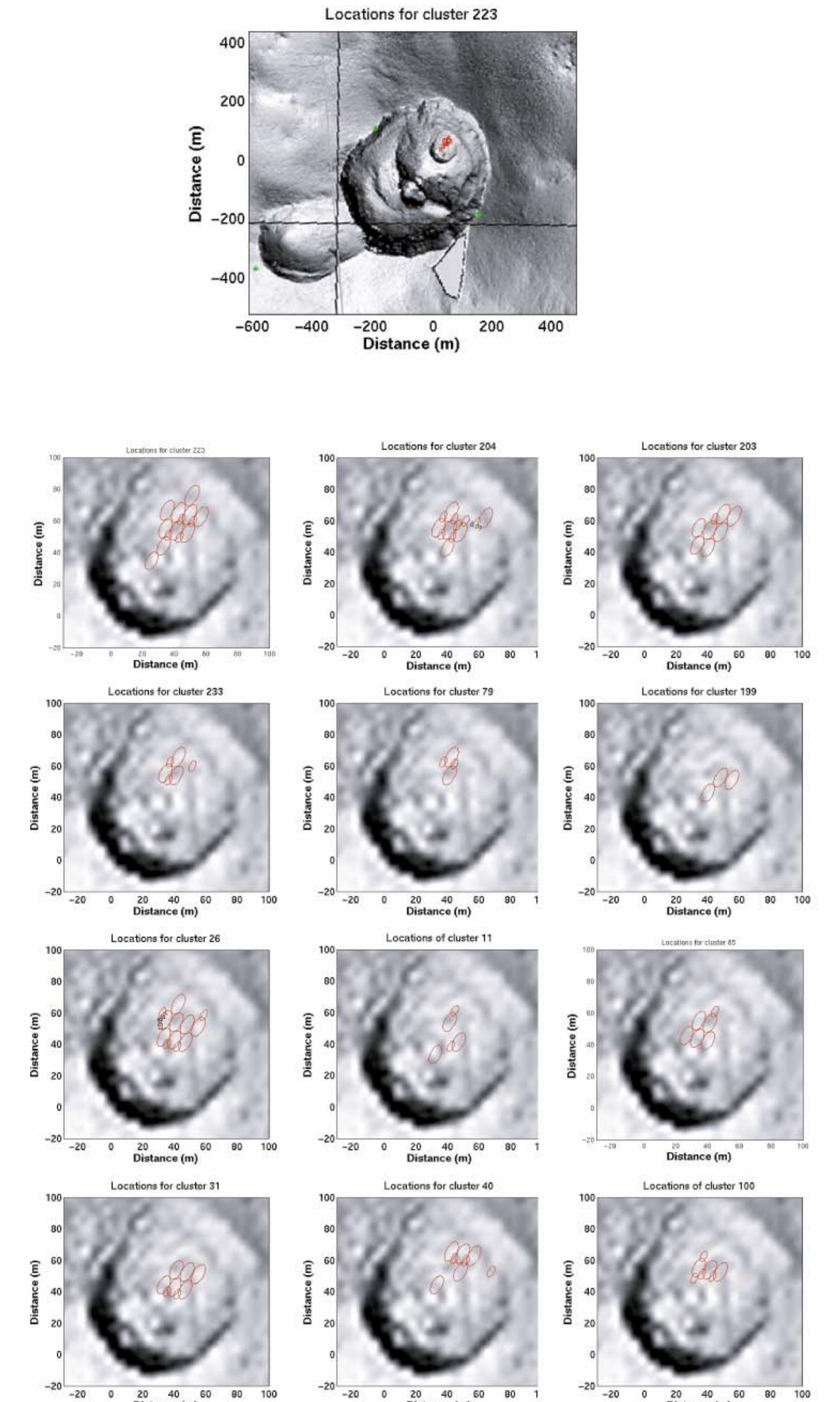

Figure 5.19 – Infrasound locations for the largest seismic clusters within the Inner Crater of Erebus, characterized by waveform similarity, recorded at E1S BB between January and April 2006 from *Jones et al.* [2007]. There does appear to be some variability in source locations, but there is significant overlap. Cluster 233 at the top of the page shows what the crater looks like before zooming in on the Inner Crater.

When the infrasound locations (determined by *Jones et al.* [2007]) of the seismic clusters were examined, there appeared to be a possible location preference for each cluster. However, the majority of events within a cluster overlapped the events in the other clusters (Figure 5.19). Unfortunately, the accuracy of the grid search program may not be high enough to produce robust results with this limited infrasound data set. The grid search spacing resolution is set at 5 meters right now. However, one sample of an infrasound time series equates to approximately 10 m of shockwave propagation. The resolution of the grid search program can be increased, but due to the ~10 m propagation for each (40 samples/s) sample, the improved resolution would be insignificant (J. Johnson, pers. com.).

When the time series for the infrasound were clustered, they had an expected very high degree of similarity (Figure 5.20). The only places where there were significant variations was in the first motion rise time character, and the amplitude of the first motion (oscillation). After that the clusters were almost identical, including an apparent reflection off the crater wall at about 6.5 seconds (Figure 5.20) [*Jones et al.*, 2007]. It is interesting to note that size does not affect how the data is broken into clusters near as much for the infrasound, as it does for the seismic data (Figure 5.21). This suggests that the extent of lava lake disruption may be a contributor to seismogram differences. From looking at the video of the eruptions, it is evident that there are several ways for an eruption to initiate in the early bubble burst phase (bulging of the lava lake, no pre eruptive bulge, and vertical or angled rupture of the bubble). These differences may be what is causing the initial differences at the beginning of the infrasound signal. It is also useful to point out that the infrasound locations appear to be insensitive the rupture initiation point, with the location of the bubble centroid being more important (J. Johnson, pers. com.)

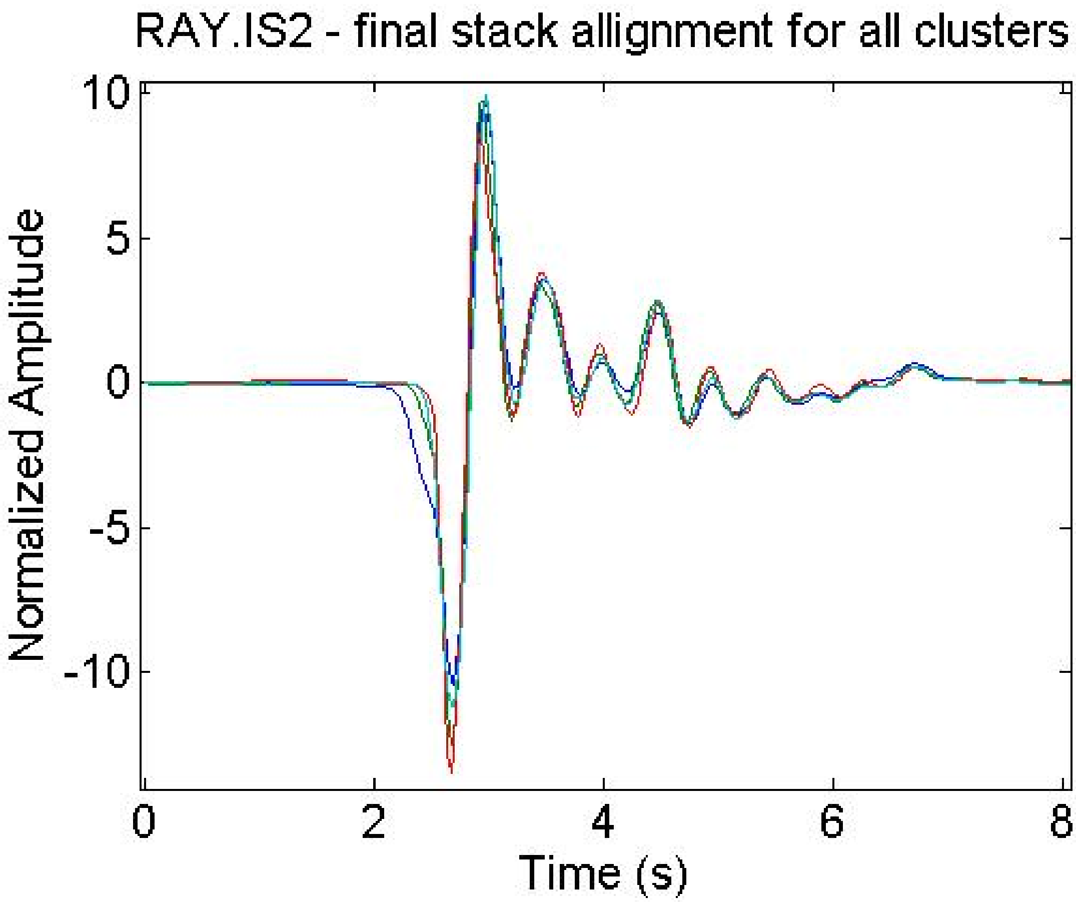

Figure 5.20 – Four normalized RAY.IS2 unfiltered infrasound clusters plotted on top of each other. The only difference is in how fast the first motion began, and the amplitude of the fist motion down and up. The infrasound coda may be influenced by crater wall echoes. Variability in the early infrasound signal may represent differing source characteristics related to rapid acceleration of the erupting bubble (J. Johnson, pers. com.).

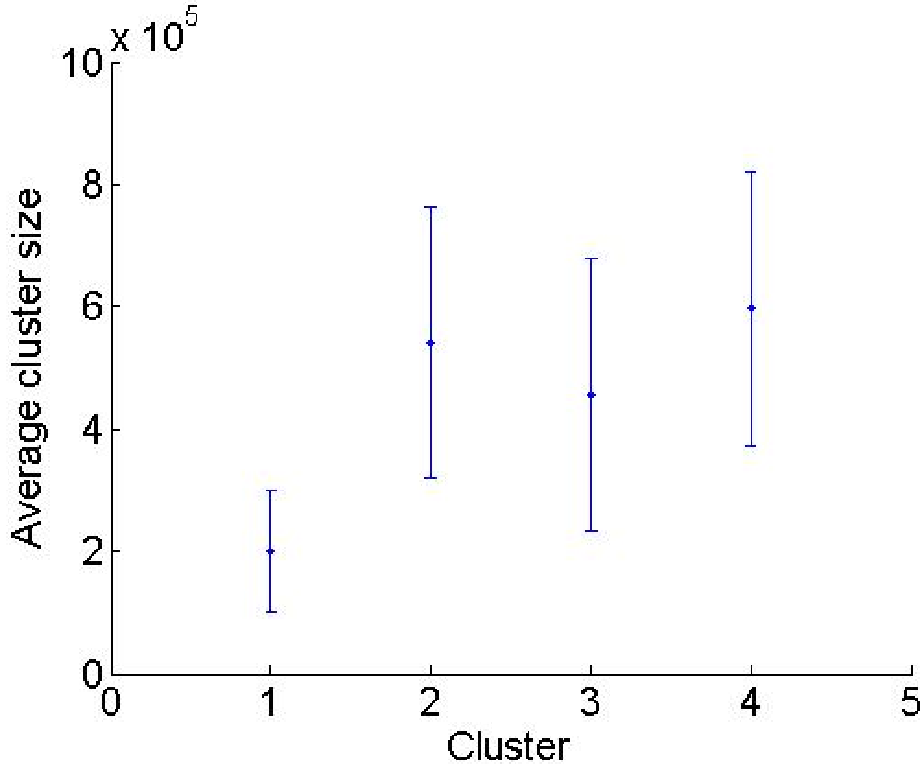

Figure 5.21 – Size ranges of the clusters for RAY.IS2. Except for the cluster containing the smallest events, size does not seem to be a significant factor in how the infrasound events cluster for this small set of event groups.

CHAPTER 6

Discussion and Conclusions

Discussion

It was possible to reproduce a similar decorrelation of the coda in 1999-2000 (the so-called "Gret period") as reported by *Gret et al.* [2005]. However, the analysis also showed a hint of decorrelation of the initial part during this period as well, which is not shown in the author's paper. We conclude that the results of *Gret et al.* [2005] were incomplete, in that other effects (besides changes in the medium) are now shown to be important. Particularly, clipping (for the short period station) and event size were two important sources of seismogram variability. Clipping was the most important effect that had been overlooked. The initial parts of the time series are clipped for many events, with the clipping being more pronounced as the events got larger in January 2000. This created an artificial similarity for the initial part of the time series. Performing the same analysis on the unclipped high-dynamic range broadband data, from the same period, showed that the decorrelation of the coda occurred in unclipped data, but the initial part of the seismogram also showed a decorrelation. The decorrelation of the seismograms over time was also shown to be strongly correlated with an increase in event size, as is shown by the moving window analysis (Chapter 3).

The moving window analysis showed that there is only one band of relatively consistent high correlation in the initial part of the seismogram that is stable through time (3 s for broadband data set, and 4 s for the short period data from the Gret period). The moving window analysis showed that even much of the initial part, not just the coda, is susceptible to variability. It was also possible to show that there are stable bands of correlation within the coda that can persist for years. When the lags for the band of strong correlation were examined, they were typically zero (or very close to zero), showing that the timing of these reflectors in the subsurface is stable over time. The lags for the areas of decorrelation, relative to the master/stack, show time bands of negative and positive lags that are stable through time. The lack of increasing or decreasing lags later in the coda suggests that the path is surprisingly stable (no changes in the medium).

By plotting up the maximum correlations of bands of strong reflectors versus event size, it was also possible to show that size is an important factor for some of the bands. This size-associated variability does not just affect the coda, but is also seen within 3 s or less of the directly arriving energy. It is very likely that size is not the only factor that affects the correlations of the bands, but it does appear to be the most important. Using the scatter analysis it was also possible to show that these bands of high correlation are not due to energy trapped in the magma conduit, but instead arise from scatterers that are at appreciable distance from the explosion source (of the order of km).

It was also possible to use local data from the Socorro area to show that these bands of high correlation could be caused by the large magmatic system of the volcano. It is thus consistent to suppose that at least some of the strong reflections seen at Mount

Erebus are also due to similar reflections, and possibly trapped energy, in the magma body (bodies?) under Mount Erebus.

Clustering the whole seismogram showed that the eruption seismograms break into discrete clusters. Looking at the events in the individual clusters, and looking at stacks of each cluster, showed that there could be significant and obvious differences between clusters. The clustering analysis also shows that source effects are very important in clustering. The clearest factor that affects how the events cluster is, again, event size. However, because there can be more than one cluster with the same size range, there must also be other source effects responsible for changes in the signal.

The most obvious secondary source of variability is the location of the gas slug in the lave lake when it ruptures. Plotting up grid search infrasound locations for the seismic clusters determined in associated research at NM Tech, and looking at videos of the events in the cluster, showed that location may be affecting clustering.

The video clusters also generally showed a tendency for the gas slugs to rupture in the same region of the lava lake. There were some events that looked like outliers, and these may be events that barely cluster above the threshold. In fact, looking at the seismograms of events within a single cluster and examining the cluster structures showed that there can be several subfamilies of events within a single cluster. For the largest eruptions, the gas slug appears to fill most of the lake, limiting source effects from variability in gas slug location. Other source variability seen from the video clusters is that the lava lake sometimes bulges before the bubble ruptures. The possibility of more then one active cluster being active at a time, shown through the cluster dominance analysis, indicates that the source processes are variable and not mutually exclusive.

A few smaller clusters were also shown to exist over long periods of time, indicating gradual changes in the volcano are not responsible for changes in how the clusters form. It was possible to show that the clusters can persist for years, and that more than one cluster can be active at the same time. Even clusters with the same average size range can coexist. These results strengthen the argument that the clusters are due to source processes, rather than controlled by gradual changes in the structure of the volcano. From clustering the data at the broadband station EE1S, it became apparent that the Gret period just happened to coincide with two distinct clusters with almost no overlap. It appears that the Gret period was a time of unusual relative source stability as well.

Clustering the initial part and coda of the time series separately showed that some of the events from one cluster at E1S would cluster at the other stations, but many would also break into other clusters. Some of the difficulties here are probably due to the clustering variability mentioned in the previous section. It is not surprising that the coda clusters in a similar manner as the initial part since there are bands of stability that within the coda that can be stable for many years. This, again, indicates that there are few, if any, changes to the path, making the source processes the basis of variability seen in the clusters.

The infrasound had been expected to be a good indicator of source processes since it only passes through the air. When the infrasound was clustered (with a very high correlation threshold), it only broke into 4 very similar clusters. Only the initial motion showed any variability, possibly due to rupture processes (bulge vs. no bulge). The initial motion did not result in a change in the coda, which was surprising. It was also interesting to see that except for the smallest eruptions, size had no effect on how the infrasound clustered. I must conclude that there is little or no relation between the seismic clusters and the infrasound clusters. The seismograms are heavily affected by the convolved propagation response and source effects, while clustering of infrasound appears to only be exclusively a measure of source characteristics.

Conclusions

This research has resulted in several conclusions. First, the Gret et al. results were premature. Second, size is a very important factor influencing event similarity. Third, the volcano is surprisingly stable through time, to the best of our ability to probe it using Strombolian eruption signal as repeating events. While the volcano has a highly repeatable source, it still shows significant source variability that must be accommodated for these signals to be used for coda wave interferometry. More refined studies in this regard should be restricted to a clustered group of only the most similar seismograms. However, the lack of trends in the lags and other coda features (seen in the moving window analysis) and the overall heterogeneity of source processes, suggests that it is unlikely that coda wave interferometry for medium change recovery will work at Mount Erebus while it remains in its present state.

REFERENCES

Aki, K., Analysis of the seismic coda of local earthquakes as scattered waves, *JGR*, *74* (2), 615-631, 1969.

Aki, K., and B. Chouet, Origin of Coda Waves: Source, Attenuation, and Scattering Effects, *Journal of Geophysical Research*, *80* (23), 3322-3342, 1975.

Antolik, M., R.M. Nadeau, R.C. Aster, and T.V. McEvilly, Differential Analysis of Coda Q Using Similar Microearthquakes in Seismic Gaps. Part 2: Application to Seismograms Recorded by the Parkfield High Resolution Seismic Network, *Bulletin of the Seismological Society of America*, *86* (3), 890-910, 1996.

Aster, R., B. Borchers, and C. Thurber, *Parameter Estimation and Inverse Problems*, 301 pp., Elsevier Academic Press, 2004a.

Aster, R., S. Mah, P. Kyle, W. McIntosh, N. Dunbar, J. Johnson, M. Ruiz, and S. McNamara, Very long period oscillations of Mount Erebus Volcano, *Journal of Geophysical Research*, *108* (B11), 1-20, 2003.

Aster, R., W. McIntosh, P. Kyle, R. Esser, B. Bartel, N. Dunbar, B. Johns, J. Johnson, R. Karstens, C. Kurnik, M. McGowan, S. McNamara, C. Meertens, B. Pauly, M. Richmond, and M. Ruiz, Real-Time Data Received from Mount Erebus Volcano, Antarctica, *EOS*, *85* (10), 97-104, 2004b.

Aster, R., and C. Rowe, Automatic phase pick refinement and similar event association in large seismic datasets, in *Advances in Seismic Event Location*, edited by C.

Thurber, E. Kissling, and N. Rabinowicz, pp. 231-263, Kluwer Academic Publishers, Dordrecht, 2000.

Aster, R., P. Shearer, and J. Berger, Quantitative measurements of shear-wave polarizations at the Anza seismic network, southern California -- implications for shear-wave splitting and earhtquake prediction, *Journal of Geophysical Research*, *95* (12), 12,449-12,474, 1990.

Aster, R.C., G. Slad, J. Henton, and M. Antolik, Differential Analysis of Coda Q Using Similar Microearthquakes in Seismic Gaps. Part 1: Techniques and Application to Seismograms Recorded in the Anza Seismic Gap, *Bulletin of the Seismological Society of America*, *86* (3), 868-889, 1996.

Balch, R.S., Earthquake Swarm Studies in the Central Rio Grande Rift: Specific and General Results, University of New Mexico, Socorro, 1997.

Dibble, R., velocity modeling in the erupting magma column of Mount Erebus, Antarctica, in *Volcanological and Environmental Studies of Mount Erebus, Antarctica, Antarctic Research Series, American Geophysical Union*, edited by P. Klye, pp. 17-32, 1994.

Dominguez, T., F. Flores, and G. Reyes, Temporal change in coda wave attenuation observed at Volcan de Colima, Mexico before the 1998 eruption, *Journal of Volcanology and Geothermal Research*, *125*, 215-223, 2003.

Fehler, M., P. Roberts, and T. Fairbanks, A temporal change in coda wave attenuation observed during an eruption of Mount St. Helens, *JGR*, *93* (B5), 4367-4373, 1988.

Giggenbach, W.F., P.R. Kyle, and G.L. Lyon, Present volcanic activity on Mt Erebus, Ross Island, Antarctica, *Geology*, *1*, 135-135, 1973.

Gret, A., R. Snieder, R.C. Aster, and P.R. Kyle, Monitoring rapid temporal change in a volcano with coda wave interferometry, *GRL*, *23*, 2005.

Gret, A., R. Snieder, and U. Ozbay, Monitoring in situ stress changes in a mining environment with coda wave interferometry, *Geophysical Journal International*, *167*, 504-508, 2006a.

Gret, A., R. Snieder, and J. Scales, Time-lapse Monitoring of Rock Properties with Coda Wave Interferometry, *Journal of Geophysical Research*, *111*, B03305 1-11, 2006b.

Hartse, H.E., Simultaneous hypocenter and velocity model estimation using direct and reflected phases from microearthquakes recorded within the central Rio Grande Rift, New Mexico, New Mexico Tech, Socorro, 1991.

Jones, K., J. Johnson, R. Aster, P. Kyle, and W. McIntosh, Infrasonic tracking of large bubble bursts and ash venting at Erebus Volcano, Antarctica, *J. Volcanol. Geotherm. Res.*, *submitted*, 2007.

Karageorgi, E., R. Clymer, and T. McEvilly, Seismological studies at Parkfield: I. Search for temporal variations in wave propagation using Vibroseis, *Bulletin of the Seismological Society of America*, *82*, 1388-1415, 1992.

Kyle, P., Preface, in *Volcanological and Environmental Studies of Mount Erebus, Antarctica*, edited by P. Kyle, pp. xiii-xiv, 1994.

Pandolfi, D., C.J. Bean, and G. Saccorotti, Coda wave interferometric detection of seismic velocity changes associated with the 1999 M = 3.6 event at Mt. Vesuvius, *Geophysical Research Letters*, *33*, L06306 1-4, 2006.

Peng, Z., and Y. Ben-Zion, Temporal Changes of Shallow Seismic Velocity Around the Karadere-Duzce Branch of the North Anotolian Fault and Strong Ground Motion, *Pure and Applied Geophysics*, *163*, 567-600, 2006.

Revenaugh, J., The contribution of topographic scattering to teleseismic coda in Southern California, *Geophysical Research Letters*, *22* (5), 543-546, 1995.

Rowe, C.A., Seismic Velocity Structure and Seismicity of Mount Erebus Volcano, Ross Island Antarctica, University of Alaska, Fairbanks, 1988.

Rowe, C.A., R.C. Aster, B. Borchers, and C.J. Young, An Automatic, Adaptive Algorithm for Refining Phase Picks in Large Seismic Data Sets, *Bulletin of the Seismological Society of America*, *92* (5), 1600-1674, 2002.

Rubinstein, J.L., and G.C. Beroza, Evidence for Widespread Nonlinear Strong Ground Motion in the Mw 6.9 Loma Prieta Earthquake, *Bulletin of the Seismological Society of America*, *94* (5), 1595-1608, 2004.

Ruiz, M., Analysis of Tremor Activity At Mt. Erebus Volcano, Antarctica, New Mexico Tech, Socorro, 2004.

Skov, M., Digital Seismic Data Acquisition and Processing as Applied to Seismic Networks in the Rio Grande Rift and on Mount Erebus, Antarctica, New Mexico Institute of Mining and Technology, Socorro, 1994.

Snieder, R., Coda Wave Interferometry, in *2004 McGraw-Hill Yearbook of Science & Technology*, pp. 54-56, McGraw-Hill, 2004.

Snieder, R., The Theory of Coda Wave Interferometry, *Pure and Applied Geophysics*, *163*, 455-473, 2006.

Snieder, R., A. Gret, H. Dauma, and J. Scales, Coda Wave Interferometry for Estimating Nonlinear Behavior in Seismic Velocity, *Science*, *295*, 2253-2255, 2002.

Snieder, R., and M. Hagerty, Monitoring change in volcanic interiors using coda wave interferometry: Application of Arenal Volcano, Costa Rica, *Geophysical Research Letters*, *31*, L09608, 2004.

Snieder, R., and M. Vrijlandt, Constraining the source separation with coda wave interferometry: Theory and application to earthquake doublets in the Hayward fault, California, *Journal of Geophysical Research*, *110*, B04301 1-15, 2005.

Stankova, J., S.L. Bilek, R.C. Aster, and C.A. Rowe, Characteristics of the October 2005 Microearthquake Swarm in the Socorro Region, New Mexico, *Eos Trans. AGU*, *87*, 2006.

Waldhauser, F., and W.L. Ellsworth, A Double-Difference Earthquake Location Algorithm: Method and Application to the Northern Hayward Fault, California, *Bulletin of the Seismological Society of America*, *90* (6), 1353-1368, 2000.

Wegler, U., Analysis of multiple scattering at Vesuvius volcano, Italy, using data of the TomoVes active seismic experiment, *Journal of Volcanology and Geothermal Research*, *128*, 45-63, 2003.

Wegler, U., and B.-G. Luhr, Scattering behavior at Merapi volcano (Java) revealed from an active seismic experiment, *Geophysical Journal International*, *145*, 579-592, 2001.

Appendix 1

Broadband Events Used in Research

Date yyyy-mm-dd hh:mm:ss	Maximum Amplitude Vertical counts at station E1S BB (for conversion to ground velocity, see Table 2.1).
2001-01-06 02:59:58	5.05E+04
2001-01-06 15:59:57	6.90E+04
2001-01-07 02:59:53	2.87E+04
2001-01-07 07:59:59	3.50E+04
2001-01-08 01:59:51	2.95E+04
2001-01-08 13:59:57	5.40E+04
2001-01-08 15:59:54	7.14E+04
2001-01-08 18:59:53	6.39E+04
2001-01-08 20:59:55	7.30E+04
2001-01-09 05:59:55	1.44E+05
2001-01-10 04:00:00	2.68E+05
2001-01-10 16:59:55	1.86E+05
2001-01-11 10:59:52	1.70E+05
2001-01-11 20:59:58	1.46E+05
2001-01-12 13:59:54	1.60E+05
2001-01-15 05:59:57	1.99E+05
2001-01-18 20:59:56	6.02E+04
2001-01-22 01:59:59	1.03E+05
2001-01-22 21:59:53	2.92E+04
2001-01-22 23:00:00	3.14E+04
2001-01-25 09:59:54	1.50E+05
2001-01-25 23:59:57	3.47E+05
2001-01-26 21:59:53	1.53E+05
2001-01-30 04:59:53	1.26E+05
2001-01-30 20:59:52	9.39E+04
2001-02-01 06:59:53	1.66E+05
2001-02-01 21:59:54	4.71E+04
2001-02-03 01:59:58	3.62E+05
2001-02-04 10:59:53	3.00E+05
2001-02-06 00:59:54	1.52E+05
2001-02-06 16:59:51	1.17E+05
2001-02-07 13:59:52	1.86E+05
2001-02-10 16:00:00	1.26E+05
2001-02-13 08:59:53	8.01E+04
2001-02-14 05:59:57	1.44E+05
2001-02-14 17:59:52	1.94E+05
2001-02-18 03:00:00	1.21E+05
2001-02-18 04:00:00	1.78E+05
2001-02-25 04:59:58	5.56E+04
2001-02-25 11:59:59	1.31E+05
2001-03-01 15:59:59	9.14E+04
2001-03-02 17:00:00	1.06E+05
2001-03-04 00:59:55	1.51E+05
2001-03-05 06:00:00	6.45E+04
2001-03-06 02:59:57	1.05E+05
2001-03-07 08:59:58	1.18E+05
2001-03-08 03:59:59	9.03E+04
2001-03-08 22:59:57	5.84E+04
2001-03-09 10:59:58	2.70E+04
2001-03-16 04:59:52	4.29E+04
2001-04-05 19:59:57	1.44E+05
2001-04-06 02:59:55	4.43E+04
2002-03-17 21:00:00	5.04E+04
2002-03-18 04:00:00	1.71E+05
2002-04-01 06:59:54	1.57E+05
2002-04-01 07:59:58	2.28E+04
2002-04-02 17:59:55	4.44E+04
2002-04-06 16:59:57	5.53E+04
2002-04-08 10:59:54	8.58E+04
2002-04-08 18:00:00	9.08E+04
2002-04-08 18:59:56	1.63E+05
2002-04-10 15:00:00	1.18E+05

2002-04-11 11:59:57	2.01E+05
2002-04-11 13:59:57	1.00E+05
2002-04-12 06:59:54	8.10E+04
2002-04-12 07:59:59	1.01E+05
2002-04-12 08:59:57	4.74E+04
2002-04-12 21:59:57	8.50E+04
2002-04-13 09:59:57	2.79E+05
2002-04-13 19:00:00	5.15E+04
2002-04-17 03:00:00	9.34E+04
2002-04-17 06:59:57	4.72E+04
2002-04-18 19:59:54	4.20E+04
2002-04-19 04:59:57	7.48E+04
2002-04-19 15:59:59	7.53E+04
2002-04-20 02:59:51	1.90E+05
2002-04-20 18:59:59	1.42E+05
2002-04-21 00:59:59	1.19E+05
2002-04-22 00:59:51	1.38E+05
2002-04-22 17:59:54	1.60E+05
2002-04-23 11:59:59	1.39E+05
2002-04-24 03:59:56	1.10E+05
2002-04-25 00:59:53	1.84E+05
2002-04-26 03:59:59	1.60E+05
2002-04-29 05:59:56	7.25E+04
2002-04-29 06:59:56	8.51E+04
2002-04-29 09:59:59	1.18E+05
2002-04-29 10:59:52	4.89E+04
2002-04-30 23:59:53	4.58E+04
2002-05-04 10:59:58	6.40E+04
2002-05-04 18:59:51	8.66E+04
2002-05-04 20:59:59	1.83E+05
2002-05-05 17:59:51	5.26E+04
2002-05-09 23:59:59	1.25E+05
2002-05-11 07:00:00	4.07E+04
2002-05-11 17:59:55	1.02E+05
2002-05-13 03:59:59	1.15E+05
2002-05-13 08:59:59	6.90E+04
2002-05-13 16:59:59	4.29E+04
2002-05-14 02:59:59	6.91E+04
2002-05-18 17:00:00	7.46E+04
2002-05-19 19:59:59	5.13E+04
2002-05-20 11:59:59	8.35E+04
2002-05-22 10:59:54	8.60E+04
2002-05-24 09:59:51	1.05E+05
2002-05-28 05:59:51	6.14E+04
2002-05-30 07:59:57	5.65E+04
2002-06-03 08:59:59	3.92E+04
2002-06-05 05:59:56	2.16E+05
2002-06-06 19:59:58	1.29E+05
2002-06-08 10:59:57	1.05E+05
2002-06-08 15:00:00	9.95E+04
2002-06-09 14:00:00	1.08E+05
2002-06-10 02:59:54	7.33E+04
2002-06-11 15:59:54	4.28E+04
2002-06-11 16:59:54	4.91E+04
2002-06-13 19:59:55	6.25E+04
2002-06-14 03:59:54	1.19E+05
2002-06-15 04:59:59	1.24E+05
2002-06-15 08:59:57	1.27E+05
2002-06-16 12:00:00	1.43E+05
2002-06-22 14:59:56	1.19E+05
2002-06-23 12:59:52	6.83E+04
2002-06-23 19:59:52	8.93E+04
2002-06-26 05:59:59	5.75E+04
2002-07-02 07:00:00	1.39E+05
2002-07-03 09:59:56	1.03E+05
2002-07-03 15:59:59	1.04E+05
2002-07-04 05:59:59	1.37E+05
2002-07-05 08:59:53	1.67E+05
2002-07-08 09:59:54	6.26E+04
2002-07-11 23:59:55	1.29E+05
2002-08-16 01:59:56	1.13E+05
2002-08-16 02:59:59	8.19E+04
2002-08-19 06:59:53	5.50E+04
2002-08-22 21:59:53	6.89E+04
2002-09-03 23:59:53	7.47E+04
2002-09-10 00:59:51	7.15E+04
2002-09-10 06:59:53	5.18E+04
2002-09-10 09:59:54	2.81E+04
2002-09-19 02:59:52	4.19E+04
2004-02-22 18:59:46	4.11E+04
2004-03-18 09:59:53	4.28E+04
2004-03-19 07:59:54	2.08E+04
2004-03-19 15:59:57	2.70E+04
2004-03-21 23:59:58	2.79E+04
2004-03-25 02:59:52	1.85E+04
2004-03-25 17:59:56	4.67E+04
2004-03-25 23:59:53	3.78E+04
2004-03-28 09:59:56	4.38E+04
2004-03-30 19:59:54	3.55E+04
2004-03-31 19:59:58	2.56E+04
2004-04-01 05:59:53	2.44E+04
2004-04-02 10:59:54	4.63E+04

2004-04-02 18:59:54	1.09E+04
2004-04-03 02:59:54	2.41E+04
2004-04-04 00:59:54	3.44E+04
2004-09-08 11:42:59	4.47E+04
2004-09-09 15:47:20	3.93E+04
2004-10-15 06:00:00	5.74E+04
2004-10-16 01:00:00	2.80E+04
2004-10-19 01:00:00	2.36E+04
2004-10-19 05:00:00	8.99E+03
2004-10-29 13:00:00	1.27E+04
2004-10-29 21:00:00	1.86E+04
2004-10-30 05:00:00	4.99E+03
2004-10-30 09:00:00	5.84E+03
2004-10-30 21:00:00	4.91E+03
2004-10-31 06:00:00	1.08E+04
2004-10-31 07:00:00	1.46E+04
2004-10-31 09:00:00	7.44E+03
2004-10-31 11:00:00	1.04E+04
2004-10-31 13:00:00	9.16E+03
2004-11-01 15:00:00	1.27E+04
2004-11-02 14:00:00	2.73E+04
2004-11-03 02:00:00	1.07E+05
2004-11-03 19:00:00	4.65E+03
2004-11-03 21:00:00	9.05E+03
2004-11-04 23:00:00	1.96E+04
2004-11-05 10:00:00	3.77E+04
2004-11-05 20:00:00	1.02E+04
2004-11-07 20:00:00	2.03E+04
2004-11-09 00:00:00	1.98E+04
2004-11-09 16:00:00	2.22E+04
2004-11-19 02:00:00	2.28E+04
2004-11-19 11:00:00	1.92E+04
2004-11-20 06:00:00	2.00E+04
2004-11-30 00:00:00	3.59E+04
2004-12-01 21:00:00	4.64E+04
2004-12-03 00:00:00	1.26E+04
2004-12-03 01:00:00	3.28E+04
2005-01-30 06:00:00	8.75E+03
2005-01-30 10:00:00	1.16E+04
2005-02-01 06:00:00	1.63E+04
2005-02-02 06:00:00	4.04E+04
2005-02-07 05:00:00	2.14E+04
2005-02-07 07:00:00	3.17E+04
2005-02-07 08:00:00	2.34E+04
2005-02-07 09:00:00	7.91E+03
2005-02-07 10:00:00	6.04E+03
2005-02-07 11:00:00	3.14E+04
2005-02-09 11:00:00	1.19E+04
2005-02-10 16:00:00	2.50E+04
2005-02-17 04:00:00	2.76E+04
2005-02-19 04:00:00	1.38E+04
2005-02-22 16:00:00	1.69E+04
2005-02-22 22:00:00	7.05E+03
2005-02-23 20:00:00	1.33E+04
2005-02-24 15:00:00	1.16E+04
2005-02-24 19:00:00	3.46E+04
2005-02-25 04:00:00	2.54E+03
2005-02-25 06:00:00	6.98E+03
2005-02-25 09:00:00	9.04E+03
2005-02-25 14:00:00	1.43E+04
2005-02-25 17:00:00	1.67E+04
2005-02-25 20:00:00	8.45E+03
2005-02-26 01:00:00	4.84E+04
2005-02-26 10:00:00	1.43E+04
2005-02-26 11:00:00	8.25E+03
2005-02-26 23:00:00	4.57E+03
2005-02-27 14:00:00	8.35E+03
2005-02-27 23:00:00	1.62E+04
2005-02-28 02:00:00	1.76E+04
2005-02-28 04:00:00	3.12E+04
2005-02-28 13:00:00	7.15E+03
2005-02-28 21:00:00	1.38E+04
2005-03-01 01:00:00	9.29E+03
2005-03-01 12:00:00	2.11E+04
2005-03-15 15:00:00	2.02E+04
2005-03-15 18:00:00	1.92E+04
2005-03-16 00:00:00	8.56E+03
2005-03-16 05:00:00	3.74E+03
2005-03-16 09:00:00	1.64E+04
2005-03-16 14:00:00	1.02E+04
2005-03-16 23:00:00	1.32E+04
2005-03-17 10:00:00	2.36E+04
2005-03-17 13:00:00	8.29E+03
2005-03-17 20:00:00	1.43E+04
2005-03-18 04:00:00	5.46E+04
2005-03-18 15:00:00	1.46E+04
2005-03-18 16:00:00	5.56E+03
2005-03-18 22:00:00	3.60E+04
2005-03-19 17:00:00	5.31E+03
2005-03-19 23:00:00	1.06E+04
2005-03-21 05:00:00	5.14E+04
2005-03-22 00:00:00	2.28E+04

2005-03-23 00:00:00	1.24E+04
2005-03-23 16:00:00	1.95E+04
2005-03-23 23:00:00	1.58E+04
2005-03-24 18:00:00	1.19E+04
2005-03-25 12:00:00	4.46E+04
2005-04-02 21:00:00	1.42E+04
2005-04-06 12:00:00	1.99E+04
2005-04-06 13:00:00	1.25E+04
2005-04-08 16:00:00	2.08E+04
2005-04-13 06:00:00	1.28E+04
2005-04-17 13:00:00	1.93E+04
2005-04-18 19:00:00	9.43E+03
2005-04-21 07:00:00	2.13E+04
2005-04-27 22:00:00	2.55E+04
2005-05-07 10:00:00	7.03E+04
2005-05-07 13:00:00	4.04E+04
2005-05-07 15:00:00	4.17E+04
2005-05-07 23:00:00	2.41E+04
2005-05-09 12:00:00	2.27E+04
2005-05-13 19:00:00	9.70E+03
2005-05-16 07:00:00	1.46E+04
2005-05-19 01:00:00	2.39E+04
2005-05-21 17:21:59	1.00E+04
2005-05-24 02:49:28	8.63E+03
2005-05-24 07:20:44	2.64E+04
2005-05-25 23:40:24	1.38E+04
2005-05-26 20:59:19	5.84E+03
2005-05-28 02:00:00	3.94E+04
2005-05-30 03:55:43	5.43E+04
2005-05-30 16:37:06	2.20E+04
2005-05-30 17:35:00	2.44E+04
2005-05-31 23:09:55	5.56E+03
2005-06-02 17:32:35	2.54E+04
2005-06-02 20:19:09	4.06E+03
2005-06-04 15:12:36	9.24E+03
2005-06-05 02:58:51	4.41E+03
2005-06-06 20:39:01	4.62E+03
2005-06-07 22:45:53	2.21E+03
2005-06-08 10:48:49	1.40E+03
2005-06-10 00:16:00	1.63E+03
2005-06-16 00:10:46	3.66E+03
2005-06-16 00:53:08	1.06E+04
2005-06-17 12:52:45	1.98E+04
2005-06-19 15:00:00	5.25E+03
2005-06-20 21:00:00	8.43E+03
2005-06-22 03:00:00	3.63E+04
2005-06-23 04:11:48	3.82E+03
2005-06-23 04:41:36	2.00E+04
2005-06-23 21:10:49	4.18E+03
2005-06-26 05:00:00	9.51E+04
2005-06-28 19:47:21	1.23E+05
2005-07-02 23:18:47	5.26E+04
2005-07-03 11:33:17	1.62E+04
2005-07-04 02:08:43	1.35E+03
2005-07-04 07:11:18	2.49E+04
2005-07-04 10:25:16	1.41E+04
2005-07-05 10:44:21	8.09E+03
2005-07-09 09:22:01	3.62E+03
2005-07-10 03:38:49	2.63E+03
2005-07-10 10:18:41	2.09E+04
2005-07-12 11:21:16	2.62E+04
2005-07-14 13:40:00	1.95E+04
2005-07-15 03:14:11	1.66E+04
2005-07-15 06:57:22	9.36E+04
2005-07-16 00:32:19	1.25E+04
2005-07-16 02:05:28	3.06E+04
2005-07-16 05:35:58	1.31E+04
2005-07-17 04:39:55	3.13E+04
2005-07-18 13:11:49	8.11E+03
2005-07-18 16:20:21	3.79E+04
2005-07-19 10:23:08	2.74E+04
2005-07-19 11:02:39	2.20E+04
2005-07-20 05:04:55	2.18E+03
2005-07-20 08:25:58	1.74E+04
2005-07-22 00:29:13	2.95E+04
2005-07-23 01:08:31	4.32E+04
2005-07-23 13:08:37	5.47E+03
2005-07-23 15:43:31	4.63E+03
2005-07-26 00:05:31	6.77E+03
2005-07-26 08:34:01	5.50E+03
2005-07-26 12:54:48	2.79E+04
2005-07-27 04:53:40	7.23E+03
2005-07-27 15:20:06	8.86E+03
2005-07-27 19:00:00	1.78E+04
2005-07-28 01:10:11	8.30E+04
2005-07-29 06:40:20	1.05E+05
2005-07-29 06:57:57	1.55E+03
2005-07-29 07:36:49	2.49E+03
2005-07-29 10:00:00	1.50E+04
2005-07-29 11:53:49	4.48E+04
2005-07-29 15:34:51	1.45E+03
2005-07-29 23:23:26	6.73E+03

2005-07-29 23:53:38	2.79E+03
2005-07-30 21:22:42	1.08E+05
2005-08-01 09:51:03	5.60E+04
2005-08-01 19:43:55	2.95E+04
2005-08-01 19:48:36	6.38E+04
2005-08-02 00:58:21	1.68E+04
2005-08-02 13:58:54	1.47E+04
2005-08-02 20:53:32	2.14E+04
2005-08-03 10:45:27	8.86E+03
2005-08-03 16:40:13	2.22E+03
2005-08-03 18:01:35	3.35E+04
2005-08-03 21:50:17	3.21E+04
2005-08-05 14:04:35	8.37E+03
2005-08-05 18:09:56	1.91E+04
2005-08-05 20:15:43	3.88E+04
2005-08-06 05:37:43	8.96E+03
2005-08-06 11:57:23	5.98E+03
2005-08-06 13:19:29	9.23E+04
2005-08-06 14:40:09	6.29E+04
2005-08-07 10:58:45	8.82E+04
2005-08-08 01:17:04	3.65E+04
2005-08-08 10:38:15	4.83E+04
2005-08-08 18:43:16	1.08E+04
2005-08-08 22:08:09	7.15E+04
2005-08-09 07:04:28	5.51E+04
2005-08-10 04:52:03	1.01E+05
2005-08-10 15:18:51	6.07E+04
2005-08-26 10:00:00	9.85E+03
2005-08-29 03:00:00	1.79E+04
2005-08-29 10:00:00	1.27E+04
2005-08-30 02:00:00	2.12E+04
2005-08-30 18:38:31	2.37E+04
2005-08-31 16:33:02	2.78E+04
2005-09-05 05:00:00	8.33E+04
2005-09-06 01:00:00	2.73E+05
2005-09-06 09:00:00	3.64E+03
2005-09-07 10:00:00	4.98E+03
2005-09-20 22:27:03	2.61E+04
2005-09-21 01:57:13	3.03E+04
2005-09-21 07:10:01	1.94E+04
2005-09-21 17:52:14	8.85E+04
2005-09-21 21:33:01	6.24E+04
2005-09-22 07:24:58	3.16E+04
2005-09-22 19:07:42	3.72E+03
2005-09-23 02:42:42	1.27E+04
2005-09-23 23:16:36	4.93E+03
2005-09-24 03:13:36	3.46E+04
2005-09-24 05:58:44	6.90E+04
2005-09-24 11:22:17	1.18E+04
2005-09-24 16:02:26	3.03E+03
2005-09-24 16:29:08	2.71E+03
2005-09-24 17:12:07	3.55E+04
2005-09-24 19:34:27	3.63E+03
2005-09-25 22:30:43	5.05E+04
2005-09-25 23:58:44	3.55E+04
2005-09-26 03:17:50	2.47E+04
2005-09-26 09:11:13	9.90E+04
2005-09-27 03:22:20	2.13E+04
2005-09-27 03:30:04	3.38E+04
2005-09-27 04:42:41	2.18E+04
2005-09-27 04:50:14	2.95E+03
2005-09-27 09:43:42	6.91E+04
2005-09-27 10:38:26	1.99E+03
2005-09-28 01:15:14	1.84E+04
2005-09-28 03:07:23	1.14E+04
2005-09-28 07:56:56	1.61E+04
2005-09-28 10:05:31	4.46E+04
2005-09-28 14:24:22	1.42E+04
2005-09-28 15:41:39	4.28E+03
2005-09-28 15:56:19	1.40E+04
2005-09-28 16:10:40	8.64E+03
2005-09-28 16:20:39	1.29E+04
2005-09-28 17:03:58	4.92E+03
2005-09-28 17:26:10	1.33E+04
2005-09-28 18:00:15	9.52E+03
2005-09-28 18:25:35	2.66E+04
2005-09-28 18:30:55	7.80E+03
2005-09-28 19:10:12	2.75E+03
2005-09-28 19:15:19	3.35E+03
2005-09-28 19:58:09	2.15E+03
2005-09-28 20:29:12	3.37E+04
2005-09-29 03:04:19	9.72E+04
2005-09-29 05:45:17	2.46E+04
2005-09-29 16:37:47	7.27E+04
2005-09-30 06:20:39	7.78E+04
2005-09-30 15:04:31	7.70E+03
2005-09-30 21:12:42	4.27E+04
2005-10-01 14:55:31	3.15E+04
2005-10-02 17:06:00	3.33E+04
2005-10-03 01:32:48	1.94E+04
2005-10-03 02:03:31	4.13E+04
2005-10-03 04:38:05	8.17E+04

2005-10-03 15:12:18	1.08E+04
2005-10-04 02:25:40	4.57E+04
2005-10-04 05:37:46	1.37E+05
2005-10-04 11:54:25	9.18E+03
2005-10-04 19:35:00	1.08E+05
2005-10-05 14:36:45	6.00E+04
2005-10-07 10:18:26	1.30E+05
2005-10-07 20:30:16	4.33E+04
2005-10-08 02:47:11	1.47E+04
2005-10-08 13:30:23	6.59E+04
2005-10-08 21:55:02	1.76E+04
2005-10-09 04:25:03	3.97E+04
2005-10-09 22:33:31	4.45E+04
2005-10-09 23:52:17	2.56E+03
2005-10-10 00:15:23	2.98E+03
2005-10-10 01:55:43	5.64E+04
2005-10-10 11:53:36	4.79E+04
2005-10-11 07:11:55	1.08E+05
2005-10-12 04:42:55	4.22E+04
2005-10-12 09:53:21	4.45E+04
2005-10-12 12:36:45	2.98E+04
2005-10-12 12:44:14	5.22E+04
2005-10-13 01:13:13	8.44E+03
2005-10-13 08:22:44	7.06E+04
2005-10-13 09:22:34	6.38E+04
2005-10-14 03:02:10	5.43E+04
2005-10-14 05:07:05	4.77E+04
2005-10-14 10:21:16	1.40E+05
2005-10-15 00:47:23	6.46E+03
2005-10-15 01:44:26	5.11E+04
2005-10-15 02:42:35	2.29E+04
2005-10-15 03:27:10	8.13E+03
2005-10-15 03:39:15	4.50E+03
2005-10-15 05:44:32	2.73E+03
2005-10-15 06:52:22	2.95E+04
2005-10-15 17:24:25	3.79E+03
2005-10-15 19:13:59	8.99E+04
2005-10-15 22:24:26	3.64E+04
2005-10-16 11:17:54	4.94E+04
2005-10-16 16:00:15	3.70E+04
2005-10-16 18:21:45	1.75E+04
2005-10-16 20:58:28	8.71E+03
2005-10-16 21:12:15	6.08E+03
2005-10-16 22:13:03	8.21E+03
2005-10-17 03:00:07	1.11E+05
2005-10-17 04:09:00	6.68E+04
2005-10-17 09:26:53	8.93E+02
2005-10-17 14:23:59	6.14E+02
2005-10-17 14:54:55	6.89E+02
2005-10-17 15:54:37	7.57E+04
2005-10-17 17:57:06	6.62E+02
2005-10-17 20:04:22	3.72E+04
2005-10-17 21:42:55	3.49E+03
2005-10-18 05:23:06	5.72E+04
2005-10-18 10:14:28	4.57E+04
2005-10-18 10:30:30	3.80E+04
2005-10-19 01:15:23	1.01E+05
2005-10-19 03:55:12	3.64E+04
2005-10-19 11:10:45	1.93E+05
2005-10-20 04:58:35	7.42E+04
2005-10-20 21:34:08	4.17E+04
2005-10-21 16:31:21	5.92E+04
2005-10-21 23:15:06	9.27E+04
2005-10-21 23:55:00	3.13E+04
2005-10-22 05:38:50	3.54E+03
2005-10-22 06:41:11	1.11E+05
2005-10-22 12:09:45	3.14E+04
2005-10-22 22:29:58	8.64E+04
2005-10-23 05:47:59	3.75E+04
2005-10-23 14:16:32	4.84E+04
2005-10-24 06:21:12	1.48E+05
2005-10-24 16:03:54	3.52E+03
2005-10-24 16:55:16	1.28E+05
2005-10-24 21:57:06	6.26E+02
2005-10-24 23:34:23	2.44E+04
2005-10-25 04:19:22	7.90E+04
2005-10-25 04:23:13	7.90E+04
2005-10-25 13:28:33	9.70E+03
2005-10-25 14:17:29	1.50E+04
2005-10-25 16:16:35	1.45E+05
2005-10-26 00:52:45	1.29E+04
2005-10-26 02:23:52	2.49E+03
2005-10-26 05:00:00	1.11E+05
2005-10-26 16:56:40	1.24E+05
2005-10-27 00:41:48	2.64E+03
2005-10-27 12:01:53	9.41E+04
2005-10-27 15:46:26	1.73E+03
2005-10-27 17:13:49	2.13E+03
2005-10-27 19:42:47	6.60E+04
2005-10-28 09:44:34	2.40E+03
2005-10-28 11:07:10	2.00E+03
2005-10-28 12:25:50	6.02E+04

2005-10-28 14:51:43	1.01E+05	2005-11-07 06:22:06	5.28E+03
2005-10-28 21:00:36	1.05E+03	2005-11-07 06:26:36	6.43E+03
2005-10-28 21:29:58	2.48E+03	2005-11-07 06:51:58	1.30E+04
2005-10-28 23:19:35	9.15E+03	2005-11-07 08:38:42	3.76E+03
2005-10-29 01:09:34	3.55E+03	2005-11-07 12:00:01	4.61E+03
2005-10-29 11:30:45	9.44E+02	2005-11-07 15:48:21	1.01E+05
2005-10-29 11:44:33	2.51E+03	2005-11-07 16:19:10	2.64E+04
2005-10-29 12:47:08	6.42E+04	2005-11-07 19:00:00	1.28E+05
2005-10-29 16:16:02	1.07E+03	2005-11-08 05:03:30	6.53E+04
2005-10-29 21:21:23	1.50E+03	2005-11-08 12:51:44	6.17E+04
2005-10-30 01:17:14	1.55E+03	2005-11-08 14:07:10	7.71E+04
2005-10-30 03:13:09	9.22E+02	2005-11-08 14:35:04	7.73E+02
2005-10-30 06:02:47	4.93E+04	2005-11-08 16:58:49	6.96E+03
2005-10-30 07:09:32	3.47E+03	2005-11-09 08:08:33	2.38E+04
2005-10-30 07:12:56	5.98E+03	2005-11-09 08:38:48	4.08E+04
2005-10-30 11:28:28	1.20E+05	2005-11-09 11:16:29	7.13E+03
2005-10-31 01:40:45	6.39E+02	2005-11-09 11:25:19	1.31E+03
2005-10-31 01:47:42	1.38E+04	2005-11-09 11:38:31	4.81E+03
2005-10-31 11:42:37	4.68E+04	2005-11-09 17:06:05	9.04E+04
2005-10-31 17:27:52	8.24E+03	2005-11-09 19:34:28	9.77E+04
2005-10-31 18:34:54	6.24E+04	2005-11-09 22:25:06	6.25E+04
2005-11-01 04:46:09	9.06E+03	2005-11-10 07:52:02	8.15E+04
2005-11-01 07:11:39	5.23E+04	2005-11-10 09:34:23	1.35E+05
2005-11-02 01:22:10	1.28E+05	2005-11-10 11:00:00	6.40E+04
2005-11-03 15:54:37	1.74E+04	2005-11-10 12:48:26	5.84E+03
2005-11-04 00:21:16	6.96E+04	2005-11-10 15:08:35	6.02E+03
2005-11-04 09:52:14	3.05E+04	2005-11-10 16:12:26	1.15E+04
2005-11-04 15:50:29	1.10E+05	2005-11-10 16:55:44	5.82E+03
2005-11-04 23:08:37	7.72E+04	2005-11-10 18:37:28	4.19E+04
2005-11-05 01:28:10	5.01E+04	2005-11-11 00:02:35	1.15E+04
2005-11-05 03:42:47	2.02E+04	2005-11-11 00:32:54	4.49E+03
2005-11-05 13:59:44	1.22E+05	2005-11-11 02:29:40	8.08E+04
2005-11-05 16:01:30	1.06E+04	2005-11-11 03:41:19	6.64E+04
2005-11-05 19:24:33	1.32E+05	2005-11-11 11:07:22	8.10E+04
2005-11-06 00:26:39	3.42E+03	2005-11-11 16:25:49	2.02E+04
2005-11-06 00:54:03	1.29E+04	2005-11-11 17:25:52	1.32E+05
2005-11-06 14:50:41	3.34E+04	2005-11-12 08:12:16	3.75E+04
2005-11-06 20:08:59	3.14E+03	2005-11-12 12:43:19	2.16E+05
2005-11-06 20:47:56	2.53E+03	2005-11-12 19:13:48	5.98E+04
2005-11-06 23:25:55	1.68E+05	2005-11-13 05:47:17	1.63E+04
2005-11-07 03:39:37	1.12E+03	2005-11-13 09:47:22	1.14E+05
2005-11-07 04:16:41	7.59E+03	2005-11-13 18:24:47	1.39E+05
2005-11-07 04:19:47	2.55E+03	2005-11-13 23:47:37	3.19E+05
2005-11-07 04:46:31	2.85E+03	2005-11-14 22:33:03	3.93E+04
2005-11-07 05:19:38	1.37E+05	2005-11-15 00:27:10	1.28E+05
2005-11-07 06:11:39	6.44E+03	2005-11-15 04:28:39	3.66E+04

2005-11-15 07:55:26	2.11E+04
2005-11-15 10:42:26	4.06E+03
2005-11-15 16:55:10	5.02E+04
2005-11-15 21:28:06	8.20E+04
2005-11-15 22:39:45	1.11E+05
2005-11-16 03:30:37	1.93E+04
2005-11-16 08:55:09	1.17E+05
2005-11-16 10:43:02	1.63E+04
2005-11-16 16:26:31	1.42E+05
2005-11-17 00:11:07	4.14E+04
2005-11-17 02:44:38	1.19E+05
2005-11-17 03:27:32	2.90E+03
2005-11-17 04:17:14	3.41E+03
2005-11-17 05:42:23	8.03E+03
2005-11-17 08:39:42	1.10E+03
2005-11-17 09:14:26	9.08E+03
2005-11-17 11:22:06	9.95E+04
2005-11-17 12:26:04	1.29E+05
2005-11-17 13:27:45	8.81E+03
2005-11-18 13:52:14	6.51E+04
2005-11-19 19:05:19	1.71E+04
2005-11-20 04:51:49	1.17E+05
2005-11-20 07:11:36	8.17E+04
2005-11-20 16:40:23	6.24E+03
2005-11-20 16:48:43	4.57E+04
2005-11-20 17:00:51	6.45E+04
2005-11-21 07:59:39	4.56E+04
2005-11-21 13:26:08	1.23E+05
2005-11-21 22:48:06	1.00E+05
2005-11-21 23:08:35	8.38E+04
2005-11-22 08:57:43	1.48E+05
2005-11-22 11:01:21	1.29E+04
2005-11-22 15:09:30	9.01E+03
2005-11-23 11:43:43	1.76E+05
2005-11-24 00:30:51	1.06E+05
2005-11-24 01:51:11	4.54E+03
2005-11-24 06:25:50	1.89E+04
2005-11-24 08:59:50	1.25E+03
2005-11-24 14:45:59	3.69E+04
2005-11-24 16:23:56	2.43E+04
2005-11-24 19:41:31	4.21E+04
2005-11-24 21:08:53	1.10E+05
2005-11-25 03:28:42	1.18E+04
2005-11-25 05:44:22	8.35E+04
2005-11-25 15:34:44	7.30E+04
2005-11-25 17:22:52	1.87E+04
2005-11-26 03:06:08	4.73E+04
2005-11-26 15:34:36	5.63E+04
2005-11-26 19:52:42	1.15E+04
2005-11-28 08:13:31	3.45E+04
2005-11-28 23:30:53	1.13E+04
2005-11-29 06:45:06	6.24E+04
2005-11-29 11:38:32	1.07E+05
2005-11-29 13:47:52	1.18E+05
2005-11-29 21:46:30	1.13E+05
2005-11-30 05:46:22	1.09E+05
2005-11-30 09:00:31	2.43E+04
2005-11-30 09:34:03	4.65E+04
2005-12-01 02:15:38	2.56E+04
2005-12-01 05:14:53	1.32E+05
2005-12-01 07:44:15	8.47E+04
2005-12-01 10:09:04	5.79E+04
2005-12-02 05:01:20	1.03E+05
2005-12-03 13:49:49	8.74E+04
2005-12-03 15:57:42	1.27E+04
2005-12-03 18:08:47	8.85E+04
2005-12-03 20:44:28	5.90E+04
2005-12-04 04:34:45	2.07E+04
2005-12-04 08:22:24	1.21E+05
2005-12-04 17:05:14	9.99E+04
2005-12-04 18:50:49	2.42E+05
2005-12-05 07:04:58	1.54E+05
2005-12-05 14:55:17	2.80E+04
2005-12-05 17:26:07	1.31E+04
2005-12-06 04:52:14	1.35E+04
2005-12-06 09:58:09	1.20E+05
2005-12-06 10:53:30	1.49E+05
2005-12-07 06:00:00	2.19E+05
2005-12-07 16:16:28	4.66E+04
2005-12-08 05:32:03	5.70E+03
2005-12-08 09:54:56	1.34E+04
2005-12-08 15:27:10	3.93E+04
2005-12-08 22:00:00	1.83E+05
2005-12-09 02:00:00	1.93E+05
2005-12-09 12:52:12	1.20E+04
2005-12-09 14:46:00	3.73E+03
2005-12-09 15:09:40	1.03E+05
2005-12-09 16:43:17	2.16E+04
2005-12-09 19:26:27	3.55E+03
2005-12-09 20:00:21	3.40E+03
2005-12-09 20:14:48	2.11E+03
2005-12-09 21:19:47	2.39E+03

2005-12-10 08:01:23	4.18E+03
2005-12-10 09:54:38	1.15E+05
2005-12-10 10:09:17	2.72E+05
2005-12-10 11:05:41	1.58E+03
2005-12-10 11:17:45	1.11E+03
2005-12-10 11:38:38	1.08E+03
2005-12-10 12:15:15	2.03E+03
2005-12-10 12:55:00	2.11E+03
2005-12-10 13:21:43	2.63E+03
2005-12-10 14:29:32	2.48E+03
2005-12-10 15:02:28	2.11E+03
2005-12-10 20:14:58	1.53E+03
2005-12-10 23:55:09	2.17E+03
2005-12-11 03:22:52	2.16E+04
2005-12-11 11:09:06	1.22E+05
2005-12-11 11:40:31	3.35E+03
2005-12-11 13:10:54	2.20E+03
2005-12-11 14:03:33	4.35E+04
2005-12-11 14:27:04	1.64E+03
2005-12-11 15:48:00	8.97E+04
2005-12-11 18:10:35	1.33E+03
2005-12-12 06:55:54	1.20E+04
2005-12-12 09:07:05	1.97E+04
2005-12-12 10:38:55	3.44E+03
2005-12-12 15:07:46	1.54E+04
2005-12-12 16:00:14	8.06E+04
2005-12-13 11:00:39	1.88E+03
2005-12-13 11:19:37	1.43E+03
2005-12-13 16:03:11	7.87E+03
2005-12-13 16:57:05	2.24E+05
2005-12-14 05:20:35	9.30E+04
2005-12-14 05:44:47	1.19E+04
2005-12-14 06:01:47	5.36E+03
2005-12-14 11:45:18	1.68E+05
2005-12-15 09:19:15	1.34E+05
2005-12-15 11:42:20	4.65E+03
2005-12-15 11:54:32	2.35E+03
2005-12-15 13:02:25	1.62E+05
2005-12-15 21:30:00	2.60E+05
2005-12-16 05:51:26	5.31E+04
2005-12-16 06:06:08	1.44E+03
2005-12-16 07:06:34	4.33E+03
2005-12-16 10:43:53	5.25E+04
2005-12-17 01:33:13	4.13E+04
2005-12-17 04:21:42	1.31E+05
2005-12-17 08:48:02	2.95E+05
2005-12-17 21:42:15	5.17E+03
2005-12-18 06:53:12	1.75E+04
2005-12-18 07:40:58	9.69E+04
2005-12-18 07:51:26	3.13E+03
2005-12-18 10:27:20	1.08E+05
2005-12-18 16:12:00	3.34E+04
2005-12-19 00:40:45	8.73E+04
2005-12-19 06:29:45	5.66E+04
2005-12-19 09:39:41	2.29E+05
2005-12-19 13:55:20	2.65E+04
2005-12-20 07:38:14	6.11E+04
2005-12-20 09:21:35	4.13E+04
2005-12-21 16:42:39	3.71E+04
2005-12-24 15:11:29	1.95E+04
2005-12-24 18:45:33	3.15E+05
2005-12-25 00:42:37	4.16E+05
2005-12-25 02:21:41	1.97E+03
2005-12-25 07:53:39	2.22E+05
2005-12-25 20:09:14	2.44E+05
2005-12-26 00:59:22	5.10E+03
2005-12-26 03:00:00	3.96E+05
2005-12-26 10:38:54	2.35E+03
2005-12-26 13:39:04	7.86E+03
2005-12-26 15:56:16	2.55E+05
2005-12-27 11:35:30	1.18E+04
2005-12-27 17:44:19	6.84E+03
2005-12-28 04:09:38	1.60E+05
2005-12-28 22:03:02	4.26E+04
2005-12-29 08:20:30	9.42E+03
2005-12-29 10:49:57	3.62E+04
2005-12-29 11:01:01	3.22E+04
2005-12-29 13:42:16	6.87E+04
2005-12-29 15:27:04	6.49E+04
2005-12-29 18:20:06	2.56E+04
2005-12-30 03:21:04	2.07E+03
2005-12-30 03:53:27	7.94E+04
2005-12-30 04:59:39	6.44E+04
2005-12-30 05:35:12	1.12E+05
2005-12-30 20:41:18	7.66E+04
2005-12-30 20:54:01	5.76E+04
2005-12-30 22:18:44	3.26E+03
2005-12-31 04:32:13	6.35E+03
2005-12-31 06:11:44	4.70E+04
2005-12-31 06:36:18	8.80E+04
2005-12-31 10:53:30	1.83E+05
2005-12-31 11:44:22	7.18E+04

2005-12-31 18:21:13	2.58E+03
2005-12-31 21:24:01	5.61E+04
2006-01-01 03:21:43	1.08E+05
2006-01-01 12:41:37	5.62E+03
2006-01-01 14:27:14	5.23E+04
2006-01-01 16:40:01	2.39E+03
2006-01-01 17:46:19	8.46E+04
2006-01-01 20:16:11	5.23E+03
2006-01-02 13:07:19	6.80E+04
2006-01-02 18:45:26	1.54E+05
2006-01-02 22:27:43	1.07E+04
2006-01-03 03:30:46	1.20E+04
2006-01-03 07:15:32	5.71E+04
2006-01-03 15:11:45	2.77E+04
2006-01-05 07:14:06	3.83E+04
2006-01-05 15:09:50	1.43E+05
2006-01-05 16:10:01	5.21E+04
2006-01-05 20:18:26	1.26E+05
2006-01-06 06:01:04	1.80E+04
2006-01-07 01:58:58	3.23E+04
2006-01-07 05:12:15	4.56E+04
2006-01-07 13:09:29	7.37E+03
2006-01-07 17:55:44	8.38E+04
2006-01-07 19:30:22	8.41E+04
2006-01-07 21:57:14	6.90E+04
2006-01-07 23:04:42	4.15E+04
2006-01-08 08:18:56	1.20E+05
2006-01-08 12:04:28	2.12E+04
2006-01-08 15:25:20	8.46E+04
2006-01-08 19:54:55	1.04E+05
2006-01-09 10:21:41	1.20E+04
2006-01-09 11:14:45	4.60E+03
2006-01-09 13:08:53	3.66E+04
2006-01-09 14:08:42	5.62E+04
2006-01-09 14:26:28	6.87E+04
2006-01-09 17:33:51	7.08E+04
2006-01-10 04:07:48	6.45E+04
2006-01-10 09:14:55	1.53E+05
2006-01-10 13:06:12	2.73E+04
2006-01-10 19:18:48	1.71E+05
2006-01-10 21:12:45	5.89E+04
2006-01-11 08:54:37	6.72E+03
2006-01-11 18:20:20	2.82E+04
2006-01-11 20:51:56	1.27E+04
2006-01-12 00:36:20	9.36E+03
2006-01-12 04:00:02	8.52E+04
2006-01-12 15:10:46	1.10E+04
2006-01-12 20:08:56	1.73E+04
2006-01-12 20:54:39	3.80E+04
2006-01-13 05:04:40	2.95E+04
2006-01-13 10:21:24	1.70E+05
2006-01-13 12:20:26	5.86E+04
2006-01-13 16:36:30	8.26E+03
2006-01-13 17:13:23	1.88E+04
2006-01-13 19:23:31	1.62E+05
2006-01-15 08:42:36	2.91E+05
2006-01-15 12:26:40	2.16E+04
2006-01-15 20:59:16	5.65E+04
2006-01-16 00:23:20	6.51E+04
2006-01-16 03:35:33	9.22E+04
2006-01-16 06:18:58	8.11E+04
2006-01-16 20:47:22	9.01E+04
2006-01-17 01:21:13	3.21E+05
2006-01-17 18:47:53	6.22E+04
2006-01-18 00:50:41	8.86E+04
2006-01-18 15:10:57	9.81E+04
2006-01-18 20:50:19	9.88E+04
2006-01-19 18:54:16	6.23E+04
2006-01-19 19:42:09	5.31E+04
2006-01-20 01:55:19	7.30E+04
2006-01-21 19:47:57	7.66E+04
2006-01-22 02:53:19	1.02E+04
2006-01-22 07:34:39	1.86E+05
2006-01-22 09:01:04	2.08E+04
2006-01-22 11:09:36	6.23E+04
2006-01-22 23:38:44	6.50E+04
2006-01-23 09:48:44	5.88E+04
2006-01-23 11:25:07	3.61E+04
2006-01-23 15:19:30	1.29E+04
2006-01-23 16:39:52	6.86E+04
2006-01-23 19:58:48	4.53E+04
2006-01-24 01:59:43	3.66E+03
2006-01-24 02:09:39	8.67E+04
2006-01-24 04:32:12	1.09E+05
2006-01-25 06:58:29	1.13E+05
2006-01-25 18:09:59	9.19E+04
2006-01-26 08:14:12	8.48E+04
2006-01-26 14:16:18	3.01E+04
2006-01-27 12:29:30	6.80E+04
2006-01-27 19:29:57	8.34E+04
2006-01-28 03:05:26	1.02E+04
2006-01-28 12:40:45	2.63E+04

2006-01-29 06:32:58	5.33E+03
2006-01-29 18:02:34	1.28E+05
2006-01-30 03:49:21	4.92E+03
2006-01-30 04:53:35	2.80E+04
2006-01-30 09:58:52	1.77E+04
2006-01-30 17:08:45	1.97E+05
2006-01-30 19:11:34	3.09E+04
2006-01-31 06:15:57	6.93E+03
2006-01-31 10:56:29	6.50E+03
2006-01-31 11:19:53	1.40E+03
2006-01-31 12:03:42	3.38E+05
2006-01-31 14:08:14	1.30E+05
2006-01-31 22:49:31	2.46E+03
2006-02-01 08:00:32	1.15E+05
2006-02-01 13:11:45	3.10E+04
2006-02-01 13:50:17	3.85E+03
2006-02-01 14:07:16	5.32E+03
2006-02-01 22:47:18	1.35E+04
2006-02-01 23:39:29	1.21E+04
2006-02-02 01:56:24	1.12E+05
2006-02-02 03:23:44	8.05E+03
2006-02-02 08:33:46	7.07E+03
2006-02-02 10:43:42	8.98E+03
2006-02-02 20:58:00	1.46E+04
2006-02-03 03:44:48	9.24E+04
2006-02-03 07:19:42	2.01E+04
2006-02-03 10:35:11	8.37E+04
2006-02-03 20:54:11	7.72E+04
2006-02-03 23:52:45	2.35E+05
2006-02-05 00:55:26	6.93E+04
2006-02-05 06:17:58	7.78E+04
2006-02-05 08:12:49	1.75E+04
2006-02-05 14:08:26	7.18E+04
2006-02-06 06:28:25	1.43E+05
2006-02-06 11:45:40	6.81E+04
2006-02-06 16:10:07	1.58E+05
2006-02-07 06:36:57	1.68E+05
2006-02-07 10:37:04	2.83E+04
2006-02-07 18:43:22	8.21E+04
2006-02-07 21:23:52	1.03E+04
2006-02-07 22:54:17	1.30E+05
2006-02-08 02:29:07	1.55E+05
2006-02-09 00:59:53	1.08E+05
2006-02-09 09:41:33	2.14E+04
2006-02-09 15:58:46	1.24E+05
2006-02-09 21:06:46	5.01E+04
2006-02-10 08:29:34	8.13E+04
2006-02-10 13:57:45	6.24E+04
2006-02-10 15:16:06	4.73E+04
2006-02-10 21:39:30	8.85E+04
2006-02-10 23:26:15	1.21E+05
2006-02-11 01:38:15	9.02E+04
2006-02-11 14:30:33	2.03E+04
2006-02-11 21:42:21	1.00E+04
2006-02-17 08:26:49	2.17E+05
2006-02-17 19:39:18	2.74E+04
2006-02-18 01:09:43	1.06E+05
2006-02-18 05:41:13	2.15E+04
2006-02-18 07:15:25	1.42E+05
2006-02-18 12:42:38	1.38E+04
2006-02-18 21:43:51	8.18E+04
2006-02-19 08:14:12	3.74E+04
2006-02-20 02:16:45	1.76E+04
2006-02-20 09:19:07	6.37E+04
2006-02-20 11:50:32	2.56E+05
2006-02-20 17:30:14	6.49E+04
2006-02-20 20:03:21	2.22E+04
2006-02-21 02:04:05	1.04E+05
2006-02-21 12:33:00	7.31E+03
2006-02-21 21:02:29	5.85E+04
2006-02-22 01:17:17	1.44E+05
2006-02-22 02:51:48	6.61E+03
2006-02-22 11:21:07	4.87E+04
2006-02-22 13:17:11	4.95E+04
2006-02-22 16:47:54	3.76E+03
2006-02-23 00:11:30	5.79E+04
2006-02-24 07:51:45	3.86E+04
2006-02-24 13:56:48	5.99E+04
2006-02-25 02:38:59	1.16E+04
2006-02-25 06:57:54	1.47E+05
2006-02-25 07:26:47	4.62E+03
2006-02-25 22:26:01	2.18E+05
2006-02-26 01:13:12	1.06E+05
2006-02-26 03:29:40	4.87E+04
2006-02-26 06:42:09	1.32E+05
2006-02-26 08:06:39	4.42E+05
2006-02-27 23:54:39	9.05E+03
2006-02-28 15:30:42	2.33E+05
2006-02-28 15:31:39	3.59E+04
2006-03-01 10:26:48	7.16E+04
2006-03-03 19:09:31	5.75E+04
2006-03-04 10:05:09	4.46E+03

2006-03-04 10:55:13	6.62E+04	2006-03-18 03:59:58	6.66E+04
2006-03-04 11:56:45	4.03E+04	2006-03-19 16:01:50	8.97E+04
2006-03-04 16:52:15	1.06E+05	2006-03-20 01:03:37	1.29E+05
2006-03-05 06:20:20	5.03E+04	2006-03-20 03:50:34	4.83E+03
2006-03-05 06:48:18	6.07E+04	2006-03-20 05:47:37	3.83E+04
2006-03-05 19:35:33	2.33E+05	2006-03-20 07:48:54	1.11E+05
2006-03-06 09:01:48	9.29E+04	2006-03-20 12:18:45	1.45E+05
2006-03-07 04:09:55	6.30E+04	2006-03-20 14:32:16	7.80E+04
2006-03-07 06:15:58	2.27E+04	2006-03-20 17:34:07	1.42E+04
2006-03-07 06:43:01	1.16E+05	2006-03-21 09:39:33	3.29E+05
2006-03-07 08:26:56	1.72E+04	2006-03-22 08:06:50	1.31E+05
2006-03-07 11:35:11	3.19E+04	2006-03-22 18:11:53	1.03E+05
2006-03-07 17:28:14	7.32E+04	2006-03-23 21:25:42	1.26E+04
2006-03-08 12:52:43	6.31E+04	2006-03-23 22:08:58	2.47E+04
2006-03-08 20:20:16	7.64E+03	2006-03-24 05:38:51	2.55E+04
2006-03-09 10:31:44	5.12E+04	2006-03-24 05:58:11	1.02E+04
2006-03-09 13:29:22	9.63E+03	2006-03-24 07:14:55	6.28E+04
2006-03-10 01:28:55	1.07E+05	2006-03-24 08:44:06	8.09E+04
2006-03-10 04:41:29	2.61E+05	2006-03-24 09:56:03	1.55E+04
2006-03-10 10:47:32	4.01E+04	2006-03-24 13:07:37	1.90E+04
2006-03-10 17:45:59	3.31E+04	2006-03-24 18:43:08	5.02E+03
2006-03-10 19:17:35	2.15E+04	2006-03-24 21:23:36	1.70E+05
2006-03-10 21:11:36	6.60E+03	2006-03-25 02:13:39	9.29E+03
2006-03-11 02:36:16	2.32E+05	2006-03-25 03:53:40	2.14E+04
2006-03-11 22:24:45	1.36E+05	2006-03-25 06:16:41	4.06E+04
2006-03-12 15:21:17	1.40E+05	2006-03-25 09:11:01	2.06E+05
2006-03-13 17:01:20	1.10E+05	2006-03-26 03:33:48	1.15E+05
2006-03-13 18:08:03	8.47E+04	2006-03-26 19:43:36	5.81E+04
2006-03-13 21:02:50	4.46E+04	2006-03-27 09:01:19	3.85E+04
2006-03-14 09:54:19	8.16E+04	2006-03-27 12:47:18	1.12E+04
2006-03-14 17:20:46	5.35E+04	2006-03-27 17:42:39	9.73E+04
2006-03-15 04:03:02	1.89E+04	2006-03-29 19:44:58	6.17E+03
2006-03-15 10:25:04	3.40E+04	2006-03-29 20:46:51	1.10E+04
2006-03-15 13:58:56	9.00E+04	2006-03-29 23:31:27	5.55E+03
2006-03-15 16:06:35	5.79E+04	2006-03-30 00:47:32	3.47E+04
2006-03-15 19:15:11	1.55E+04	2006-03-30 05:48:50	1.56E+04
2006-03-15 23:04:38	5.94E+04	2006-03-30 12:09:22	3.89E+03
2006-03-16 01:17:36	9.82E+04	2006-03-30 12:42:46	3.31E+04
2006-03-16 05:21:04	2.42E+04	2006-03-30 19:48:24	7.28E+03
2006-03-16 07:32:34	1.46E+05	2006-03-30 21:04:45	1.17E+04
2006-03-16 12:56:34	1.28E+05	2006-03-31 02:36:48	4.07E+04
2006-03-17 09:56:16	7.22E+03	2006-03-31 03:53:23	1.15E+04
2006-03-17 10:41:34	1.06E+04	2006-03-31 05:17:19	2.08E+03
2006-03-17 15:31:49	5.53E+03	2006-03-31 05:53:26	3.42E+04
2006-03-17 16:48:22	1.24E+04	2006-03-31 09:50:53	4.83E+04
2006-03-18 00:36:41	4.28E+04	2006-03-31 10:08:29	5.99E+04

2006-03-31 14:33:47	3.75E+04
2006-03-31 19:03:10	1.14E+04
2006-03-31 23:45:05	7.71E+03
2006-04-01 05:46:48	1.28E+05
2006-04-01 08:11:34	8.72E+04
2006-04-02 21:14:01	1.16E+05
2006-04-03 00:36:59	7.63E+04
2006-04-03 10:13:50	3.15E+03
2006-04-03 10:37:42	5.72E+03
2006-04-03 13:35:59	1.60E+05
2006-04-03 21:58:58	1.63E+05
2006-04-04 01:55:57	2.15E+04
2006-04-04 02:58:10	2.01E+04
2006-04-04 07:41:08	7.57E+04
2006-04-04 18:49:25	2.15E+05
2006-04-05 03:46:15	7.83E+03
2006-04-05 04:59:14	5.97E+04
2006-04-05 16:13:29	2.20E+05
2006-04-05 18:35:45	1.05E+05
2006-04-05 22:36:35	5.87E+04
2006-04-06 06:27:45	3.76E+04
2006-04-06 08:48:51	4.66E+03
2006-04-06 12:19:47	6.13E+04
2006-04-06 17:48:08	8.68E+04
2006-04-06 23:08:40	5.83E+04
2006-04-07 04:14:11	1.40E+05
2006-04-07 08:02:01	5.57E+03
2006-04-07 11:23:23	1.30E+05
2006-04-07 12:18:44	6.88E+03
2006-04-08 01:00:48	1.53E+05
2006-04-08 01:23:25	2.67E+03
2006-04-08 03:26:00	4.02E+02
2006-04-09 22:49:56	1.86E+05
2006-04-10 08:52:52	1.86E+05
2006-04-10 10:16:46	3.10E+03
2006-04-10 10:49:31	2.38E+03
2006-04-10 11:31:27	6.54E+02
2006-04-10 12:05:03	2.88E+04
2006-04-10 12:39:44	1.80E+03
2006-04-10 12:50:21	5.54E+03
2006-04-10 13:21:40	1.68E+03
2006-04-10 19:56:55	1.24E+05
2006-04-11 06:23:54	9.73E+03
2006-04-11 09:52:54	4.41E+03
2006-04-11 18:59:03	3.96E+03
2006-04-11 20:10:22	2.17E+04

2006-04-11 23:46:46	5.23E+04
2006-04-12 03:50:04	3.75E+03
2006-04-12 12:55:25	2.61E+03
2006-04-12 15:36:18	6.41E+03
2006-04-12 15:50:08	3.73E+03
2006-04-13 00:20:45	4.62E+04
2006-04-13 01:15:06	7.59E+04
2006-04-13 01:30:31	5.78E+04
2006-04-13 04:35:45	1.04E+05
2006-04-13 05:12:54	2.04E+05
2006-04-13 06:05:21	1.50E+05
2006-04-13 07:52:35	5.00E+03
2006-04-14 00:49:54	1.69E+05
2006-04-14 03:31:37	4.77E+03
2006-04-14 17:18:48	6.81E+04
2006-04-14 20:30:31	1.19E+05
2006-04-15 04:49:14	1.04E+05
2006-04-15 23:50:18	5.22E+04
2006-04-16 18:34:54	2.16E+05
2006-04-16 20:25:43	1.06E+05
2006-04-16 23:30:26	4.54E+04
2006-04-17 03:54:08	1.10E+04
2006-04-17 11:08:34	4.85E+03
2006-04-17 11:16:53	3.94E+03
2006-04-17 14:31:51	1.95E+03
2006-04-17 17:23:35	1.04E+05
2006-04-17 18:33:24	5.39E+03
2006-04-17 23:21:20	7.37E+03
2006-04-18 00:06:31	1.82E+05
2006-04-18 01:39:31	1.03E+04
2006-04-18 05:31:05	1.04E+04
2006-04-18 06:11:17	4.78E+03
2006-04-18 10:52:50	9.78E+03
2006-04-18 12:26:15	1.47E+04
2006-04-18 13:08:06	6.63E+03
2006-04-18 15:12:17	1.23E+04
2006-04-18 15:26:56	1.34E+05
2006-04-18 19:43:17	2.49E+03
2006-04-18 23:19:52	2.32E+03
2006-04-19 02:19:21	3.11E+03
2006-04-19 05:47:59	7.26E+03
2006-04-19 07:15:11	2.81E+03
2006-04-19 10:35:07	5.19E+04
2006-04-19 14:51:01	9.28E+04
2006-04-19 21:56:42	1.52E+04
2006-04-19 23:59:27	5.16E+04

2006-04-20 00:16:51	9.76E+04
2006-04-20 03:29:36	7.08E+03
2006-04-20 05:54:05	1.96E+05
2006-04-20 17:42:21	1.19E+04
2006-04-21 00:50:07	7.19E+04
2006-04-21 09:52:35	1.36E+04
2006-04-21 12:40:45	1.14E+05
2006-04-21 23:39:03	1.86E+04
2006-04-22 09:04:26	1.17E+03
2006-04-22 13:34:39	1.32E+04
2006-04-22 14:13:47	5.17E+04
2006-04-22 14:28:57	6.96E+04
2006-04-22 15:15:58	8.24E+03
2006-04-22 15:56:52	6.06E+04
2006-04-22 23:23:52	3.52E+04
2006-04-23 18:53:04	3.15E+04
2006-04-23 21:08:08	1.18E+05
2006-04-24 04:38:38	4.06E+03
2006-04-24 09:30:39	2.59E+04
2006-04-24 18:55:51	1.16E+05
2006-04-25 15:00:56	7.57E+04
2006-04-25 15:32:03	6.86E+04
2006-04-25 20:45:14	8.96E+04
2006-04-26 04:36:33	2.89E+03
2006-04-26 16:08:00	4.71E+04
2006-04-26 17:32:39	4.47E+03
2006-04-26 19:52:36	1.10E+04
2006-04-26 22:27:06	6.00E+03
2006-04-27 03:21:44	6.20E+04
2006-04-27 11:49:55	2.01E+03
2006-04-27 12:42:11	4.24E+03
2006-04-27 17:46:38	3.34E+03
2006-04-28 00:06:01	1.24E+04
2006-04-28 04:13:40	2.15E+04
2006-04-28 14:05:19	5.45E+03
2006-04-28 16:50:54	1.08E+05
2006-04-29 08:50:44	7.22E+03
2006-04-29 11:24:54	1.10E+04
2006-04-29 11:38:48	4.80E+03
2006-04-29 15:24:28	1.22E+04
2006-04-29 23:34:45	7.00E+03
2006-04-30 03:43:51	1.06E+04
2006-04-30 05:02:25	1.37E+05
2006-04-30 19:41:36	7.81E+04
2006-04-30 20:53:14	6.02E+04
2006-05-01 04:50:22	1.86E+05
2006-05-01 10:05:01	3.84E+04
2006-05-01 13:14:45	1.60E+05
2006-05-02 01:51:54	5.32E+04
2006-05-02 02:53:36	1.00E+04
2006-05-02 05:12:30	1.71E+05
2006-05-02 10:27:16	1.10E+04
2006-05-02 19:02:40	1.86E+05
2006-05-03 02:35:36	1.59E+05
2006-05-03 07:42:37	2.83E+05
2006-05-03 14:31:11	3.85E+04
2006-05-04 00:00:07	3.33E+03
2006-05-04 01:22:25	2.75E+05
2006-05-04 06:10:02	4.58E+04
2006-05-04 09:13:32	5.49E+04
2006-05-04 11:04:47	1.22E+05
2006-05-05 10:21:52	2.16E+04
2006-05-05 12:56:46	3.25E+04
2006-05-05 23:15:56	7.71E+04
2006-05-06 00:37:39	3.60E+04
2006-05-06 04:42:00	2.77E+04
2006-05-06 13:34:56	4.36E+04
2006-05-06 18:27:57	2.55E+04
2006-05-07 04:20:08	6.90E+04
2006-05-07 06:51:30	2.60E+04
2006-05-07 10:20:07	4.17E+04
2006-05-09 04:26:02	6.04E+04
2006-05-09 05:26:43	6.04E+04
2006-05-09 13:36:57	2.49E+04

Appendix 2

Short Period events used

Date yyyy-mm-dd hh:mm:ss	Maximum Amplitude Counts at station E1S SP (for conversion coefficients see Table 2.1)
1999-12-05 07:05:16	1.51E+03
1999-12-05 14:04:26	7.73E+02
1999-12-05 23:30:08	6.96E+02
1999-12-06 10:14:14	3.13E+02
1999-12-06 21:49:27	3.59E+02
1999-12-06 22:40:34	9.18E+02
1999-12-07 17:13:30	3.82E+02
1999-12-08 03:20:11	1.65E+03
1999-12-09 07:25:42	1.70E+03
1999-12-09 14:29:59	8.84E+02
1999-12-09 16:07:07	8.88E+02
1999-12-10 10:43:48	6.09E+02
1999-12-10 12:51:36	1.46E+03
1999-12-10 14:44:04	7.51E+02
1999-12-10 22:29:14	6.06E+02
1999-12-11 18:19:57	1.59E+03
1999-12-11 19:36:38	3.91E+02
1999-12-11 19:41:44	4.82E+02
1999-12-16 05:22:56	1.04E+03
1999-12-16 06:34:30	1.26E+03
1999-12-16 08:11:38	3.91E+02
1999-12-16 18:25:03	5.92E+02
1999-12-16 21:23:57	1.08E+03
1999-12-17 18:04:22	2.56E+02
1999-12-18 03:09:58	5.92E+02
1999-12-19 00:56:54	6.68E+02
1999-12-20 04:06:06	1.51E+03
1999-12-20 04:46:59	1.15E+03
1999-12-21 03:20:11	7.97E+02
1999-12-21 22:56:24	2.55E+02
1999-12-22 02:29:05	2.00E+03
1999-12-22 11:56:29	1.16E+03
1999-12-22 15:20:57	8.82E+02
1999-12-23 01:22:47	8.62E+02
1999-12-23 04:52:22	1.86E+03
1999-12-23 10:39:58	2.38E+03
1999-12-24 05:48:17	1.54E+03
1999-12-24 11:51:13	1.88E+03
1999-12-25 00:31:35	1.82E+03
1999-12-25 06:49:51	2.05E+03
1999-12-25 16:53:03	2.42E+03
1999-12-25 20:43:05	2.27E+03
1999-12-26 14:45:00	2.29E+03
1999-12-27 02:18:46	1.15E+03
1999-12-27 13:02:51	1.93E+03
1999-12-28 00:31:35	2.45E+03
1999-12-28 08:01:25	1.66E+03
1999-12-28 15:26:09	2.44E+03
1999-12-28 18:25:04	2.64E+03
1999-12-29 16:42:41	1.92E+03
1999-12-29 21:20:27	2.38E+03
1999-12-30 06:49:51	8.28E+02
1999-12-30 13:23:28	3.40E+02
1999-12-30 18:35:17	2.33E+03
1999-12-30 20:02:11	3.52E+02
1999-12-31 15:21:13	2.37E+03
1999-12-31 22:40:50	1.74E+03
2000-01-01 04:36:52	7.16E+02
2000-01-01 10:24:28	1.04E+03
2000-01-01 12:47:36	2.22E+03
2000-01-02 01:43:14	2.45E+03
2000-01-02 13:58:23	9.33E+02
2000-01-02 18:24:12	2.52E+03
2000-01-03 05:29:19	2.15E+03

2000-01-03 07:21:47	2.09E+03
2000-01-04 09:33:26	2.39E+03
2000-01-04 17:44:10	1.93E+03
2000-01-04 22:40:39	1.68E+03
2000-01-04 23:21:33	2.65E+03
2000-01-07 02:24:03	2.01E+03
2000-01-07 03:56:03	2.19E+03
2000-01-07 09:43:40	2.45E+03
2000-01-07 16:01:56	2.54E+03
2000-01-08 15:20:47	2.56E+03
2000-01-09 04:01:06	2.52E+03
2000-01-09 15:46:32	2.65E+03
2000-01-10 04:42:09	2.43E+03
2000-01-10 19:31:36	2.77E+03
2000-01-12 01:07:17	2.33E+03
2000-01-12 04:01:05	2.70E+03
2000-01-12 13:33:37	2.18E+03
2000-01-12 23:52:08	1.34E+03
2000-01-13 06:03:57	2.68E+03
2000-01-13 11:10:40	2.54E+03
2000-01-13 20:17:38	2.45E+03
2000-01-13 23:16:32	2.60E+03
2000-01-15 00:31:25	2.58E+03
2000-01-15 14:09:18	2.43E+03
2000-01-15 21:49:22	2.56E+03
2000-01-16 22:30:26	2.62E+03
2000-01-18 00:06:02	2.56E+03
2000-01-18 16:42:50	2.19E+03
2000-01-18 23:52:13	2.57E+03
2000-01-19 05:07:27	2.53E+03
2000-01-19 18:40:14	2.47E+03
2000-01-20 07:05:07	2.43E+03
2000-01-20 08:16:41	2.50E+03
2000-01-20 11:51:22	2.51E+03
2000-01-20 16:17:11	2.58E+03
2000-01-21 07:10:23	2.52E+03
2000-01-21 12:32:26	2.68E+03
2000-01-22 04:26:39	2.50E+03
2000-01-22 14:34:57	2.49E+03
2000-01-23 00:57:16	1.33E+03
2000-01-23 02:03:43	2.15E+03
2000-01-23 02:59:57	2.31E+03
2000-01-23 09:54:00	2.52E+03
2000-01-23 11:46:28	2.62E+03
2000-01-24 03:15:10	2.46E+03
2000-01-24 09:43:39	2.57E+03
2000-01-24 18:19:57	2.53E+03
2000-01-24 20:32:51	4.39E+02
2000-01-25 04:52:08	2.57E+03
2000-01-25 11:25:45	2.25E+03
2000-01-25 13:59:06	2.53E+03
2000-01-26 01:17:30	2.69E+03
2000-01-26 09:48:41	2.63E+03
2000-01-27 00:21:24	2.52E+03
2000-01-27 05:53:40	2.62E+03
2000-01-27 09:13:02	2.67E+03
2000-01-27 23:52:15	2.50E+03
2000-01-28 09:28:14	2.57E+03
2000-01-28 15:26:04	2.55E+03
2000-01-28 17:03:11	2.67E+03
2000-01-28 23:06:08	2.60E+03
2000-01-29 04:26:45	2.25E+03
2000-01-29 07:20:33	2.35E+03
2000-01-29 07:41:00	2.72E+03
2000-01-29 16:01:57	2.01E+03
2000-01-29 17:13:31	2.48E+03
2000-01-29 19:41:46	2.47E+03
2000-01-30 05:22:52	2.51E+03
2000-01-30 15:20:57	2.66E+03
2000-01-31 05:17:51	2.56E+03
2000-01-31 13:49:02	2.52E+03
2000-01-31 17:49:17	2.52E+03

Appendix 3

Temporary Broadband Events Used

Date (Julian day) yyyy-jdy hh:mm:ss	Maximum Amplitude Vertical counts at EE1S BHZ (for conversion coefficients see Table 2.1) Counts		
1999-344 10:29	1.42E+04	1999-359 20:41	8.92E+04
1999-344 12:44	5.07E+04	1999-360 06:48	8.89E+04
1999-344 14:44	3.94E+04	1999-360 14:42	2.65E+04
1999-344 23:42	7.64E+04	1999-362 07:58	8.02E+04
1999-347 14:15	5.85E+04	1999-364 18:30	9.97E+04
1999-348 03:29	2.93E+04	1999-365 12:19	2.15E+03
1999-348 03:31	3.47E+04	2000-001 12:44	3.61E+04
1999-348 22:04	2.02E+04	2000-002 01:39	4.54E+04
1999-348 23:15	4.00E+04	2000-002 18:14	8.03E+04
1999-349 02:10	9.28E+04	2000-003 07:14	4.50E+04
1999-349 13:34	3.16E+04	2000-004 09:29	4.28E+04
1999-349 18:37	4.48E+04	2000-004 22:29	7.47E+04
1999-350 05:20	5.48E+04	2000-004 22:54	7.47E+04
1999-350 06:28	4.96E+04	2000-004 23:14	8.69E+04
1999-353 00:52	1.70E+04	2000-005 10:54	5.89E+04
1999-354 04:01	6.61E+04	2000-007 02:14	9.36E+04
1999-354 04:44	5.71E+04	2000-007 03:54	8.14E+04
1999-355 03:18	4.44E+04	2000-007 09:39	6.25E+04
1999-356 02:25	7.18E+04	2000-007 15:54	8.31E+04
1999-356 11:54	5.62E+04	2000-008 00:39	9.30E+04
1999-356 15:20	5.07E+04	2000-008 15:14	2.44E+03
1999-356 18:11	6.36E+04	2000-009 03:57	6.05E+04
1999-357 01:18	5.03E+04	2000-009 15:44	5.46E+04
1999-357 04:49	9.24E+04	2000-010 04:39	3.50E+04
1999-357 10:34	2.39E+03	2000-010 19:29	8.00E+04
1999-357 18:56	1.44E+03	2000-012 00:59	1.29E+02
1999-358 11:47	8.24E+04	2000-012 03:44	6.01E+04
1999-359 00:29	8.37E+04	2000-012 13:29	2.59E+03
1999-359 06:46	3.16E+02	2000-013 05:59	5.33E+04
1999-359 16:49	3.41E+04	2000-013 10:59	4.77E+04

2000-013 20:09	7.92E+04	2000-022 14:29	3.72E+04
2000-013 23:09	2.42E+04	2000-023 00:44	5.61E+04
2000-015 00:29	5.29E+04	2000-023 01:59	8.00E+04
2000-015 13:59	7.10E+04	2000-023 02:59	2.00E+04
2000-015 22:14	9.43E+04		

Appendix 4

Infrasound data used

Date Maximum Amplitude
yyyy-mm-dd hh:mm:ss Counts (for conversion coefficients see Table 2.1)

2006-01-02 13:07:19	4.20E+05	2006-01-10 19:18:48	6.66E+05
2006-01-02 18:45:26	3.98E+05	2006-01-10 21:12:45	2.77E+05
2006-01-02 22:27:43	6.43E+04	2006-01-11 08:54:37	3.56E+04
2006-01-03 03:30:46	4.35E+04	2006-01-11 18:20:20	1.60E+05
2006-01-03 07:15:32	3.28E+05	2006-01-11 20:51:56	8.66E+04
2006-01-03 15:11:45	1.52E+05	2006-01-12 00:36:20	5.63E+04
2006-01-05 07:14:06	2.45E+05	2006-01-12 04:00:02	4.60E+05
2006-01-05 15:09:50	5.47E+05	2006-01-12 15:10:46	6.45E+04
2006-01-05 16:10:01	3.01E+05	2006-01-12 20:08:56	1.10E+05
2006-01-05 20:18:26	6.16E+05	2006-01-12 20:54:39	2.31E+05
2006-01-06 06:01:04	1.08E+05	2006-01-13 05:04:40	1.74E+05
2006-01-07 01:58:58	1.66E+05	2006-01-13 10:21:24	6.51E+05
2006-01-07 05:12:15	2.20E+05	2006-01-13 12:20:26	2.75E+05
2006-01-07 13:09:29	4.68E+04	2006-01-13 16:36:30	4.72E+04
2006-01-07 17:55:44	4.40E+05	2006-01-13 17:13:23	9.03E+04
2006-01-07 19:30:22	3.67E+05	2006-01-13 19:23:31	6.19E+05
2006-01-07 21:57:14	3.48E+05	2006-01-15 08:42:36	8.05E+05
2006-01-07 23:04:42	2.96E+05	2006-01-15 12:26:40	1.71E+05
2006-01-08 08:18:56	4.63E+05	2006-01-15 20:59:16	3.36E+05
2006-01-08 12:04:28	1.28E+05	2006-01-16 00:23:20	2.86E+05
2006-01-08 15:25:20	4.08E+05	2006-01-16 03:35:33	4.99E+05
2006-01-08 19:54:55	2.58E+05	2006-01-16 06:18:58	3.12E+05
2006-01-09 10:21:41	6.21E+04	2006-01-16 20:47:22	4.79E+05
2006-01-09 11:14:45	4.46E+04	2006-01-17 01:21:13	7.95E+05
2006-01-09 13:08:53	2.32E+05	2006-01-17 18:47:53	3.95E+05
2006-01-09 14:08:42	3.05E+05	2006-01-18 00:50:41	4.76E+05
2006-01-09 14:26:28	3.80E+05	2006-01-18 15:10:57	4.10E+05
2006-01-09 17:33:51	2.77E+05	2006-01-18 20:50:19	3.81E+05
2006-01-10 04:07:48	3.64E+05	2006-01-19 18:54:16	3.87E+05
2006-01-10 09:14:55	6.57E+05	2006-01-19 19:42:09	2.81E+05
2006-01-10 13:06:12	1.74E+05	2006-01-20 01:55:19	5.80E+05

2006-01-21	19:47:57	4.66E+05
2006-01-22	02:53:19	5.66E+04
2006-01-22	07:34:39	7.41E+05
2006-01-22	09:01:04	8.98E+04
2006-01-22	11:09:36	3.66E+05
2006-01-22	23:38:44	3.58E+05
2006-01-23	09:48:44	2.38E+05
2006-01-23	11:25:07	2.14E+05
2006-01-23	15:19:30	7.80E+04
2006-01-23	16:39:52	3.03E+05
2006-01-23	19:58:48	2.38E+05
2006-01-24	01:59:43	1.72E+04
2006-01-24	02:09:39	3.52E+05
2006-01-24	04:32:12	5.07E+05
2006-01-25	06:58:29	4.95E+05
2006-01-25	18:09:59	4.30E+05
2006-01-26	08:14:12	4.26E+05
2006-01-26	14:16:18	1.68E+05
2006-01-27	12:29:30	2.63E+05
2006-01-27	19:29:57	3.99E+05
2006-01-28	03:05:26	4.86E+04
2006-01-28	12:40:45	1.81E+05
2006-01-29	06:32:58	8.16E+03
2006-01-29	18:02:34	6.60E+05
2006-01-30	03:49:21	8.30E+03
2006-01-30	04:53:35	1.54E+05
2006-01-30	09:58:52	1.49E+05
2006-01-30	17:08:45	7.88E+05
2006-01-30	19:11:34	2.65E+05
2006-01-31	06:15:57	4.63E+04
2006-01-31	10:56:29	1.04E+04
2006-01-31	11:19:53	1.12E+04
2006-01-31	12:03:42	8.08E+05
2006-01-31	14:08:14	2.56E+05
2006-01-31	22:49:31	4.71E+02
2006-02-01	08:00:32	6.89E+05
2006-02-01	13:11:45	1.83E+05
2006-02-01	13:50:17	2.64E+04
2006-02-01	14:07:16	3.77E+04
2006-02-01	22:47:18	3.18E+04
2006-02-01	23:39:29	7.97E+04
2006-02-02	01:56:24	6.43E+05
2006-02-02	03:23:44	4.94E+04
2006-02-02	08:33:46	6.75E+04
2006-02-02	10:43:42	4.11E+04
2006-02-02	20:58:00	1.46E+05
2006-02-03	03:44:48	5.42E+05
2006-02-03	07:19:42	1.57E+05
2006-02-03	10:35:11	5.17E+05
2006-02-03	20:54:11	4.19E+05
2006-02-03	23:52:45	7.25E+05
2006-02-05	00:55:26	2.63E+05
2006-02-05	06:17:58	3.47E+05
2006-02-05	08:12:49	1.36E+05
2006-02-05	14:08:26	4.10E+05
2006-02-06	06:28:25	6.71E+05
2006-02-06	11:45:40	4.18E+05
2006-02-06	16:10:07	6.79E+05
2006-02-07	06:36:57	5.84E+05
2006-02-07	10:37:04	1.34E+05
2006-02-07	18:43:22	3.59E+05
2006-02-07	21:23:52	6.80E+04
2006-02-07	22:54:17	7.33E+05
2006-02-08	02:29:07	6.62E+05
2006-02-09	00:59:53	4.75E+05
2006-02-09	09:41:33	9.72E+04
2006-02-09	15:58:46	5.17E+05
2006-02-09	21:06:46	3.15E+05
2006-02-10	08:29:34	4.38E+05
2006-02-10	13:57:45	2.85E+05
2006-02-10	15:16:06	2.57E+05
2006-02-10	21:39:30	4.82E+05
2006-02-10	23:26:15	5.51E+05
2006-02-11	01:38:15	2.43E+05
2006-02-11	14:30:33	2.56E+05
2006-02-11	21:42:21	2.58E+05
2006-02-11	21:55:31	1.42E+05
2006-02-17	08:26:49	2.59E+05
2006-02-17	19:39:18	1.32E+05
2006-02-18	01:09:43	5.80E+05
2006-02-18	05:41:13	1.21E+05
2006-02-18	07:15:25	6.24E+05
2006-02-18	12:42:38	9.44E+04
2006-02-18	21:43:51	4.25E+05
2006-02-19	08:14:12	3.43E+02
2006-02-20	02:16:45	1.08E+05
2006-02-20	09:19:07	3.19E+05
2006-02-20	11:50:32	7.45E+02
2006-02-20	17:30:14	3.35E+05
2006-02-20	20:03:21	1.47E+05
2006-02-21	02:04:05	5.65E+05
2006-02-21	12:33:00	4.63E+04

2006-02-21 21:02:29	3.20E+05
2006-02-22 01:17:17	2.56E+05
2006-02-22 02:51:48	2.69E+02
2006-02-22 11:21:07	2.95E+05
2006-02-22 13:17:11	3.05E+05
2006-02-22 16:47:54	4.02E+03
2006-02-23 00:11:30	3.38E+05
2006-02-24 07:51:45	3.07E+05
2006-02-24 13:56:48	3.14E+05
2006-02-25 06:57:54	6.63E+05
2006-02-25 07:26:47	6.77E+03
2006-02-25 22:26:01	7.09E+05
2006-02-26 01:13:12	4.19E+05
2006-02-26 03:29:40	2.37E+05
2006-02-26 06:42:09	6.05E+05
2006-02-26 08:06:39	7.42E+05
2006-02-27 23:54:39	7.01E+04
2006-02-28 15:30:42	6.75E+05

Appendix 5

Digital Video of Lava Lake Eruptions

Date (mm-dd-yy hh:mm)	Maximum Amplitude Vertical counts at station E1S BB (for conversion to ground velocity, see Table 2.1).		
12-03-05 13:50	8.74E+04	12-30-05 20:54	5.76E+04
12-03-05 15:57	1.27E+04	12-31-05 04:32	6.35E+03
12-11-05 11:09	1.22E+05	12-31-05 06:12	4.70E+04
12-11-05 11:40	3.35E+03	12-31-05 06:36	8.80E+04
12-11-05 14:03	4.35E+04	12-31-05 10:53	1.83E+05
12-11-05 18:10	1.33E+03	12-31-05 11:44	7.18E+04
12-13-05 16:57	7.87E+03	01-01-06 14:27	5.23E+04
12-14-05 05:21	9.30E+04	01-01-06 17:46	8.46E+04
12-14-05 05:45	1.19E+04	01-02-06 18:45	1.54E+05
12-14-05 11:45	1.68E+05	01-03-06 07:15	5.71E+04
12-15-05 09:19	1.34E+05	01-05-06 07:14	3.83E+04
12-15-05 11:42	4.65E+03	01-05-06 15:10	1.43E+05
12-15-05 11:54	2.35E+03	01-05-06 16:10	5.21E+04
12-15-05 13:02	1.62E+05	01-07-06 01:59	3.23E+04
12-18-05 06:34	1.75E+04	01-07-06 05:12	4.56E+04
12-18-05 10:27	1.08E+05	01-07-06 13:09	7.37E+03
12-19-05 00:41	8.73E+04	01-07-06 17:56	8.38E+04
12-19-05 06:30	5.66E+04	01-07-06 19:30	8.41E+04
12-19-05 09:39	2.29E+05	01-07-06 21:57	6.90E+04
12-21-05 16:42	3.71E+04	01-07-06 23:04	4.15E+04
12-27-05 11:35	1.18E+04	01-08-06 08:19	1.20E+05
12-28-05 22:03	4.26E+04	01-08-06 12:04	2.12E+04
12-29-05 10:50	3.62E+04	01-08-06 15:25	8.46E+04
12-29-05 11:01	3.22E+04	01-08-06 19:55	1.04E+05
12-29-05 13:42	6.87E+04	01-09-06 10:21	1.20E+04
12-30-05 20:41	7.66E+04	01-09-06 11:15	4.60E+03

01-09-06 13:09	3.66E+04
01-09-06 14:08	5.62E+04
01-09-06 14:26	6.87E+04
01-09-06 17:34	7.08E+04
01-10-06 04:08	6.45E+04
01-10-06 09:15	1.53E+05
01-10-06 13:06	2.73E+04
01-10-06 19:19	1.71E+05
01-10-06 21:13	5.89E+04
01-11-06 08:54	6.72E+03
01-11-06 18:20	2.82E+04
01-11-06 20:52	1.27E+04
01-17-06 01:21	3.21E+05
01-20-06 01:55	7.30E+04
01-30-06 17:09	1.97E+05
01-31-06 06:16	6.93E+03
01-31-06 14:08	1.30E+05

Appendix 6

Code Used

Code to Improve Rough Pick

```
clear

!ls 20060[4-5]*/RAY.BHZ*.sac | sort | uniq > list3.all
!cat list3.all | wc -l > list3.num

 fid1 = fopen('list3.num');
 fid2 = fopen('list3.all');
 mag=1000;
 %window time length
 dlength=2500;

 %laod data into matrix
 events=fscanf(fid1,'%d');
 for i=1:events

   sdata = fscanf(fid2,'%s.SAC\n');

   %get path from file
    if i==1
        stnames=char(sdata);
    else
        stnames=char(stnames,sdata);
    end

    %load sac data and detrend it
    [sachdr(:,i),dataZ]=load_sac(sdata);

    dataZ=detrend(dataZ);
```

```
   %create need variables
   starttime=sachdr(i).t0;
   %starttime=sachdr(i).a;
   delta=sachdr(i).delta;
   sampsec=1/delta;
   begin = sachdr(i).b;
   beginning=round(sampsec*starttime)-round(sampsec*begin);
   offset=round(10*sampsec);
   beginning=beginning-offset;
   %make sure you don't go off the beginning of the data
   if offset > beginning
       dataZ=[zeros(offset,1);dataZ(:,1)];
       beginning=round(sampsec*starttime-sampsec*begin);
   end

   dataZ=dataZ(round(beginning) : round(length(dataZ)));

   %insert in array
   if length(dataZ) >= dlength;
       data(:,i)=dataZ(1:dlength);
   else
       data(:,i)=[dataZ ; zeros(dlength-length(dataZ),1)];
   end
   clear dataZ

 end



%%%%%%%%%%%%%%%%%%%%%%%%%%%%%%%%%%%%%%%%%%%%
%filter data
 %n = order, Wn = normalized cut off frequency
  W1 = (2)/(sampsec/2);
  W2 = (5)/(sampsec/2);
  Wn = [W1,W2];
  n = 2;
  [b,a] = butter(n,Wn);
  for ii=1:events
     data(:,ii) = filtfilt(b,a,data(:,ii));
     detrend(data(:,ii));
  end

%%%%%%%%%%%%%%%%%%%%%%%%%%%%%%%%%%%%%%%%%%%%
%solve for pick adjustments

 %correlation and lag determination using the Fourier transform
```

```
%cmax is the maximum correlation
%ilag is the relative lag in samples
 k=1;
 n=length(data(:,1));
for i=1:events-1
    for j=i+1:events

        ccorr=fcorr(data(:,i),data(:,j));
        [cmax(k,1),l]=max(ccorr);

       %get the lag from the index of the maximum of ccorr;
       %lags greather than n/2 are actually negative
         if(l > n/2)
           ilag(k,:) = l-n-1;
         else
           ilag(k,:) = l-1;
         end
         k=k+1;
    end
end

%add zero at end of event lag list
ilag(k,:)=0;

%number of rows
num=events*(events-1)/2;
%create comparison matrix
G=zeros(num+1,events);%+1for row of 1's at the bottom
%G=zeros(num,events);
k=1;
for i=1:events-1
    for j=i+1:events
        G(k,i)=1*cmax(k)^2;
        G(k,j)=-1*cmax(k)^2;
        k=k+1;
    end
end

G(num+1,:)=1;

%%%%%%%%%%%%%%%%%%%%%%
%solve for lag adjustments
%irls
%lagAdjust=irls(G,ilag.*([cmax;1].^2));
%Conjugant Gradiant Lest Squares (2-norm)
[X,Rho,Eta]=cgls(G,ilag.*([cmax;1].^2),50);
```

```
lagAdjust=X(:,end);
%%%%%%%%%%%%%%%%%%%%%%%%%%%%%%%%%%%%%%%%%%%
%calculate new picks and save them to the aproprate sac headers
 for i=1:events
    if lagAdjust(i,:) > 0
       Adj=abs(round(lagAdjust(i,:)));
       sachdr(i).t0 = ((sachdr(i).t0) + ((Adj+1)/sampsec));
       %sachdr(i).t0 = ((sachdr(i).a) + ((Adj+1)/sampsec));
    elseif lagAdjust(i,:) < 0
       Adj=abs(round(lagAdjust(i,:)));
       sachdr(i).t0 =( (sachdr(i).t0) - ((Adj)/sampsec));
       %sachdr(i).t0 =( (sachdr(i).a) - ((Adj)/sampsec));
    else
        sachdr(i).t0 = sachdr(i).t0;
        %sachdr(i).t0 = sachdr(i).a;
    end
    stnames(i,:)
    write_sac_h(stnames(i,:),sachdr(i));
 end

fclose(fid1);
fclose(fid2);

%%%%%%%%%%%%%%%%%%%%%%%%%%%%%%%%%%%%%%%%%%%%%%%%%%%%
%TEST the picks to make sure they work%%%%%%%%%%%%%%%%%%%%%

fid1 = fopen('list3.num');
fid2 = fopen('list3.all');

events=fscanf(fid1,'%d');
for i=1:events

  sdata = fscanf(fid2,'%s.SAC\n');

   if i==1
      stnames=char(sdata);
   else
      stnames=char(stnames,sdata);
   end

   %load sac data and detrend it
   [sachdrp(:,i),dataZ]=load_sac(sdata);

   dataZ=detrend(dataZ);

   starttime=sachdr(i).t0;
```

```
   delta=sachdr(i).delta;
   sampsec=1/delta;
   begin = sachdr(i).b;
   beginning=round(sampsec*starttime)-round(sampsec*begin);
   offset=round(5*sampsec);
   beginning=beginning-offset;
   if beginning < 1
      dataZ=[zeros(beginning,1);dataZ(:,1)];
      beginning=1;
   end

   dataZ=dataZ(round(beginning) : round(length(dataZ)));

   %insert in array
   if length(dataZ) >= dlength;
      dataq(:,i)=dataZ(1:dlength);
   else
      dataq(:,i)=[dataZ ; zeros(dlength-length(dataZ),1)];
   end
   clear dataZ

 end

%%%%%%%%%%%%%%%%%%%%%%%%%%%%%%%%%%%%%%%%%%%%%
 %filter data
 %n = order, Wn = normalized cut off frequency
 W1 = (2)/(sampsec/2);
 W2 = (5)/(sampsec/2);
 Wn = [W1,W2];
 n = 2;
 [b,a] = butter(n,Wn);
 for ii=1:events
   dataq(:,ii) = filtfilt(b,a,dataq(:,ii));
 end

%%%%%%%%%%%%%%%%%%%%%%%%%%%%%%%%%%%%%%%%%%%%%
%divide events by their RMS values
  for ii=1:events
     vartemp=var(dataq(:,ii));
     dataq(:,ii)= dataq(:,ii)./sqrt(vartemp);
  end

 figure(2)
 imagesc(dataq)
 colormap(bone)
```

Preparation Code

```
clear
%load data into a matrix for analysis, and save pertinent variables

cmpnames={'HOO.EHZ.ER.sac'}; %CHANGE CP BELOW
for c=1:1

%CHANGE THIS AS WELL
!cp HOOgretlist list.all
!cat list.all | wc -l > list.num

SR=40;

%filtering is currently disabled right now
%filter settings
HP=1;
LP=8;
%dlength=500;
dlength=40*1*40;
%pre-pick offset (s)
offsec=2;
Wn=[HP,LP]/(SR/2);
[B,A]=butter(2,Wn);
%[B,A]=butter(2,Wn(1),'high');

fid1 = fopen('list.num');
fid2 = fopen('list.all');
%window time length (samples)

events=fscanf(fid1,'%d');

if events == 0
   disp('No Events Found')
   return
end

for i=1:events

   sdata = [fgetl(fid2),char(cmpnames(c))];

   if i==1
      stnames=char(sdata);
   else
```

```
        stnames=char(stnames,sdata);
    end

    %load sac data and detrend it
    disp(sdata)
    [sachdr(:,i),dataZ]=load_sac(sdata);

    %starttime=sachdr(i).t0;
    starttime=sachdr(i).a;

    %detrend the data
    dataZ=detrend(dataZ);

    % filter data
    % dataZ=filtfilt(B,A,dataZ);

    delta=sachdr(i).delta;
    sampsec=1/delta;
    begin = sachdr(i).b;
    beginning=round(sampsec*starttime)-round(sampsec*begin);
    offset=round(offsec*sampsec);
    beginning=beginning-offset;
    if beginning < 1
        dataZ=[zeros(abs(beginning),1);dataZ(:,1)];
        beginning=1;
    end

    dataZcut=dataZ(round(beginning) : round(length(dataZ)));

    %insert in array
    if length(dataZcut) >= dlength;
        data(:,i)=dataZcut(1:dlength);
    else
        data(:,i)=[dataZcut ; zeros(dlength-length(dataZcut),1)];
    end

end

%save the necessary variables from the reading step for explot2
save dsave delta data events dlength stnames sachdr
system(['mv dsave.mat ','dsave.',char(cmpnames(c)),'.unfiltered.gret.SP.mat']);
```

Iterative Alignment Program

```
clear
%for si=1:7
%stalist={'CON','E1S','LVA','NOE','UHT','HEL','NKB'};
si=1;
stalist={'HOO'};
sname=char(stalist(si));
load dsave.HOO.EHZ.ER.sac.unfiltered.gret.SP.mat
thresh=0.5;
minsize1 = 0;
maxsize1 = 1000000000;

%filter data
 %n = order, Wn = normalized cut off frequency
 filtband='2to5';%change this when you cange the values below
 W1 = (2)/((1/sachdr(1).delta)/2);
 W2 = (5)/((1/sachdr(1).delta)/2);
 Wn = [W1,W2];
 n = 2;%number of poles
 [b,a] = butter(n,Wn);
 [mm,nn]=size(data)
 for ii=1:nn
    data(:,ii) = filtfilt(b,a,data(:,ii));
 end

%normalize for stacking/alignment (use rms amplitude of vertical)
for i=1:events
    eventsize(i)=min((data(:,i)));
    rmsval(i)=sqrt(var(data(:,i)));
    a(i)=std(data(:,i));
    data_t0(:,i)=data(:,i)/a(i);
end
eventsize=abs(eventsize);
s=std(data_t0');
stack=sum(data_t0')/events;

%plot unnormalized data
xtime=delta*(0:dlength-1);
xnum=(1:events);
figure(1)
set(gca, 'FontSize', 16,'LineWidth',1.0);
colormap(bone)
imagesc(xnum,xtime,data)
```

```
ylabel('Time (s)')
xlabel('event number')

%plot data using original t0 picks
figure(2)
set(gca, 'FontSize', 16,'LineWidth',1.0);
colormap(bone)
imagesc(xnum,xtime,data_t0)
ylabel('Time (s)')
xlabel('event number')
nstack=stack/std(stack);
fnstack=fft(nstack');
hold on
for i=1:events
    ccf=real(ifft(fnstack.*conj(fft(data_t0(:,i)))))/dlength;
    [corr(i),ind(i)]=max(ccf);
    corr0(i)=ccf(1);
    if ind(i) > dlength/2
        ind(i)=ind(i)-dlength;
    end
end
plot(xnum,-corr*10+20)
hold off
title(sname)

figure(3)
set(gca, 'FontSize', 16,'LineWidth',1.0);
plot(delta*(0:dlength-1),stack)
hold on
plot(xtime,stack+s,'-.r')
plot(xtime,stack-s,'-.r')
xlabel('Time (s)')
hold off
title('Initial pick stack');

figure(4)
set(gca, 'FontSize', 16,'LineWidth',1.0);
plot(xtime,stack)
hold on
plot(xtime,stack+s,'-.r')
plot(xtime,stack-s,'-.r')
xlabel('Time (s)')
hold off
title([sname,'Adjusted pick stack (pre-iteration) (+- 1 \sigma)']);

%iterative realignment using stack
```

```
datatmp=data_t0;
%initial correlation (use all events)
corr=ones(1,events);

netshift=zeros(1,events);

onevents=0;
for iter=1:15

   %latest stack
   stack=zeros(dlength,1);
   j=1;
   clear dbest;
   clear dind;
   %clear hdr
   for i=1:events
      %note conditional here to use only the small events
      if corr(i) > thresh & eventsize(i) > minsize1 & eventsize(i) < maxsize1
         dbest(:,j)=datatmp(:,i);
         dind(j)=i;
         %hdr(:,j)=sachdr(:,i);
         j=j+1;
      end
   end

      nstack=mean(dbest')';
      nstack=nstack/std(nstack);
      s=std(dbest')';

   fnstack=fft(nstack);
   for i=1:events
      ccf=real(ifft(fnstack.*conj(fft(datatmp(:,i)))))/dlength;
      [corr(i),ind(i)]=max(ccf);

      if ind(i) > dlength/2
         ind(i)=ind(i)-dlength;
      end

      %4-second limit to interative alignment adjustment
      if abs(ind(i))>160
         ind(i)=sign(ind(i))*160;
      end

   end

   netshift=netshift-(ind-1);
```

```
    datatmp=colshift(datatmp,-(ind-1));

    %image sc of all data after realignment with stack
    figure(5)
    set(gca, 'FontSize', 16,'LineWidth',1.0);
    colormap(bone)
    imagesc(xnum,xtime,datatmp)
    ylabel('Time (s)')
    xlabel('Event Number')

    hold on

    plot(xnum,-corr*10+20)
    hold off

    figure(6)
    set(gca, 'FontSize', 16,'LineWidth',1.0);
    plot(xtime,nstack)
    title(sname)

    hold on
    plot(xtime,nstack+s,'-.r')
    plot(xtime,nstack-s,'-.r')
    xlabel('Time (s)')
    hold off
    title('Adjusted pick stack (+- 1 \sigma)');

    %imagesc of stack data
    figure(7)
    set(gca, 'FontSize', 16,'LineWidth',1.0);
    xbnum=j-1;
    colormap(bone)
    imagesc(1:xbnum,xtime,dbest)
    ylabel('Time (s)')
    xlabel('event number')

    figure(8)
    set(gca, 'FontSize', 16,'LineWidth',1.0);
    hist(corr,20)
    title(sname)

    disp(['iteration: ',num2str(iter),' median correlation: ',num2str(median(corr)),' number
of events: ',num2str(xbnum)])
    pause(1)
    if (onevents==xbnum) && (onmedian==median(corr))
        break
```

```
    end
    onevents=xbnum;
    onmedian=median(corr);
end

%save all realigned data
dataorig=datatmp;
dfinal=dbest;

 figure(18)
 set(gca, 'FontSize', 16,'LineWidth',1.0);
 snormplot(dfinal);
 title(sname)

%plot data by time
 figure(19)
 set(gca, 'FontSize', 16,'LineWidth',1.0);
 snormplottime(dfinal./5,sachdr(dind))

%normalized traces
dfinalnz=dfinal;
%other needed veriables
 dataz=data;
 sz=s;
 sachdrz=sachdr;

save dsave dataz dataorig dfinalnz a events dlength stnames sachdr nstack sz dind netshift
eventsize rmsval%nlagAdjust
system(['mv dsave.mat fsave.',sname,'.EHZ.gret.SP.',filtband,'.mat']);
```

Gret and Moving Window Analysis Code

```
clear

load fsave.E1S.EHZ.gret.mat

station_name='E1S.EHZ';
window = 2*round(1/sachdr(1).delta);

%create needed veriables
[m n]=size(dfinalnz);
h=sachdr(dind);
```

```
eventSize=eventsize(dind);
dataseg=dfinalnz;
dhdr=h;

[m1,n1]=size(dataseg);

%calculate time distrubution through time
for i=1:n1
   stationtime(i)=(pick2unixsecs_sac(dhdr(i),'t0'));
   stationtime(i)=stationtime(i)/(60*60*24*365)+1970;
end
xaxis=1:n1;
figure(1)
plot(xaxis,stationtime,'.')
title(station_name)
xlabel('Number of Events')
ylabel('Date')

%find correlations for moving window using the stack
[px,py]=size(dataseg);
for ii=1:py
   [corr(:,ii), lag(:,ii)]=movcor(nstack,dataseg(:,ii),window);
end

figure(2)
set(gca, 'FontSize', 16,'LineWidth',1.0);
imagesc(corr)
title([station_name ' moving correlation with repsect to the stack'])
ylabel('time(s)')
xlabel('number of events')
colormap('default')
colorbar

figure(3)
set(gca, 'FontSize', 16,'LineWidth',1.0);
snormplottime(dataseg./1,dhdr)
title(station_name)

x1axis=1:m1;
figure(4)
set(gca, 'FontSize', 16,'LineWidth',1.0);
plot(x1axis.*sachdr(i).delta,nstack)
title(['stack for ' station_name])
xlabel('time (s)')

%correlations of reflectors
```

```
[r,c]= size(corr);
%set wich row to look at
row=7;
for i = 1:c
   reflection(i)=corr(row,i);
end
% figure(5)
% plot(stationtime,reflection)
% title([station_name 'Correlation of a reflector with the stack over time'])
% ylabel('Correlation')
% xlabel('Date')

%find event most simlar to stack
[maxcorr,maxcol]=max(sum(corr))
%override this value if desired
%maxcol=16

%find correlations for all columns
for i = 1:r
   for j=1:c
      reflection2(i,j)=j+corr(i,j);
   end
end

%moving correlation with respect to a master event
for ii=1:py
   [corr2(:,ii), lag2(:,ii)]=movcor(dataseg(:,maxcol),dataseg(:,ii),window);
end

figure(7)
set(gca, 'FontSize', 16,'LineWidth',1.0);
imagesc(corr2)
title([station_name ' moving correlation with respect to a master event'])
ylabel('time(s)')
xlabel('number of events')
colormap('default')
colorbar

figure(6)
set(gca, 'FontSize', 16,'LineWidth',1.0);
plot(stationtime,eventSize,'.')
title([station_name ' Size of Event with time'])
ylabel('Maximum Size')
xlabel('Date')

for i = 1:c
```

```
    reflection(i)=corr(row,i);
end

% figure(8)
% plot(stationtime,reflection)
% title('Correlation of a reflector with the best event over time')
% ylabel('Correlation')
% xlabel('Date')

%gret analysis
offset=(2)*round(1/sachdr(1).delta)
initial=(2+7)*round(1/sachdr(1).delta);%offset + initial part (also used 4.5 s)
coda=(7+2+7)*round(1/sachdr(1).delta);%offset+initial+length of coda (also used 13 s)

%find max correlation of the initial part
for i=1:c
    ccorrinitial=fcorr(nstack(offset:initial),dataseg(offset:initial,i));
    [cmax1(i,1),l]=max(ccorrinitial);
    ccorrinitialb=fcorr(dataseg(offset:initial,7),dataseg(offset:initial,i));
    [cmax2(i,1),l]=max(ccorrinitialb);
end
%find max correlation of the coda
for i=1:c
    ccorrcoda=fcorr(nstack(initial:coda),dataseg(initial:coda,i));
    [cmax3(i,1),l]=max(ccorrcoda);
    ccorrcodab=fcorr(dataseg(initial:coda,7),dataseg(initial:coda,i));
    [cmax4(i,1),l]=max(ccorrcodab);
end

figure(9)
set(gca, 'FontSize', 16,'LineWidth',1.0);
plot(stationtime,cmax1,'r.')
hold on
plot(stationtime,cmax2,'b.')
title('Correlation of the inital part - red(stack), blue(induvidual event)')
ylabel('Correlation')
xlabel('Date')
hold off

figure(10)
set(gca, 'FontSize', 16,'LineWidth',1.0);
plot(stationtime,cmax2,'r.')
hold on
plot(stationtime,cmax4,'b.')
title('Correlation of the later part - red(stack), blue(induvidual event)')
ylabel('Correlation')
```

```
xlabel('Date')
hold off

figure(11)
set(gca, 'FontSize', 16,'LineWidth',1.0);
reflectors=[3,6,7,9,16];
reflength=length(reflectors)+1;
for i=1:length(reflectors)
   for j=1:n1
      reflection3(i,j)=corr(reflectors(i),j);
   end
   subplot(reflength,1,i),plot(stationtime,reflection3(i,:),'.')
   grid minor
   axis([stationtime(1)-.001 stationtime(n1)+.001 0 1])%stationtime(1)-.001 2004.8
   ylabel([num2str(reflectors(i)) ' s'])
end
subplot(reflength,1,1)
title([station_name ' correlation of reflector with time with respect to the stack'])
subplot(reflength,1,i+1),
plot(stationtime,eventSize./max(eventSize),'r.')
title([station_name ' Size of Event with time'])
grid minor
axis([stationtime(1)-.001 stationtime(n1)+.001 0 1])
ylabel('Max value')
xlabel('Date')

%plot(stationtime,reflection3)
title([station_name ' Correlation of major reflections over time'])
ylabel('Correlation')
xlabel('Date')

% rdiff=reflection3(1,:)-reflection3(4,:);
% figure(12)
% set(gca, 'FontSize', 16,'LineWidth',1.0);
% plot(stationtime,rdiff)

figure(13)
set(gca, 'FontSize', 16,'LineWidth',1.0);
%title([station_name ' correlation of reflector with time with respect to a master event'])
for i=1:length(reflectors)
   for j=1:n1
      reflection3(i,j)=corr2(reflectors(i),j);
   end
   subplot(reflength,1,i),plot(stationtime,reflection3(i,:),'.')
   axis([stationtime(1)-.001 stationtime(n1)+.001 0 1])
   ylabel([num2str(reflectors(i)) ' s'])
```

```
    grid minor
end
subplot(reflength,1,1)
title([station_name ' correlation of reflector with time with respect to a master event'])
subplot(reflength,1,i+1),
plot(stationtime,eventSize./max(eventSize),'r.')
title([station_name ' Size of Event with time'])
grid minor
axis([stationtime(1)-.001 stationtime(n1)+.001 0 1])
ylabel('RMS value')
xlabel('Date')

figure(14)
set(gca, 'FontSize', 16,'LineWidth',1.0);
plot(x1axis.*sachdr(i).delta,dataseg(:,maxcol))
title([station_name ' master event'])
xlabel('Time (s)')

figure(444)
set(gca, 'FontSize', 16,'LineWidth',1.0);
 for j=1:n1
        reflection3(7,j)=corr2(7,j);
    end
   plot(stationtime,reflection3(7,:),'.')
    axis([stationtime(1)-.001 stationtime(n1)+.001 0 1])
    ylabel('Max Correlation of 7s refector')
xlabel('date')
title('Maximum correlation of a reflector(blue),event size(red)')
hold on
plot(stationtime,eventSize./max(eventSize),'r.')
hold off
```

Scatterer Analysis Code

```
clear

%!ls 20051028212958/E1S.BHZ*.sac 20051028212958/CON.BHZ*.sac
20051028212958/LEH.BHZ*.sac | sort | uniq > list2.all
!cat list2.all | wc -l > list2.num

fid1 = fopen('list2.num');
fid2 = fopen('list2.all');
```

```
events=fscanf(fid1,'%d');
dlength = 60*40;

%load data
[stnames,data,delta]=load_events(events,fid2, dlength, 't0');
%filter data
 sampsec=1/delta;
  W1 = (2)/(sampsec/2);
  W2 = (5)/(sampsec/2);
  Wn = [W1,W2];
  n = 2;
  [b,a] = butter(n,Wn);
  for ii=1:events
     data(:,ii) = filtfilt(b,a,data(:,ii));
     detrend(data(:,ii));
  end

%stack the data to improve signal to noise ration
constack=data(:,1)+data(:,3)+data(:,2);
e1sstack=data(:,4)+data(:,5)+data(:,6);
abbstack=data(:,7)+data(:,8)+data(:,9);
bomstack=data(:,10)+data(:,11)+data(:,12);
brdstack=data(:,13)+data(:,14)+data(:,15);

%normalize data
constack=constack./max(constack);
e1sstack=e1sstack./max(e1sstack);
abbstack=abbstack./max(abbstack);
bomstack=bomstack./max(bomstack);
brdstack=brdstack./max(brdstack);

%line up the stacks at their maximum correlation
[cmax,ind]=max(xcorr(abs(hilbert(e1sstack)),abs(hilbert(constack)),'coeff'));
if(ind>length(e1sstack)/2)
    ilag=ind-dlength-1;
else
    ilag=ind-1;
end
constack=colshift(constack , -(ilag-1));
%line up the stacks at their maximum correlation
[cmax,ind]=max(xcorr(abs(hilbert(e1sstack)),abs(hilbert(bomstack)),'coeff'));
if(ind>length(e1sstack)/2)
    ilag=ind-dlength-1;
else
    ilag=ind-1;
```

```
end
bomstack=colshift(bomstack , -(ilag-1));
%line up the stacks at their maximum correlation
[cmax,ind]=max(xcorr(abs(hilbert(e1sstack)),abs(hilbert(brdstack)),'coeff'));
if(ind>length(e1sstack)/2)
   ilag=ind-dlength-1;
else
   ilag=ind-1;
end
brdstack=colshift(brdstack , -(ilag-1));

%plot all stations with respect to E1S for comparison
xtime=(1:dlength).*delta;
% figure(1)
% plot(xtime,constack)
% figure(2)
% plot(xtime,e1sstack)
figure(3)
plot(xtime,abs(hilbert(constack)),xtime,abs(hilbert(e1sstack)),'r')
figure(4)
plot(xtime,constack,xtime,e1sstack,'r')
figure(5)
plot(xcorr(abs(hilbert(e1sstack(12.5*sampsec:2400,:))),abs(hilbert(constack(12.5*sampse
c:2400,:))),'coeff'))
figure(6)
plot(xcorr(abs(hilbert(e1sstack)),abs(hilbert(abbstack)),'coeff'))
figure(7)
plot(xcorr(abs(hilbert(e1sstack)),abs(hilbert(bomstack)),'coeff'))
figure(31)
plot(xtime,abs(hilbert(bomstack)),xtime,abs(hilbert(e1sstack)),'r')
figure(32)
plot(xtime,bomstack,xtime,e1sstack,'r')
figure(8)
plot(xcorr(abs(hilbert(e1sstack)),abs(hilbert(brdstack)),'coeff'))
figure(9)
plot(xtime,abs(hilbert(brdstack)),xtime,abs(hilbert(e1sstack)),'r')
figure(10)
plot(xtime,brdstack,xtime,e1sstack,'r')
```

Clustering Code

```
clear
for si=5:5
   %stalist={'CON','E1S','NKB','LEH','RAY','HOO'};
   sname='E1S';
   %eval(['load dsave.',sname,'.BHZ.ER.sac.SP.mat']); %also chance save location at the
bottom
   load dsave.E1S.BHZ.ER.sac.video.SP.mat
   method='average';% 'weighted''average'
   threshold=0.6;
   thresh=1-threshold;
   minclustersize=8;

    %filter data
    %n = order, Wn = normalized cut off frequency
    W1 = (1)/((1/sachdr(1).delta)/2);
    W2 = (8)/((1/sachdr(1).delta)/2);
    Wn = [W1,W2];
    n = 2;
    [b,a] = butter(n,Wn);
    [mm,nn]=size(data)
    for ii=1:nn
       data(:,ii) = filtfilt(b,a,data(:,ii));
    end

   %save local versions of the entire input mat file
   for i=1:events
        datal(:,i)=detrend(data(:,i));
   end
   sachdrl=sachdr;
   stnamesl=stnames;
   eventsl=events;

   %save maximum size of events
   for i=1:events
      eventsizes(i)=max(abs(data(:,i)));
      rmsval(i)=sqrt(var(data(:,i)));
   end
   maxsize=max(eventsizes);
   minsize=min(eventsizes);

   %compute correlations
   k=1;
```

```
    for i=1:events-1
        for j=i+1:events
           c(k)=max(xcorr(datal(:,i),datal(:,j),'coeff'));
           cc(i,j)=c(k);
           k=k+1;
        end
    end
    figure(2)
    hist(c)
    title('Crosscorrelation Coefficients')

    %create simularity tree
    dist=1.00001-c;
    %z=linkage(dist,'weighted');
    z=linkage(dist,method);

    figure(3)
    dendrogram(z,0,'COLORTHRESHOLD',thresh);
    clustind=cluster(z,'Cutoff',thresh,'criterion','distance');
end

[cnum,sind]=sort(clustind);

for i=1:events
    years(i)=sachdr(i).nzyear+sachdr(i).nzjday/365+sachdr(i).nzhour/(365*24)-2001;
end

clist=unique(clustind(sind)); %number of uniqe clusters
figure(4)
hist(clustind,length(clist))
title('cluster populations')
evlist=(1:events)';
[evlist(sind),clustind(sind),years(sind)']

for i=1:length(clist)
     ii=find(clustind == clist(i));
     if length(ii) >= minclustersize
        figure(5)
        plot(years(ii)*365,evlist(ii),'*')
        title(['cluster ',num2str(i)])
        xlabel('Day since 1/1/2001')
        ylabel('event number')
        figure(6)

        % create a cluster output dsave file
```

```
        data=datal(:,evlist(ii));
        snormplot(data);
        sachdr=sachdrl(evlist(ii));
        events=length(evlist(ii));
        stnames=stnamesl(ii,:);
        eventsize=eventsizes(ii);

        % save dsave delta data events dlength stnames sachdr eventsize minsize maxsize
        % system(['mv dsave.',sname,'.',num2str(clist(i)),'.',num2str(threshold),'.SP.mat
clusters/E1Scompare'])
        % pause
    end
end

%plot time distribution of clusters
figure(7)
s=['.-b'; '.-g'; '.-r'; '.-c'; '.-m'; '.-y'; '.-k'];
count=2;
for pp=1:length(clist)
   qq=find(clustind==clist(pp));
   if length(qq)>=minclustersize
      plot(years(qq)+2001,count*ones(length(qq),1),s((1+mod(count,6)),:))%,clustind(qq)
      hold on
      count=count+1;
   end
end
plot(years+2001,ones(length(years),1),'.')
hold off
axis([min(years)-.05+2001 max(years)+.05+2001 0 count])
xlabel('Date')
title(['Clusters of similar events (', num2str(threshold), ' or better correlation)'])
ylabel('cluster')
% figure(7)
% plot(years(sind),cnum,'.')

%  save dsave sachdrl stnamesl eventsl clist years datal sind clustind z c dist cnum
eventsizes maxsize minsize threshold evlist rmsval
%  system(['mv dsave.mat', '
clusters/EE1Sclusters6a/','alldata.',num2str(threshold),'.',method,'.',sname,'.unfiltered.SP.
mat'])
```

Code to Examine the Character of the Clusters

```
clear

%load RAYIS2clusters9a/alldata.0.97.average.SP.mat
%load E1Scompare/alldata.0.6.average.compare.SP.mat
load E1S.alldata.0.6.average.SP.v6.mat

thresh=1-0.98;
minclustersize=8;
step=50;
set(gca, 'FontSize', 16,'LineWidth',1.0);

%look at cluster activity in data
for i=step:step:1200
   clear temp;
   clear clustnum;
   temp=unique(clustind(i-step+1:i));
   timedist=unique(years(i-step+1:i));
   for pp=1:length(temp)
      clear temp2;
      temp2=find(clustind(i-step+1:i)==temp(pp));
      clustnum(pp)=length(temp2);
   end
   bar(temp, clustnum')
   title(['Active clusters from ', num2str(min(timedist)+2001), ' to ',
num2str(max(timedist)+2001)])
   xlabel('Cluster Index')
   ylabel('Number of events in cluster')
   pause
end

figure(2)
set(gca, 'FontSize', 16,'LineWidth',1.0);
s=['.-b'; '.-g'; '.-r'; '.-c'; '.-m'; '.-k'];
count=2;
for pp=1:length(clist)
   qq=find(clustind==clist(pp));
   if length(qq)>=minclustersize
      plot(years(qq)+2001,count*ones(length(qq),1),s((1+mod(count,6)),:))%,clustind(qq)
      hold on
      count=count+1;
   end
end
```

```
ylabel('cluster')
xlabel('date')

plot(years+2001,ones(length(years),1),'.')
hold off
axis([min(years)-.05+2001 max(years)+.05+2001 0 count])
xlabel('Date')
title(['Clusters of similar events (', num2str(threshold), ' or better correlation)'])
ylabel('cluster')

figure(33)
dendrogram(z,0,'COLORTHRESHOLD',thresh);
clustind=cluster(z,'Cutoff',thresh,'criterion','distance');

figure(3)
set(gca, 'FontSize', 16,'LineWidth',1.0);
plot(2001,maxsize,'*')
hold on
plot(2001,minsize,'*')
count=1;
count2=1;
eventsizes2=eventsizes;
for pp=1:length(clist)
   qq=find(clustind==clist(pp));
   s=['.-b'; '.-g'; '.-r'; '.-c'; '.-m'; '.-k'];
   eventsizes2(qq)=mean(eventsizes(qq));
   if length(qq)>=minclustersize
      plot(years(qq)+2001,eventsizes2(qq),s((1+mod(count,6)),:))
      avesize(count)=mean(eventsizes(qq));
      numingroup(count)=length(qq);
      count=count+1;
   end
   avesize2(count2)=mean(eventsizes(qq));
   numingroup2(count2)=length(qq);
   count2=count2+1;
end
%title('test')
xlabel('Date')
ylabel('Average Cluster Size')
hold off

figure(4)
plot(maxsize,'*')
hold on
plot(minsize,'*')
plot(numingroup,avesize,'.')
```

```
set(gca, 'FontSize', 16,'LineWidth',1.0);
%title('Number of Events in Cluster Vs avergage size of events in cluster ')
ylabel('Average size of events in cluster')
xlabel('Number of events in cluster')
hold off

figure(5)
plot(maxsize,'*')
hold on
plot(minsize,'*')
set(gca, 'FontSize', 16,'LineWidth',1.0);
plot(numingroup2,avesize2,'.')
%title('Number of Events in Cluster Vs avergage size of events in cluster ')
ylabel('Average size of events in cluster')
xlabel('Number of events in cluster')
hold off

figure(6)
set(gca, 'FontSize', 16,'LineWidth',1.0);
plot(years+2001, eventsizes,'.')
xlabel('Date')
ylabel('Event Size')

figure(7)
set(gca, 'FontSize', 16,'LineWidth',1.0);
plot(years+2001,eventsizes2,'.')
title('plot of average cluster sizes vs time')
xlabel('Data')
ylabel('Average Eventsize')
```

Code for Examining Cluster Stacks

```
clear

%load E1S.alldata.0.6.average.SP.v6.mat
load alldata.0.97.average.RAY.unfiltered.SP.v6.mat
%load alldata.0.6.average.EE1S.SP.v6.mat

stn = 'RAY.IS2';

%making sure veriables are named right
c= c;
```

```
cnum =  cnum;
eventsize= eventsizes;
maxsize = maxsize;
sind =  sind;
years=  years;
clist = clist;
datal = datal;
eventsl=  eventsl;
minsize= minsize;
stnamesl = stnamesl;
z = z;
clustind = clustind;
dist= dist;
evlist = evlist;
sachdr= sachdrl ;
threshold  = threshold;

dlength=length(datal);

count=1;
for pp=1:length(clist)
   qq=find(clustind==clist(pp));
   if length(qq)>=8
      events=length(qq);
      data=datal(:,qq);

                  %start alignment program
                  delta=sachdr(1).delta;
                  thresh=0.4;
                  minsize1 = 0;  %0
                  maxsize1 = 100000000; %50000
                  sname='E1S';
                  %normalize for stacking/alignment (use rms amplitude of vertical)
                  for i=1:events
         a(i)=std(data(:,i));
         data_t0(:,i)=data(:,i)/a(i);
                  end
                  stack=sum(data_t0')/events;
                  xtime=delta*(0:dlength-1);
                  xnum=(1:events);

                  nstack=stack/std(stack);
                  fnstack=fft(nstack');
                  %find correlation coefficients
                  for i=1:events
         ccf=real(ifft(fnstack.*conj(fft(data_t0(:,i)))))/dlength;
```

```
[corr(i),ind(i)]=max(ccf);
corr0(i)=ccf(1);
if ind(i) > dlength/2
   ind(i)=ind(i)-dlength;
end
         end

         %data from iterative realignment using stack
         datatmp=data_t0;
         %initial correlation (use all events)
         corr=ones(1,events);

         netshift=zeros(1,events);

         %lince up events
         onevents=0;
         for iter=1:15

%latest stack
stack=zeros(dlength,1);
j=1;
clear dbest;
clear dind;
for i=1:events
   %note conditional here to use only the small events if
   %desired
   if corr(i) > thresh & eventsize(i) > minsize1 & eventsize(i) < maxsize1
      dbest(:,j)=datatmp(:,i);
      dind(j)=i;
      j=j+1;
   end
end

   nstack=mean(dbest')';
   nstack=nstack/std(nstack);
   s=std(dbest')';

fnstack=fft(nstack);
for i=1:events
   ccf=real(ifft(fnstack.*conj(fft(datatmp(:,i)))))/dlength;
   [corr(i),ind(i)]=max(ccf);

   if ind(i) > dlength/2
      ind(i)=ind(i)-dlength;
   end
```

```
   %4-second limit to interative alignment adjustment
   if abs(ind(i))>160
      ind(i)=sign(ind(i))*160;
   end

end

%netshift=netshift-(ind-1);
datatmp=colshift(datatmp,-(ind-1));

figure(2)
set(gca, 'FontSize', 16,'LineWidth',1.0);
plot(eventsizes(qq))
hold on
plot(maxsize,'*')
plot(minsize, '*')
xlabel('Event Number')
ylabel('Maximum Event Size(in counts)')
hold off
title([stn ' - Cluster ' num2str(count)])

figure(5)
set(gca, 'FontSize', 16,'LineWidth',1.0);
colormap(bone)
imagesc(xnum,xtime,datatmp)
ylabel('Time (s)')
xlabel('Event Number')
      hold on
            plot(xnum,-corr*10+20)
hold off

figure(6)
set(gca, 'FontSize', 16,'LineWidth',1.0);
            plot(xtime,nstack)
title(sname)
                  hold on
plot(xtime,nstack+s,'-.r')
plot(xtime,nstack-s,'-.r')
xlabel('Time (s)')
ylabel('Amplitude')
hold off
title([stn ' - Cluster ' num2str(count) ' stack (+- 1 \sigma)']);

figure(7)
set(gca, 'FontSize', 16,'LineWidth',1.0);
xbnum=j-1;
```

```
        colormap(bone)
        imagesc(1:xbnum,xtime,dbest)
        ylabel('Time (s)')
        xlabel('Event Number')
        title([stn ' - Cluster ' num2str(count)])

        figure(8)
        set(gca, 'FontSize', 16,'LineWidth',1.0);
        hist(corr,20)
        title(sname)

        disp(['iteration: ',num2str(iter),' median correlation: ',num2str(median(corr)),'
number of events: ',num2str(xbnum)])
        pause(1)
        %stop alignment only when the median correlation and number of
        %events used are stable
        if (onevents==xbnum)  && (onmedian==median(corr))
           break
        end
        onevents=xbnum;
        onmedian=median(corr);
    end

            dataorig=datatmp;
            dfinal=dbest;
    figure(4)
    set(gca, 'FontSize', 16,'LineWidth',1.0);
    snormplot(dfinal)
    title([stn ' - Cluster ' num2str(count)])
    xlabel('Time (s)')
    ylabel('Event Number')

    %create stack of cluster
    cluststack(:,count)=sum(dfinal,2);
    %normalize stack
    cluststack(:,count)=cluststack(:,count)./max(cluststack(:,count));

    %plot events in cluster plus stack at the top
    figure(1)
    set(gca, 'FontSize', 16,'LineWidth',1.0);
    for ii=1:length(qq)
        plot(xtime,dfinal(:,ii)./max(dfinal(:,ii))*0.6+ii)
        hold on
    end
    plot(xtime,cluststack(:,count)*0.6+ii+1,'r')
    hold off
```

```
        xlabel('Time (s)')
        ylabel('Event Number')
        title([stn ' - Cluster ' num2str(count)])

        figure(10)
        snormplottime(dfinal, sachdr(qq))

        'Cluster Number to go with cluster distribution with time'
        count
        'Actual cluster'
        pp

        pause
        count=count+1;
    end
end

%line up stacks, and look at the size ranges of the clusters
figure(9)
set(gca, 'FontSize', 16,'LineWidth',1.0);
for ii=1:count-1
    plot(cluststack(:,ii)*0.6+ii)
    hold on
end
hold off

   clear data_t0
   clear a
         [ooo,events]=size(cluststack);
        data=cluststack;

                        %start alignment program
                        delta=sachdr(1).delta;
                        thresh=0.4;
                        minsize1 = 0;  %0
                        maxsize1 = 100000000; %50000
                        sname='E1S';
                        %normalize for stacking/alignment (use rms amplitude of vertical)
                        for i=1:events
            a(i)=std(data(:,i));
            data_t0(:,i)=data(:,i)/a(i);
                        end
                        stack=sum(data_t0')/events;
                        xtime=delta*(0:dlength-1);
                        xnum=(1:events);
```

```
            nstack=stack/std(stack);
            fnstack=fft(nstack');
            %find correlation coefficients
            for i=1:events
    ccf=real(ifft(fnstack.*conj(fft(data_t0(:,i)))))/dlength;
    [corr(i),ind(i)]=max(ccf);
    corr0(i)=ccf(1);
    if ind(i) > dlength/2
       ind(i)=ind(i)-dlength;
    end
            end

            %iterative realignment using stack
            datatmp=data_t0;
            %initial correlation (use all events)
            corr=ones(1,events);

            netshift=zeros(1,events);

            %lince up events
            onevents=0;
thresh=.2;
            for iter=1:15

    %latest stack
    stack=zeros(dlength,1);
    j=1;
    clear dbest;
    clear dind;
    %clear hdr
    for i=1:events
       %note conditional here to use only the small events
       if corr(i) > thresh & eventsize(i) > minsize1 & eventsize(i) < maxsize1
          dbest(:,j)=datatmp(:,i);
          dind(j)=i;
          j=j+1;
       end
    end

       nstack=mean(dbest')';
       nstack=nstack/std(nstack);
       s=std(dbest')';

    fnstack=fft(nstack);
    for i=1:events
       ccf=real(ifft(fnstack.*conj(fft(datatmp(:,i)))))/dlength;
```

```
    [corr(i),ind(i)]=max(ccf);

    if ind(i) > dlength/2
        ind(i)=ind(i)-dlength;
    end

    %4-second limit to interative alignment adjustment
    if abs(ind(i))>160
        ind(i)=sign(ind(i))*160;
    end

end

%netshift=netshift-(ind-1);
datatmp=colshift(datatmp,-(ind-1));

figure(5)
set(gca, 'FontSize', 16,'LineWidth',1.0);
colormap(bone)
imagesc(xnum,xtime,datatmp)
ylabel('Time (s)')
xlabel('Event Number')
title([stn ' - Cluster ' num2str(count)])

figure(6)
                set(gca, 'FontSize', 16,'LineWidth',1.0);
plot(xtime,nstack)
title(sname)
                hold on
plot(xtime,nstack+s,'-.r')
plot(xtime,nstack-s,'-.r')
xlabel('Time (s)')
hold off
title([stn ' - Cluster ' num2str(count) ' stack (+- 1 \sigma)']);


figure(7)
set(gca, 'FontSize', 16,'LineWidth',1.0);
xbnum=j-1;
colormap(bone)
imagesc(1:xbnum,xtime,dbest)
ylabel('Time (s)')
xlabel('Event Number')
title([stn ' - Cluster ' num2str(count)])

figure(8)
```

```
        set(gca, 'FontSize', 16,'LineWidth',1.0);
        hist(corr,20)
        title(sname)
                disp(['iteration: ',num2str(iter),' median correlation:
',num2str(median(corr)),' number of events: ',num2str(xbnum)])
        pause(1)
        if (onevents==xbnum)  && (onmedian==median(corr))
          break
        end
        onevents=xbnum;
        onmedian=median(corr);
      end

              dataorig=datatmp;
              dfinal=dbest;
      figure(4)
      set(gca, 'FontSize', 16,'LineWidth',1.0);
      snormplot(dfinal)
      title([stn ' - final stack allignment for all clusters'])
      xlabel('Time (s)')
      ylabel('Event Number')

      figure(3)
      set(gca, 'FontSize', 16,'LineWidth',1.0);
      plot(xtime,dfinal)
      xlabel('Time (s)')

      count=1
for pp=1:length(clist)
   qq=find(clustind==clist(pp));
   if length(qq)>=8
      cmean(count)=mean(eventsizes(qq));
      cstd(count)=std(eventsizes(qq));
      stdmax(count)=cmean(count)+cstd(count);
      stdmin(count)=cmean(count)-cstd(count);
      count=count+1;
   end
end
figure(2)
set(gca, 'FontSize', 16,'LineWidth',1.0);
xaxis=1:count-1;
errorbar(cmean,cstd,'.')
xlabel('Cluster')
ylabel('Average cluster size')
```

Functions Called

movcor.m

```
%[maxcorr, lag]=function movcor(stack, data, window)
%stack can either be a stack or a specific master event

function [c, l]= movcor(stack, data, window)

step=window/2;
n=length(stack);
nn=length(data);
if (n ~= nn)
   disp('movcor:  dissimilar data file lengths')
   return
end
k=1;
%find maximum correlation and lags to that correlation
for ii = 1:step:n
   [corrs,lags]=xcorr(stack(ii:ii+step-1),data(ii:ii+step-1));
   [c(k,1),l(k,1)]=max(corrs);
   c(k)=c(k)/(norm(stack(ii:ii+step-1))*norm(data(ii:ii+step-1)));
   k=k+1;
end
l=l-step;
```

snormplot.m

```
%plot a set of traces in offset fashion in the current figure
function snormplot(data)
clf
[n,m]=size(data);
xaxis=1:n;
hold on
for i=1:m
   d=data(:,i)/8;
   plot(xaxis./40,d+i)
   %plot(d+i)
end
hold off
```

snormplottime.m

```
%plot a set of traces in offset fashion in the current figure
%snormplot(data,sachdr)
function snormplot(data,sachdr)
clf
[n,m]=size(data);
length=round(30/sachdr(1).delta); %15 length of time window
hold on
for i=1:m
   d=data(1:length,i)./300;
   secs=pick2unixsecs_sac(sachdr(i),'t0');
   xaxis=1:length;
   eptime=secs/(60*60*24*365)+1970;
   set(gca, 'FontSize', 16,'LineWidth',1.0);
   plot(xaxis.*sachdr(i).delta,d+eptime)
end
xlabel('Time (s)')
ylabel('Date')
hold off
```

pick2unixsecs_sac.m

```
function secs=pick2unixsecs_sac(sachdr,tmarker);
%function secs=pick2unixsecs_sac(sachdr,tmarker);
%returns an epoch time (seconds since Jan 1, 1970) for the given sac header and
appropriate tmarker
%where tmarker is a recognized sac header time marker (b,e,o,a,t[0-9])
begint=sachdr.b;
eval(['endt=sachdr.',tmarker,';']);
secs=sachdr.delta*(endt-
begint)+date2unixsecs2(sachdr.nzyear,sachdr.nzjday,sachdr.nzhour,sachdr.nzmin,sachdr.
sec);
```